



Norwegian University of
Science and Technology

Development of new heat pump cloth drum dryer with CO₂ as working fluid

Åsmund Elnan

Master of Energy and Environmental Engineering

Submission date: December 2011

Supervisor: Trygve Magne Eikevik, EPT

Co-supervisor: Inge Håvard Rekstad, EPT

EPT-M-2011-79

MASTER THESIS

for

Stud. Techn. Åsmund Elnan

Autumn 2011

Development of new heat pump cloth drum dryer with CO₂ as working fluid*Utvikling av ny varmepumpe tørketrommel for klær med CO₂ som kuldemedium***Background and objective**

Drying of cloths has over generations been dried in outdoor air, where the drying have been influenced by temperature, relative humidity (and rain) and wind. During the last 30-40 years the drum dryer for family houses has been developed. The first versions had direct electric heating of the air and the humid air was rejected directly to the surroundings (indoor or to outside of the building). Focus on energy use for these dryers introduced the heat pump system with closed drying loop, where the air is cooled in an air cooler (evaporator) to remove the moisture and then the air is reheated in the air heater (condenser). In this Master thesis the focus will be introduction CO₂ as working fluid for the heat pump. The CO₂ system will be implemented in an existing drum dryer and compared with the existing system using R134a as working fluid.

The following tasks are to be considered:

1. Literature review of heat pump drum dryers for cloths
2. Construction and building of the new CO₂ heat pump systems
3. Instrumentation and plan for experimental tests
4. Measuring performance data of the drying cycle
5. Comparison of initial calculations and the measured data
6. Evaluation of different control strategies
7. Writing of a draft paper from the results of the work
8. Suggestions for further work

-- " --

Within 14 days of receiving the written text on the master thesis, the candidate shall submit a research plan for his project to the department.

When the thesis is evaluated, emphasis is put on processing of the results, and that they are presented in tabular and/or graphic form in a clear manner, and that they are analyzed carefully.

The thesis should be formulated as a research report with summary both in English and Norwegian, conclusion, literature references, table of contents etc. During the preparation of the text, the candidate should make an effort to produce a well-structured and easily readable report. In order to ease the evaluation of the thesis, it is important that the cross-references are correct. In the making of the report, strong emphasis should be placed on both a thorough discussion of the results and an orderly presentation.


The candidate is requested to initiate and keep close contact with his/her academic supervisor(s) throughout the working period. The candidate must follow the rules and regulations of NTNU as well as passive directions given by the Department of Energy and Process Engineering.

Risk assessment of the candidate's work shall be carried out according to the department's procedures. The risk assessment must be documented and included as part of the final report. Events related to the candidate's work adversely affecting the health, safety or security, must be documented and included as part of the final report.


Pursuant to "Regulations concerning the supplementary provisions to the technology study program/Master of Science" at NTNU §20, the Department reserves the permission to utilize all the results and data for teaching and research purposes as well as in future publications.

The final report is to be submitted digitally in DAIM. An executive summary of the thesis including title, student's name, supervisor's name, year, department name, and NTNU's logo and name, shall be submitted to the department as a separate pdf file. Based on an agreement with the supervisor, the final report and all other material and documents have to be given to the supervisor in digital format on a CD.

Department of Energy and Process Engineering, August 20th 2011



Prof. Olav Bolland
Department Head



Prof. Trygve M. Eikevik
Academic Supervisor

Research Advisors:

Summary

Since early the early 20th century the electrical tumble dryer became an appliance to dry clothes. During many years of improvements different configurations to solve issues on decreased drying time and more energy efficient solutions has been performed. Several different configurations have been developed; air vented dryers, condensing dryers and the most recent heat pump dryers. The heat pumps in drying technology became the next solution based on improved drying time and decreased energy consumption. With today's focus on energy consumption, with energy demanding appliance such as the clothes dryer; new technology that satisfy the customers need must be available.

By introducing the heat pump to the drying technology, a suitable refrigerant must be chosen. The choice should be based on several factors; the performance of the heat pump and the refrigerants GWP and ODP values, its toxicity and safety for the consumer. This report is based on a heat pump dryer made for an R134a system. R134a has a global warming potential (GWP) 1300 times the value of R744 (carbon dioxide). This report will present the feasibility of replacing the R134a system with a system designed for carbon dioxide as refrigerant.

Carbon dioxide or R744 is a natural refrigerant, and it is in contrast to other commonly used refrigerants operating in the transcritical region. This implies that the heat rejection is performed with gliding temperature exchange, not by condensation as for the R134a. This is due to the low critical temperature of carbon dioxide; a critical pressure of 73.8 Bara and a critical temperature of 31.1°C. Despite the required high pressures, the heat exchange properties of carbon dioxide in the critical region are very good, and new technology can take advantage of this.

By SINTEF developed simulation tool HX SIM Basic 2007, based on results from the R134a cycle, heat exchangers have been designed to reach the optimal solution. The capacity of the heat changers and the compressor will be the same as the R134a system.

The system is built with a manual throttling valve in parallel to a capillary tube, during the experiments the system will be tested to find the most optimal set point. Evaporating pressures from 40 to 50 Bara and gas cooler pressures from critical pressures to 120 Bara have been applied in the experiments. The main purpose of the experiments is to find a system design that will fulfil both energy saving requirements and have a simple enough construction for it to be a market product. Based on the experiments on this first prototype and the results obtained; a conclusion is that the dryer with CO₂ as refrigerant is using marginally more energy than the R134a system. However this is a first prototype and its potential should be investigated further.

Sammendrag

Siden tidlig på 1900-tallet har elektriske tørketromler vært aktuelle produkter for å tørke klær. Gjennom mange år har det blitt arbeidet med utvikling av nye konsepter for å løse problemer med tørketid og energi effektivitet. Flere ulike modeller har blitt utviklet og utprøvet ventilert tørketrommel, kondenseringstørketrommel og den mest aktuelle tørketrommel med varmepumpe. Å basere en tørketrommel på varmepumpe er en smart måte å utnytte både varm og kald side i prosessen. Med dagens fokusering på energibruk i teknologiske applikasjoner er bruk av varmepumpe en steg i riktig retning.

For en varmepumpe må et passende arbeidsmedium velges med bakgrunn i flere faktorer; termodynamisk ytelse, global oppvarming og andre miljøaspekter. I denne rapporten vil et system basert på R134a bli ersatt og sammenlignet med et system basert på karbondioksid. R134a har globalt oppvarmingspotensiale på 1300 sammenlignet med CO₂ på 1; muligheten for å bruke CO₂ i en tørketrommel skal undersøkes. CO₂ er et naturlig arbeidsmedium som i motsetning til andre arbeidsmedier opererer transkritisk; det vil si at varmeavgivelsen foregår med nedkjøling av høytrykks gass uten at det er kondensering. Dette er på grunn av det lave kritiske punktet til CO₂ på 31.1 °C og 73.8 bar. Selv med høye trykk i gasskjøleren er de termodynamiske egenskapene til CO₂ i den superkritiske regionen veldig bra og ny teknologi er utviklet for å kunne gjøre det til en fordel.

Med programvare utviklet fra SINTEF HX SIM Basic 2007 basert på luftverdier fra R134a systemet har størrelse og design av varmevekslere blitt utviklet. Kapasiteter til varmevekslere og kompressor er i samme størrelsesorden som det gamle R134a systemet.

Det nye systemet er bygget med to muligheter for strupning av arbeidsmediet; en manuell strupeventil og et kapillærrør i parallell. Systemet blir testet med fordampningstrykk på 40-50 bar og gasskjølertrykk fra kritisk trykk opp til 120 bar, dette vil indikere ved hvilken trykkklasse systemet vil operere best mulig. Hovedgrunnen for å utføre disse eksperimentene er for å finne en løsning som er både bra energimessig, men som også er enkel nok for å kunne selges på markedet.

Ut i fra resultater og beregninger på den nye CO₂ prototypen vil energibruken øke marginalt i forhold til R134a systemet, likevel bør det fortsettes med arbeid for å utvikle konseptet videre.

Preface

This report is a result of a heat and energy processes master thesis TEP4900 at the Norwegian University of Science and Technology. It was commenced in the fall of 2011 and handed in December 2011. The thesis accounts for 30 credits of the master degree in Energy and Environmental Engineering with a specialization within Energy- and Process engineering.

The thesis investigates the possibilities of replacing R134a with carbon dioxide as refrigerant in clothing dryer. The process of this thesis includes a theoretical part with assessment of the R134a system and a design and order of new parts for the system. The new parts include compressor, evaporator and two gas coolers as well as tubes and valves.

During this thesis I have learned a great deal; I have been challenged in a practical and theoretical manner. I want to thank my main supervisor Trygve Magne Eikevik for his support and contact during the thesis. I also want to thank my secondary supervisor Håvard Rekstad at SINTEF, which has been very supporting during all parts of the project.

When working at the laboratory I want to thank Martin Bustadmoen for his exceptional work and assistance to build the system and Reidar Tellebon and Gunnar Lohse for theoretical and practical advices during building and operation. Thanks to Erik Løvseth Seehuus and Odin Hoff Gardå which helped me with instrumentation and the electrical set up for the system. Also thanks to all the people at the university which have been helpful and made this a great finish to my study here at Norwegian University of Technology.

Trondheim 03.12.2012

Asmund Euan

Nomenclature

CO_2 = Carbon dioxide

R134a = Tetrafluoroethane (CH_2FCF_3)

EC= Energy consumption

COP = Coefficient of performance

SMER = Specific moisture extraction rate

h = Enthalpy

VRC = Volumetric refrigerating capacity

GWP = Global warming potential

x = Absolute humidity

cSt = Centi-stroke

C_v = Throttle valve flow coefficient

L = Length

M = Mass flux

Bara = Absolute bar pressure

v = Specific volume

λ = Volumetric efficiency

f = Frequency

RH = φ = Relative humidity

η_{is} = Isentropic efficiency

m_0 = Mass water vapour

m_g = Mass dry air

p_0 = Partial pressure

p_m = Saturated pressure

q_0 = Evaporator capacity

I = Electric current

P = Electric power

R = Electric resistance

PF = Power factor

f_{sp} = Friction factor single phase

ε = Roughness height

d_i = Inner diameter

L_{sp} = Length single phase

ΔP = Pressure drop

V = Mean flow velocity

ρ = Density

M_{ref} = Refrigerant flux

M_{ref} = Refrigerant mass flow

A = Flow area

f_l = Liquid friction factor

Φ = Multiphase flow coefficient

Fr_h = Froude number

We_h = Weber number

g = Gravity

δX_i = Total uncertainty

$S_{\text{Measurement}}$ = Measurement error

$S_{\text{Controller}}$ = Controller error

Table of contents

1.	Literature review and CO ₂ system basics.....	1
1.1.	Background	1
1.2.	Purpose and goal	5
1.3.	Transcritical CO ₂ cycle properties	5
1.4.	The air cycle	10
2.	Designing and building the new CO ₂ heat pump system.....	15
2.1.	Process of building	16
2.2.	Component documentation.....	16
2.2.1.	Compressor	16
2.2.2.	Heat exchangers.....	24
2.2.2.1.	Main gas cooler	25
2.2.2.2.	External gas cooler.....	28
2.2.2.3.	Evaporator.....	30
2.2.3.	Expansion devices	33
2.2.4.	Tubes and fittings.....	42
3.	Instrumentation and plan for experimental tests	44
3.1.	Instrument overview.....	45
3.1.1.	Temperature measurement.....	45
3.1.2.	Pressure measurement	48
3.1.3.	Mass flow measurement – Rheonik RHM 04 – Coriolis mass flow meter	52
3.1.4.	Air temperature and humidity measurement	54
3.1.5.	Electrical power measurement	56
3.2.	Uncertainly analysis	57
4.	Plan for experiments.....	61
4.1.	Experiment overview	62
5.	Measuring performance data of the drying cycle.....	62
5.1.	R134a results.....	62
5.2.	Experiment 1: Manual throttle valve, no external fan	65
5.3.	Experiment 2: Manual throttling external gas cooler fan connected.....	69

5.4.	Experiment 3: Capillary tube (900 mm), external fan.....	73
5.5.	Experiment 4: Capillary tube (740 mm), external fan.....	76
5.6.	Experiment 5: Capillary tube (660 mm), no external fan	79
5.7.	Experiment 6: Capillary tube (660 mm) no external fan – reduced refrigerant charge	82
5.8.	Experiment 7: Capillary tube (660 mm) no external fan – increased refrigerant charge.....	85
5.9.	Experiment 8: Capillary tube (660 mm) external fan connected.....	87
6.	Discussion of initial theoretical and experimental data	90
7.	Evaluation of control strategies	97
8.	Conclusion.....	98
9.	Suggestion of further work	99
	References	101
	Table of figures	102
	Table of tables.....	107
	Table of equations	108
	Appendices.....	109
	Appendix A: Experiment performance figures	109
	Experiment 1: Manual throttle valve, no external fan	109
	Experiment 2: Manual throttling external gas cooler fan connected.....	111
	Experiment 3: Capillary tube (900 mm), external fan.....	112
	Experiment 4: Capillary tube 740 mm	114
	Experiment 5: Capillary tube 660 mm – 1.....	116
	Experiment 6: Capillary tube 660 mm – 2: reduced refrigerant charge	117
	Experiment 7: Capillary tube 660 mm – 3: increased refrigerant charge.....	118
	Experiment 8: Capillary tube 660 mm – 3: increased refrigerant charge.....	120
	Appendix B: Dew point table.....	122
	Appendix C: Dryer template ASKO – CO ₂	123
	Appendix D: Dryer template ASKO – R134a	124
	Appendix E: Draft article	125
	Appendix F: Safety report	135

1. Literature review and CO₂ system basics

1.1. Background

Since the early 20th century when the first electrical tumble dryer became an appliance for drying clothes, the drying appliances have been developed to become a more efficient product. The first traditional dryers had a long drying time due to inefficient heating mechanisms, but as the competence on electricity improved, both efficiency and speed of the tumbler increased to the modern tumble dryer we know today. Attempts to improve the technology has been analysed comprehensively, but many of the proposed techniques are unacceptable either on a financially- or environmentally basis. According to (Colver, et al., 2003) 3 % of the total household consumption in the United States is from clothes dryers. As said by (Dekker, 1987) that drying consumes 50 % of the energy of manufacturing of finished textile products. Thus energy management is an essential part of the drying process and efficient energy use contributes extensively to the total cost. Measures on existing dryers includes recycling a portion of exhaust air to reduce energy consumption, air-air heat exchanger, reduce air leaks, add insulation and using more efficient motors are some measures that have been studied. The disadvantage by recycling process air is that it will also recycle lint from the fabric and cause potential fire hazard situation. The air-air heat exchanger will accumulate lint on the surface and reduce the heat transfer coefficient.

Traditionally two types of dryers for household have dominated the market; the vented dryer and the condensing dryer.

The conventional vented dryer for clothes works by that a fan blows ambient air over a heating element, the hot air is humidified from the wet clothes and is then vented out from the cycle. According to (Bansal , et al., 2001) this conventional vented dryer is simple, cheap, reliable and relatively short drying time. However the disadvantages is the requirement of ducting to the outdoors, since the hot and moist air vented indoors can lead to moisture condensation problems, and the fact that the process is energy inefficient.

The condensing dryers working principle is the implementation of a heat exchanger to recover heat from the hot and humid air leaving the drum while condensing the moisture from the air. This will increase the moisture extraction rate compared to the vented dryer, and vent less moisture to the ambient air. (Bansal , et al., 2001) reports that the condensing dryer is 14 % more efficient than the air-vented conventional dryer, but even though it is more energy efficient than the vented dryer, it does not meet the European energy efficiency standards.

The configuration that according to (Klöcker, et al., 2001) has been recognized as an optimal solution for drying is using heat pumps in convective hot air dryers. Heat pump dryers use the heating capacity in the heat pump to heat up the hot air, and the refrigeration capacity is used to dehumidify the moist air. According to (Schmidt, et al., 1998) this technology has been produced and distributed since 1997. Heat pump dryers are according to (Li, et al., 2009) widely used in many fields such as wood drying, food processing, vegetable dehumidifying, biotechnological materials and seed drying. The most commonly used working fluids are historically the HCFCs and the CFCs in heat pumps and air-conditioners. The use of these working fluids is being controlled from the Montreal Protocol of 1989, because of their ozone depleting effects. The Kyoto Protocol of December 1997 accepted by many countries decided to control the use of HFCs due to their high global warming potential, therefore the option with natural working fluids will be considered. According to (Colak, et al., 2009) the first patent on heat pump dryers started in 1973, and it was stated that energy consumption was less than conventional steam heated dryers.

Today the focus on energy consumption and environment has become more and more in the centre of attention of household appliances. To be able to maintain the luxury of a tumble dryer, the energy consumption and the environmental impacts must be set to a minimum, and the old-fashion dryers must be phased out. Heat pump in the traditional dryer system will decrease the energy consumption with 60-80% depending on the heat pump system configuration, when operating in the same temperature conditions (Strømmen, et al., 2002). The HFC refrigerants that once were accepted as long term solutions, are now on lists over substances with global warming effects, and therefore not a feasible option for the future. With the environmentally friendly natural fluids like water, air, noble gases, hydrocarbons, ammonia and carbon dioxide, the attention should rather be on develop systems suitable for the natural refrigerants rather than inventing new refrigerants (Kim, et al., 2004).

From a study done by (Schmidt, et al., 1998) where the heat pump drying technology using R134a and CO₂ as refrigerants was explored. The thermodynamic analysis shows that the air heating with the gliding temperature in the gas cooler for CO₂ is more efficient than the regular condenser for R134a. However throttling losses were considerable larger for the CO₂, due to difference in specific heat in the fluids and the position of throttling relative to the critical point of both fluids.

After a first optimization of a CO₂ heat pump prototype with a 12 kW heating capacity (Klöcker, et al., 2001) was originally an electrically hot air laundry dryer (Passat type 132E). The electrical heating element was removed and replaced by the heat pump system. With less focus on the drying time an energy saving potential of 65% can be achieved. If the high water extraction rate is the main focus,

an energy saving of 53% can be realized, that with significant shorter drying time than the conventional system.

An experimental analysis performed by (Valero, et al., 2009) where the performance of CO₂ and R134a was compared in a dryer prototype. With R134a as the reference case the system with CO₂ showed an improved energy efficiency of 7 %. However the report was prepared to explore the feasibility of CO₂ in the system, and not to optimize.

Another application was patented by (Bison, et al., 2007), this is a home laundry drier, using CO₂ as refrigerant to dry clothes. This is similar to the system in considered in this report, but the closed carbon dioxide cycle will be in a gaseous state during the drying. This means that there will be no evaporation of the refrigerant in the system, only gas cooling and heating process in supercritical state. To evaluate the performance of the heat pump dryer (Klöcker, et al., 2001) expressed that by considering the coefficient of performance for the heat pump (COP_{HP}) and by the moisture extraction rate (SMER) for the dryer.

The COP is a measure of the efficiency of the heat pump, while the SMER ratio specifies the dryer efficiency of the cycle. Below in Figure 1.1-1 a system is shown, this system is illustrated with a both capillary tube and a manual throttling valve. The external gas cooler is placed after the main gas cooler to reduce the temperature of the CO₂ after the air-heating process.

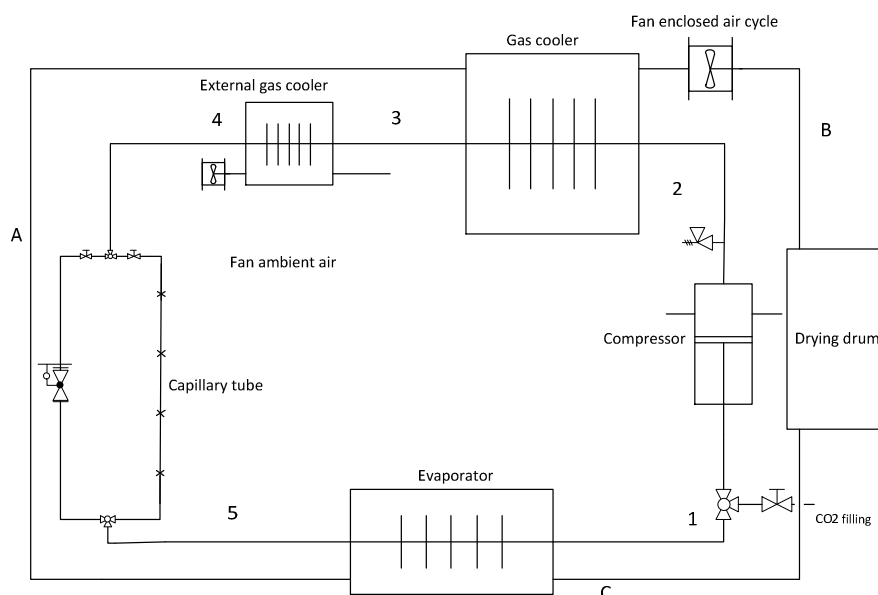


Figure 1.1-1 Heat pump and dryer cycle

The energy consumption in the cycle will be monitored from two watt transducers; one at the motor running the drum and the main fan and one at the compressor. The external fan will have more or less the same load through the cycle and a constant value will be added to the calculation. The energy consumption for the system will be considered in two ways; one for the heat pump alone and one for the total energy consumption. These are expressed in Equation 1.1-1 and Equation 1.1-2 respectively.

$$EC_{HP} = \dot{m}_{Ref}(h_3 - h_2)$$

Equation 1.1-1 Energy consumption heat pump [kW]

$$EC_{Total} = EC_{HP} + EC_{Motor} + EC_{Fan}$$

Equation 1.1-2 Total energy consumption [kW]

The coefficient of performance shown in Equation 1.1-3 of the heat pump is the ratio between the changes of enthalpy in the condenser/gas cooler to the change of enthalpy in the compressor.

$$COP_{HP} = \frac{(\Delta h_{gas\ cooler})}{(\Delta h_{Compressor})} = \frac{(h_3 - h_5)}{(h_3 - h_2)}$$

Equation 1.1-3 Heat pump coefficient of performance

The real coefficient of performance includes all the energy consuming components.

$$COP = \frac{\dot{m}_{Ref}(h_3 - h_5)}{EC_{Total}}$$

Equation 1.1-4 Coefficient of performance

A simplified conversion from COP to energy savings is shown in Equation 1.1-5. This value can be useful to show the relation between the coefficient of performance and how much energy actually is saved by applying a heat pump in the dryer.

$$Energy\ savings = 1 - \left(\frac{1}{COP}\right)$$

Equation 1.1-5 Energy savings heat pump

1.2.Purpose and goal

The purpose of investigating a new dryer concept in this project is based on the environmental aspects with HFCs as refrigerant. With the high global warming potential of R134a alternative options must be developed. However to be able to replace an existing product the operational costs of the system must be minimized, thus the energy savings must be optimized and the investment costs must be limited. This report will not consider the economical parts in detail, but the technical solutions will be based on parts that will be affordable for a market model.

The prototype should operate without any adjustments during a drying procedure where the pressure level should adjust automatically and thus the temperatures into the drum. A way to minimize investment costs for the product is by applying a capillary tube for the throttling device. The manual expansion device will only be applied in the first experiments to experience how the system will operate with and without the external fan connected. The following experiments will investigate how the length of the capillary tube and the refrigerant charge affect the system performance. Altering factors such as the pressure level, the air temperature will change and thus the drying time will be affected.

The report will first present the theoretical background for carbon dioxide as refrigerant for a dryer concept; next the new parts for the system including the instrumentation will be presented.

The main goal of the project will be to find a length of the capillary tube and a refrigerant charge that will produce a pressure level that will minimize drying time and consumed energy.

With a sufficiently high gas cooler pressure; the temperature into the drum will be sufficiently high to evaporate a large amount of water in the drum. However there must be a balance between the optimal air temperature and the energy consumed by the compressor.

1.3.Transcritical CO₂ cycle properties

Carbon dioxide as based on vapour compression systems has been applied as far back as 1850, mainly used in marine appliances. Because of the low critical point of CO₂ ($t_c = 31.1$ °C and $p_c = 73.8$ bar), the system faced several problems, and with the discovery of halocarbon refrigerants, left the focus on CO₂ as refrigerant in the shade (Bhattacharyya, et al., 2004). When the awareness of the environmentally harmful conditions from using halocarbons was discovered, the focus on the natural refrigerant carbon dioxide had its renaissance. Gustav Lorentzen among others with their pioneer studies took advantage of the low critical point of carbon dioxide by operating the system in the transcritical region. The conventional subcritical condensing heat exchange applied by other refrigerants was replaced by a gliding temperature exchange in a gas cooler in the supercritical

region. This made the carbon dioxide a feasible option as working fluid in heat pump applications with higher heat sink temperature requirements. The fact that carbon dioxide is non-toxic, non-flammable, low price, compatible with various common materials, good heat transfer properties are some of the features that makes carbon dioxide as refrigerant a good option for heat pumps.

Carbon dioxide separates itself from other commonly used refrigerants with the low critical point and thus introduces the transcritical CO₂ cycle. The CO₂ transcritical cycle is shown in Figure 1.3-1; this consists of a compression process (2-3), a gas cooling process (3-5), a throttling process (5-6) and an evaporation process (6-1). The heat exchange in the gas cooler occurs in the supercritical region with a gliding temperature and constant pressure.

The assumptions for the cycle are listed below, and the isentropic efficiency of the cycle is used in Equation 1.3-1 to calculate the enthalpy at the compressor discharge.

$$h_3 = h_2 + \frac{h_{2s} - h_2}{\eta_{is}}$$

Equation 1.3-1 Isentropic efficiency

- Evaporation temperature of 15 °C
- 5 K overheat
- 100 bar gas cooler pressure
- No pressure loss in tubes and heat exchangers
- Compressor isentropic efficiency of 0,5
- Throttling temperature of 35 °C
- External gas cooler ejects the same amount of heat as the compressor loose due to isentropic efficiency.

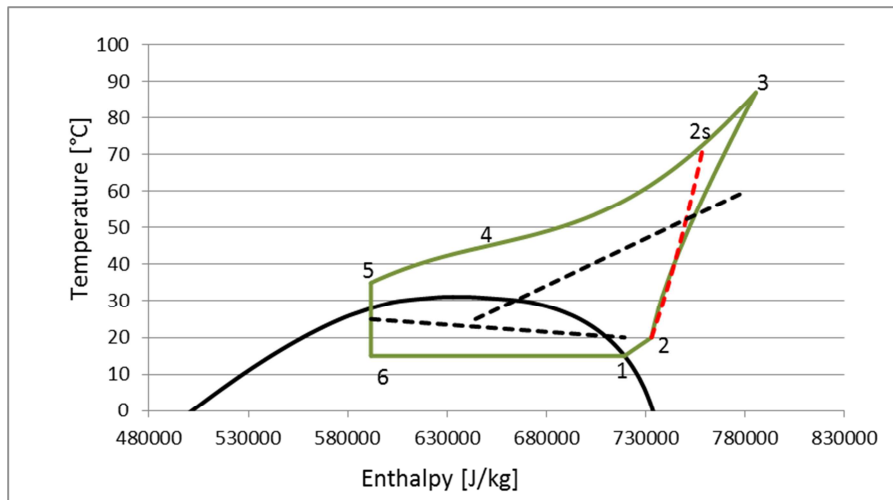


Figure 1.3-1 Transcritical CO2 cycle, gas cooler pressure of 100 bar

The dotted lines visualize the enclosed air cycle, the heating line stops in the middle of the gas cooling process; due to that it is the end of the main gas cooler. And the external gas cooler is cooling the air to the ambient air flow, not the internal one. The red line in the figure represents the isentropic compression process.

To limit the error determining the isentropic efficiency the real isentropic efficiency will be used as well, this is calculated using the real compressor consumption instead of basing it on the discharge temperature measurement. The consumed energy in Equation 1.3-2 is based on electrical measurements that will have a smaller degree of uncertainty compared to thermocouple measurements.

$$\eta_{is} = \frac{\dot{m}_{ref}(h_{2s} - h_2)}{W_{Compressor}}$$

Equation 1.3-2 Isentropic efficiency real

To determine the volumetric efficiency of the compressor the mass flow, suction specific volume, cylinder volume and frequency are used. This determines how much of the volume in the cylinder that will be effective volume. The “dead volume” in small piston compressors has large effect to the volumetric efficiency.

$$\lambda = \frac{\dot{m} \cdot v_2}{V_S \cdot f}$$

Equation 1.3-3 Compressor volumetric efficiency

In Table 1.3-1 Thermo physical properties of R134a and CO₂ physical and thermodynamically properties of CO₂ and R134a are compared at evaporation temperature of 0 °C.

Table 1.3-1 Thermo physical properties of R134a and CO₂ (Stene, 1997)

Property	R134a	CO ₂ (R744)	Units
Molecular weight	102,0	44,01	[g/mol]
Heat of evaporation	198,4	231,6	[kJ/kg]
Thermal conductivity liquid	0,092	0,105	[W/mK]
Thermal conductivity gas	0,012	0,023	[W/mK]
Specific volume liquid	0,768	1,073	[m ³ /kg]
Specific volume gas	71,0	10,2	[m ³ /kg]
Kinematic viscosity liquid	0,212	0,095	[10 ⁻⁶ m ² /s]
Kinematic viscosity gas	0,880	0,156	[10 ⁻⁶ m ² /s]

With a small molecular weight of the refrigerant it will gain the system with a smaller required mass flow [kg/s]. Thus the size of the systems heat exchangers, pipes and liquid containers can be reduced, or increase the efficiency of the system due to less pressure losses. CO₂ have this advantage with a low molecular weight compared to R134a.

Most critical relating to the heat transfer are the density in both liquid and gas state, specific heat of evaporation and the liquids' thermal conductivity. (Stene, 1997)

Carbon dioxides' high gas density and relatively high heat of evaporation gives a favourable volumetric refrigeration capacity (VRC). This is given in kJ/m³, and since the compressor have a fixed displacement volume, the mass flow of the process can be reduced.

$$VRC = \rho_{CO_2} \Delta h_{Evaporator}$$

Equation 1.3-4 Volumetric refrigeration capacity

In Figure 1.3-2 the VRC-value value is shown for different R744 and R134a values at different evaporation temperatures. The curves in this figure will be applied to find the best evaporation temperature for the prototype.

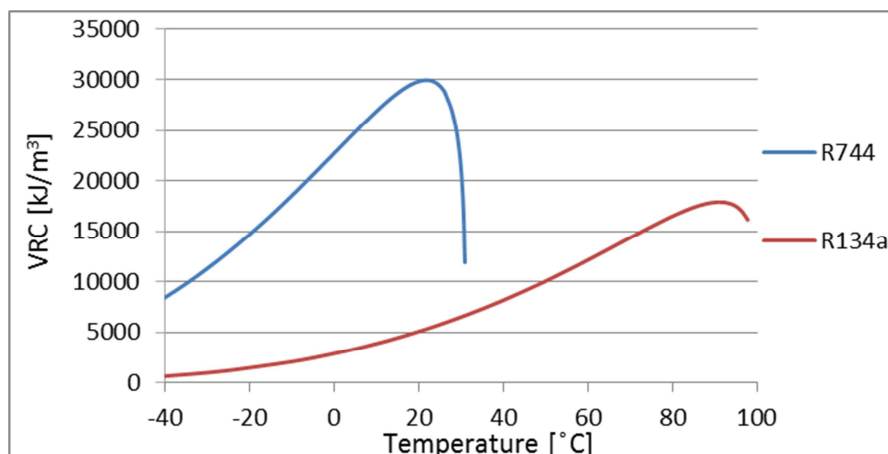


Figure 1.3-2 Volumetric refrigeration capacity vs. temperature

Considering pressure losses in a heat pump cycle CO_2 also has a benefit; the temperature drop from pressure drops in the cycle. Figure 1.3-3 illustrates the change in saturation temperature related to change in pressure. The figure simply illustrates that CO_2 cycle can accept a much higher pressure drop in evaporator, gas cooler and tubes than the conventional R134a cycle.

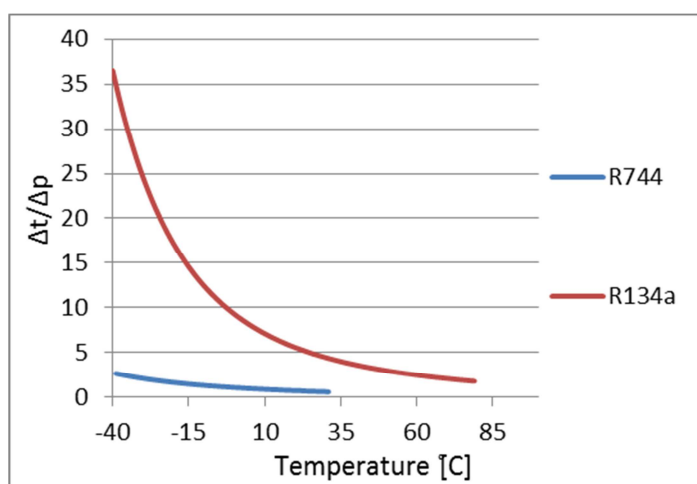


Figure 1.3-3 Temperature loss vs. pressure loss

The reasoning of substituting R134a applied in the heat pump dryer with the CO_2 is mainly due to R134a's high global warming potential (GWP) of 1300. Carbon dioxide as refrigerant has a GWP of 1 and an ozone depletion rate of 0. The costs of the system and the energy efficiency is the remaining part to be proven to be compatible with the less environmental friendly options.

The transcritical process introduces both challenges and opportunities for controlling the heat pump system. The optimal gas cooler pressure can be obtained from a relation between heating capacity and the compressor power input, thus the optimal coefficient of performance (COP) is found.

1.4.The air cycle

According to (Li, et al., 2009) researchers from Essen studied the heat pump laundry dryer with carbon dioxide and compared it to an R134a system. They found that the drying performance was more or less equal, but the CO₂ transcritical process was favoured due to environmental and thermal properties of the carbon dioxide.

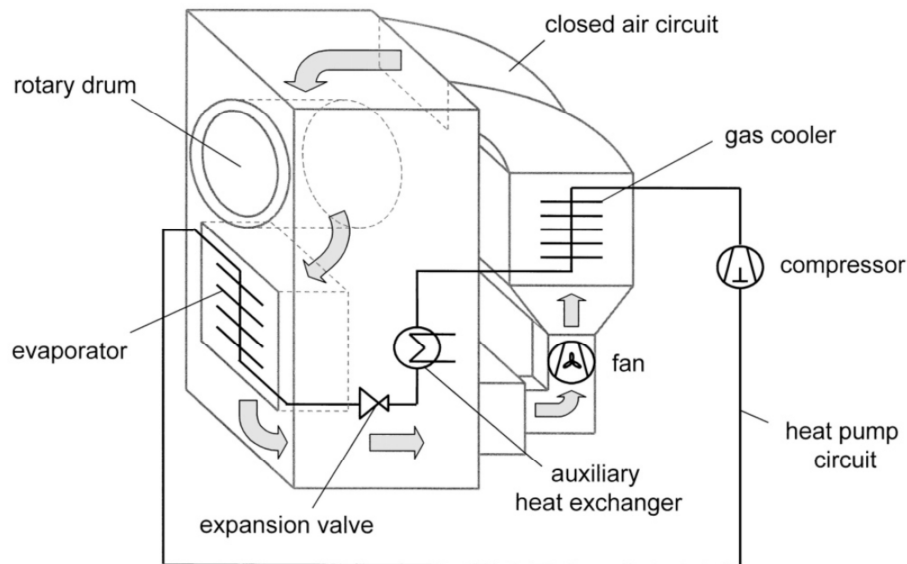


Figure 1.4-1 Carbon dioxide heat pump dryer (Klöcker, et al., 2001)

In a condensing dryer three stages are recognized during the cycle; humidification, dehumidification and heating. The humidification process takes place within the drum where the moist fabric encounters with dry hot air. The temperature of the air decreases as the moisture content in the air increases. The humid air then continues to the evaporator which will cool down the relatively hot air below its dew point, the moisture will condense on the fins of the evaporator and the water will be drained away from the cycle.

Different characteristics of the drying processes have been examined based on the moisture content of the clothes and the rate of evaporation over time. (Colver, et al., 2003) Studied the effect on energy consumption and drying time from an electrical dryer by altering various parameters. It was concluded that by increasing the drum load, the air flow would decrease and the area of mass transfer for water increases. This resulted in an increased rate of evaporation from the wet clothes, i.e. the specific energy consumption would decrease with increased load. By increasing the heater power it would increase the rate of evaporation thereby decrease the drying time, while the fan speed showed to have little influence on the evaporation rate.

A simple model for drying process was developed and tested by (Lambert, et al., 1991); here they found that by lowering the partial pressure of water in the air entering the drum increases the speed of the drying process. This was accomplished by either decrease humidity content or increase the temperature. With too high temperature it can damage the clothes, therefore the focus land on keeping the humidity content to a minimum.

An easy way to illustrate the drying process is in the h-x-diagram or the Mollier-diagram for humid air. In the Mollier diagram the absolute humidity content in the air is shown along the x-axis and the temperature along the y-axis.

The absolute humidity content, x is given by the mass relation between the water vapour, m_0 and dry air, m_g given in *kg*.

$$x = \frac{m_0}{m_g} \cdot 100\%$$

Equation 1.4-1 Absolute humidity content

The relative humidity content is given by the relation between the partial pressure, p_0 and the saturated pressure, p_m of the water vapour, given with the same dry bulb temperature.

$$\Phi = \frac{p_0}{p_m} \cdot 100\%$$

Equation 1.4-2 Relative humidity content

When humid air is cooled down under constant pressure, the relative humidity will increase until it reaches the saturated state where $\phi=1$, and water will condense from the humid air. The line in Figure 1.4-2 marked with $\phi=1$ is the dew point line and correspond to 100% relative humidity.

An important quantity to include when looking at a heat pump dryer is the dh/dx -relation. This relates to how much energy that is necessary to remove 1 kg water from the material. The relation is calculated from the heat in the evaporator to the water removed by condensation in the evaporator.

$$\frac{dh}{dx} = \frac{q_o}{\Delta x_{C-A}}$$

Equation 1.4-3 Dryer efficiency

With a decreasing drying temperature the dh/dx -relation will increase, i.e. more energy spent per mass removed water content. This means that more energy is required for low temperature drying

than for high temperature drying. Another consideration is the relative humidity at the drum outlet; if this is low, the dh/dx relation will increase, thus a proper humidification in the drum is important.

The specific moisture extraction rate (SMER) for a heat pump expresses how much moisture is removed from the drying material to the power input of the compressor in the system. The SMER value for a heat pump is given by Equation 1.4-4, and can be useful to see how much power consumption is required to remove a certain deal of water. In this report the SMER value is expressed as $[\text{kg}_w/\text{kW}]$. It is related directly to the COP of the heat pump and the dh/dx -relation.

$$SMER_{HP} = \frac{\Delta x_{C-A}}{P_{El}}$$

Equation 1.4-4 Specific moisture extraction rate heat pump $[\text{kg}_{\text{water}}/\text{kW}]$

The SMER-value is often used as an indicator of the energy efficiency of a heat pump dryer, and is useful to compare different running conditions in equal systems. The SMER-value will decrease if the drying is occurring with low temperatures, especially with negative temperatures.

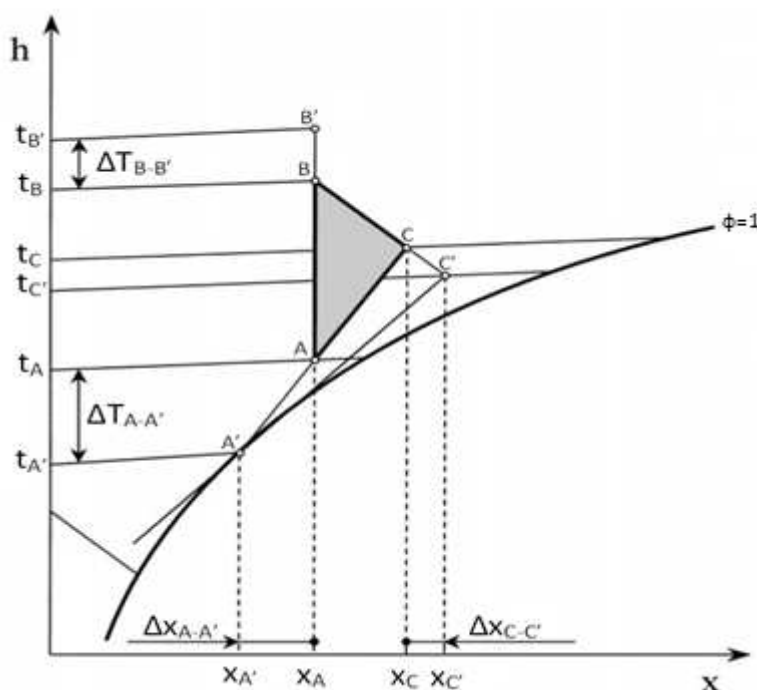


Figure 1.4-2 – h-x-Chart of the drying process; based on (Klöcker, et al., 2001)

The air cycle (A-B-C) starts from point A, where air with ambient conditions enters the gas cooler/air heater, and is heated to temperature t_b at constant absolute humidity. The hot air then continues to the drying chamber and absorbs the moisture from the drying clothes, in an adiabatic change of state. From the drying chamber the temperature decreases to t_c , before being blown into the

evaporator, where the moisture is condensed from the air. The air is cooled down to a temperature t_A , and the enclosed air cycle continues again back through the gas cooler.

The air mass flow at the reference point is a key value for the process considering the change in water content in the kiln (Δx_{C-B}). With high air flow in the closed air cycle will require a smaller temperature lift Δt_{B-A} , thus the heat pumps compressor will have a reduction in the energy consumption. However the increased air mass flow will lead to a high pressure drop in the system and thus a high power consumption of the fan. This relation between the heat pump and the air cycle will be optimized to find the best air flow rate (Klöcker, et al., 2001).

Various variables will have an effect on the total system performance. Factors related to the air cycle are the mass flow rate, system flow resistance constant and air pressure drop. The component effectiveness for the kiln Φ_{KM} , air cooler Φ_{AC} and air heater Φ_{AH} expressed below on the base of temperature and moisture content.

$$\Phi_{KM} = \frac{x_C - x_B}{x_{C'} - x_B}$$

Equation 1.4-5 Kiln efficiency

$$\Phi_{AC} = \frac{x_C - x_A}{x_C - x_{A'}}$$

Equation 1.4-6 Air cooler efficiency

$$\Phi_{AH} = \frac{t_2 - t_1}{t_{2'} - t_1}$$

Equation 1.4-7 Air heater efficiency

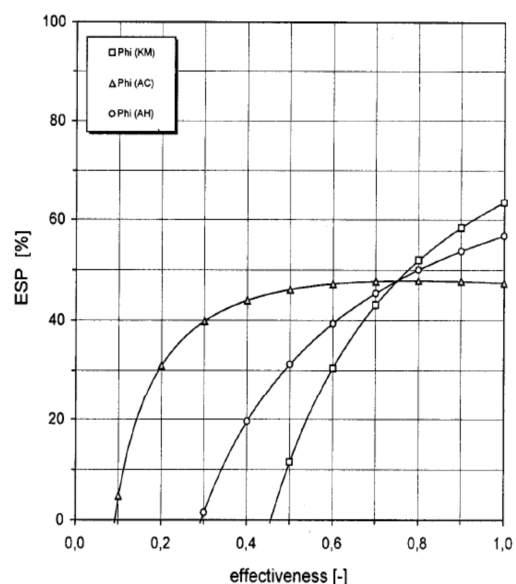


Figure 1.4-3 Energy saving potential (ESP) vs. effectiveness (Klöcker, et al., 2001)

The Figure 1.4-3 is visualizing the energy saving potential where the efficiencies common reference value is set to 0.75. The kiln and the air heater efficiency will have an impact on the energy saving potential, but the air cooler will only have a small effect on the selected reference point. If the kiln efficiency is low, a too efficient air cooler might also cut down energy savings.

During the drying of the fabric in the dryer, there are two periods of interest that determine the speed and efficiency of the drying. The first part of the drying progression includes a constant drying speed with drying from a moist surface. The drying material will contain a sufficiently amount of

moisture to keep the surface moist all during this period. The drying speed in this period is controlled by the heat transfer to the surface. The mass transfer is balancing the heat transfer, and the temperature at the surface will remain constant. If the heat transfer only occurs with convection, as it will for heat pump dryers, the surface temperature will be equal to the wet bulb temperature. To increase the drying speed in the constant drying period the difference between the dry bulb and the wet bulb temperature must be increased or optimize the outer mass and heat transfer conditions. The constant drying period does not always occur due to the initial humidity content or temperature in the drying material is too low to cause internal water transport.

The decreasing drying period is present when the water transport to the surface no longer can maintain the surface to be wet. The evaporation from the surface will be greater than the internal water transport. The drying speed is often modelled linearly as a function of the water content in the drying material.

The two periods are shown in Figure 1.4-4.

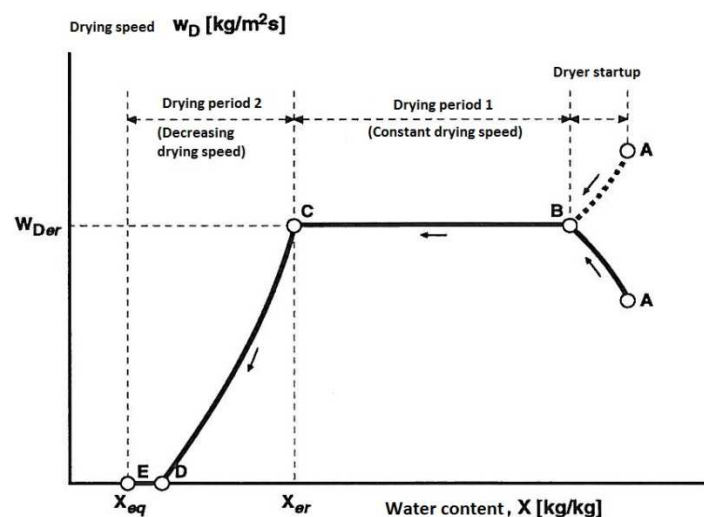


Figure 1.4-4 Drying progress

2. Designing and building the new CO₂ heat pump system

To build the new system with CO₂ as refrigerant new components made to withstand high pressures have to be used. All components in the system have been examined to determine which pressure class they belong to.

The chosen system for the prototype is shown in the process flow diagram in Figure 1.1-1. This figure illustrates the main components for the CO₂ and the air cycle.

The system design is supposed to be implemented in an existing chassis with limited space. Due to space limitations the design is without a low pressure receiver after the evaporator, instead the system is designed for 5 K overheat out of the evaporator. This will cause that some of the surface in the evaporator to be dry, thus the heat transfer efficiency will be reduced. The measurement of the refrigerant charge must be calculated and weighed into the system accurately. A charge higher than designed volume in the evaporator there will be risk of liquid compression that will damage the compressor, with a too low refrigerant charge the designed capacity of the evaporator will be reduced.

Due to the space limitations in the chassis, the prototype will have the compressor rigged outside; this was due to the outer dimensions of the compressor delivered.

Table 1.4-1 Equipment list

Equipment List				
Displayed Text	Description	Manufacturer	Material	Model
Compressor	CO2 compressor	Embraco	Iron	EK 6214 CD
Gas cooler	CO2 HX	Sierra	Cu/Al	Custom made
External gas cooler	CO2 HX	Sierra	Cu/Al	Custom made
Evaporator	CO2 HX	Sierra	Cu/Al	Custom made
Dryer components		ASKO		

Table 1.4-2 Valve and pipeline list

Valve and pipeline list				
Description	Valve Class	Manufacturer	Model	Number/length
Swagelok Tee		Swagelok	316L-400-3 Stainless Steel	#3
Manual metering valve	Cv 0.04	Swagelok	SS-31RS4	#1
Standard 2-way		Swagelok	SS-43GS4	#3
Pressure safety valve	Max t/p 121 C/ 338 Bar	Swagelok	SS-4R3A, High pressure	#1
CO2 tubes	(1/4)"		CO2 copper tubes	ca 3.7 meter
Capillary tube	Ø0.9 mm			ca 1 meter

2.1.Process of building

The system is based on the R134a casing, which means that the space to introduce the new CO₂ components is limited. The first job was to dismantle the original system and remove the original parts, including compressor, evaporator, main condenser, external condenser and expansion device. All of the old components are designed for a refrigerant working on a lower pressure, and could not be used for the carbon dioxide transcritical cycle where pressures above 100 Bara will be applied.

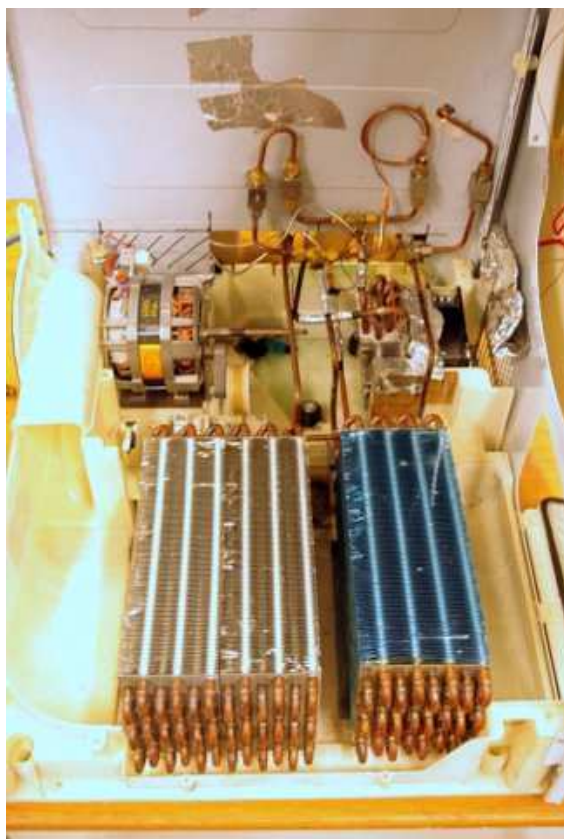


Figure 2.1-1 Complete system – inside



Figure 2.1-2 Complete system - outside

2.2.Component documentation

2.2.1. Compressor

General information

The compressor applied in the system is an Embraco EK6214 CD specially made for the CO₂ as refrigerant. The design is specially made to withstand the high pressures in the transcritical R744 cycle. Information regarding compressor running conditions is obtained from the compressor manufacturer Embraco.

All dimensions in millimeter [mm].

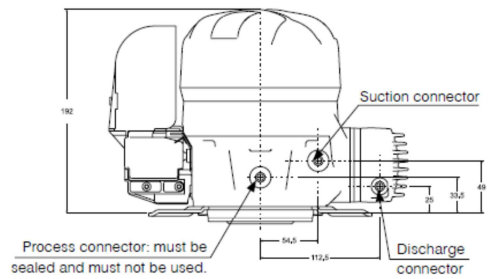


Figure 2 - Frontal view

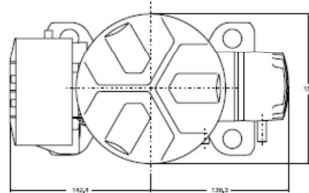


Figure 3 - Superior view

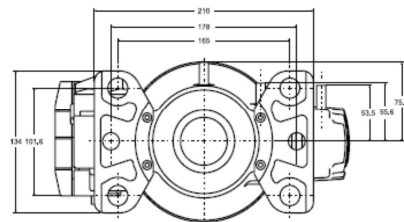


Figure 4 - Interior view

Figure 2.2-1 Compressor outer dimensions



Figure 2.2-2 Compressor EK 6214CD

Contamination of compressor

The compressor shall remain sealed until 10 minutes before welding to keep it clean, and avoid any dust, metal particles or solid residues in the system. To avoid residues cleaning of parts with dry air or nitrogen should be performed.

Table 2.2-1 Refrigerant purity degree specs

Purity Carbon Dioxide	99.95 % vol.
Water Content	Max 20 wtppm
Nitrogen	<5 ppm
Acid (Sulphur Dioxide)	0.1 wtppm

It is important that all the components are compatible with the refrigerant and the lubricant used in the compressor. Substances including chlorine, paraffin and silicone are not approved.

To avoid problems that may shorten the lifetime of the system it is important to apply components that are supplied internally, dried and properly sealed. All components should remain sealed until they are installed in the system.

If a moisture level above the limit is in the system it can cause some inconveniences for the system.

Table 2.2-2 Inconvenience caused by moisture in the system

1 Ice build-up	Reduces the cross-sectional area of the capillary tube, or expansion valve, up to their complete obstruction.
2 Acid build-up	Causes serious problems to the compressor and to the molecular sieve of the filter. Consequences: <ul style="list-style-type: none"> • Copper planting of valve plate, valve reeds, crankshaft bearings, etc. • Etching of electric motor insulation by acids, with burning of motor windings • Destruction of the filter with disintegration of molecular sieve and build-up of dusts. • Wear of reciprocating and rotating parts.
3 Oil contamination	Causes acidification and reduction of its lubricating power, with change of oil colour (brown). It can cause build-up of sludge, with subsequent poor lubrication of compressor.

It is critical to perform an evacuation of the system in order to ensure proper running of the refrigerating machine and to preserve the lifetime of the compressor. This will assure that the air and moisture levels are below the allowed limits.

The fact that the POE oils are highly hygroscopic the vacuum procedure requires great care. It is recommended for the system to be in vacuum on both sides with a vacuum level of 0.05 mbar for 10 minutes.

System refrigerant charge

The optimal way to determine the refrigerant charge of the system is to compare the R744 system to the old system using R134a. Generally R744 charge will be 35-50 % larger than for R134a system if the internal volume is kept the same. In this case the internal volume has changed some and correct procedure to charge the system must be followed.

The maximum amount of refrigerant charge in the system using this compressor is 500 g R744, if the system is approaching its maximum value, the risk of flooded start and liquid slugging is imminent.

The internal volume in the high-pressure side should be large enough to lead to a maximum density of 0.65 g/cm³ when all the refrigerant charge is distributed in this volume.

$$\text{Maximum density} = \frac{\text{Refrigerant charge}}{\text{High pressure side internal volume}} \text{ [g/cm}^3\text{]}$$

After the evacuating of the system it will be filled with the correct measured amount of refrigerant.

The refrigerant charge will be injected through a connection at the outlet of the evaporator. The expansion valve should be left open during the filling procedure and for 5 minutes after the filling is finished. Vapour phase refrigerant must be used to avoid liquid compression.

Table 2.2-3 System volume calculations

Volume location	Tube length	Tube diameter	Cross section area	Volume
	m	m	m ²	m ³
Evaporator	14,5	0,005	1,9635E-05	0,000284707
Gas cooler	21,74	0,005	1,9635E-05	0,000426864
External gas cooler	2,7	0,005	1,9635E-05	5,30144E-05
Tubes high pressure side	2,365	0,00435	1,48617E-05	3,51479E-05
Tubes low pressure side	1,35	0,00435	1,48617E-05	2,00633E-05
Volume low pressure side				0,000305
Volume high pressure side				0,000515
Total volume				0,000820

From the total volume of the system it is now possible to find the amount of refrigerant to charge the system with. The calculations are based on an evaporating pressure at 45 Bara and a gas cooling pressure at 100 Bara it was also assumed a temperature of 40 °C before throttling and isentropic efficiency of the compressor at 50%. Applying these boundary conditions the specific volume will be calculated to determine the amount of refrigerant in the system. From the data the average specific volume at the low and the high pressure side was used combined with the volume estimations.

Table 2.2-4 Refrigerant charge calculations

	Low pressure side	High pressure side	Total
Total volume [cm³]	305	515	820
Average specific volume [m³/kg]	0,00564	0,00394	
Total refrigerant charge [kg]	0,05585	0,146171	0,202

From the table it is shown that the refrigerant charge for the system will be 0.202 kg, when applying the formula for of maximum density set by the compressor manufacturer it gives a result of 0.25 g/cm³ which is well below the limit of 65 g/cm³.

Refrigerant filling procedure

- Evacuating the system
- Weighing the refrigerant
- Compressor running during the filling procedure

System standstill

Initially the refrigerant charge will be determined from the design conditions, however on the high pressure side of the cycle the internal volume is larger. This is due to a larger volume in the main gas cooler, and the extra volume from the external gas cooler and the mass flow sensor. Thus the refrigerant charge must be adjusted to meet the volume of the low pressure side of the system. With ambient temperatures lower than critical temperature of 31 °C, the refrigerant will be in saturated state. This must be considered in relation to the refrigerant charge in system standstill. With an amount of liquid higher than the internal volume on the low pressure side, liquid will drain into the compressor and cause damage once restarting. Hence the refrigerant charge determined

from the desired capacity must be adjusted to avoid this problem. When the system is in standstill after operation the refrigerant will eventually stabilize to the temperature of the surroundings. The system will be stored in a location with fairly stable temperature conditions; thus the refrigerant specific volume at saturated state has been calculated for temperatures from 25 and down to 15 °C.

Table 2.2-5 Refrigerant standstill saturated state conditions

Ambient temperature	Specific volume		Mass		
	Saturated liquid	Saturated gas	Mass liquid in evaporator	Mass gas - rest volume	Total mass volume
°C	m ³ /kg	m ³ /kg	kg	kg	kg
25	0,00140	0,00411	0,20331	0,13033	0,33364
24	0,00137	0,00431	0,20745	0,12407	0,33152
23	0,00135	0,00452	0,21126	0,11844	0,32970
22	0,00133	0,00472	0,21480	0,11331	0,32811
21	0,00131	0,00493	0,21812	0,10859	0,32672
20	0,00129	0,00513	0,22126	0,10423	0,32549
19	0,00127	0,00534	0,22423	0,10017	0,32440
18	0,00125	0,00555	0,22707	0,09637	0,32344
17	0,00124	0,00577	0,22978	0,09280	0,32258
16	0,00123	0,00598	0,23239	0,08944	0,32182
15	0,00121	0,00620	0,23489	0,08626	0,32115

Table 2.2-5 shows the standstill conditions of the CO₂ for various temperatures, the specific volume related to the internal volume of the evaporator. The total calculated refrigerant charge compared to the internal volume of the evaporator shows that the evaporator is large enough to store the full amount. The design of the system with the hot and the cold side of the system placed besides each other, there will most likely be some refrigerant that will condense in the gas coolers as well. This is another advantage to keep the liquid refrigerant away from the compressor.

Lubrication issues

Due to intrinsic characteristics, CO₂ compressors have higher oil circulation rate than that of regular HFC compressors. The compressor is delivered from the manufacturer containing polyester oil type with a kinematic viscosity of 68 cSt at 40 °C, where 1 cSt is a centistroke equals to 10⁻⁶ m²/s. The oil charge is 150 cm³ at delivery and this must not come below 100 cm³. In the lubrication process

under high pressure the oil will mix with the carbon dioxide in the system. The mixing of oil and refrigerant is highly dependent on the viscosity of the refrigerant which will be affected by the compressing temperature. Some of the oil will mix with the refrigerant and circulate in the system. To maintain a sufficient lubrication of the system it is critical that the oil in the system will return to the compressor.

Therefore it is very important to assure there is no oil trap in the system that can cause compressor failure. Top to down circulation is not recommended, if applicable: check the oil return to the compressor. Flow speed of less than 2 m/s is not recommended to force the oil to return to the compressor with the refrigerant. The chosen design of the external gas cooler (see. Figure 2.2-17) is the same as for the R134a system with a top to down circulation this can cause an oil trap. However the flow speed in the external gas cooler for CO₂ temperatures of supercritical gas will be above 2 m/s, this should be sufficiently high to return the oil to the compressor.

Maximum observed discharge pressure

Considering abnormal working conditions fan failure, gas cooler area reduction due to fouling, and/or expansion device failure. The maximum observed discharge pressure should not exceed 30 bar of the limit which is 120 Bara, to avoid any compressor failure a pressure relief valve is implemented in the system after the compressor, which will breach at 145 Bara.

System equalization

The time for the suction and the discharge pressure will take to equalize ranges from 3-6 minutes depending on the application. Compressor "off" -periods less than 5 minutes must be avoided when using capillary tubes, to allow proper equalization and for the PTC to cool down. For expansion valves it is important to check the values of allowable unbalanced pressures during start-up. It is recommended that the system equalizes right before starting the compressor in case of electronic controlling.

Table 2.2-6 Compressor boundary conditions

Maximum discharge pressure	120 bar
Maximum discharge temperature (measured 50 mm from discharge tube)	160 °C
Maximum temperature of electric motor stator windings	130 °C under normal running conditions 140 °C under tropical and extreme voltage conditions
Maximum compressor inlet temperature (measured 200 mm from far from the suction tube)	32 °C

The compressor working area is visualized in the compressor operating envelope, Figure 2.2-3 shows the limits of evaporating, condensing, ambient and return gas temperature. The compressor can only work within the limits of evaporating temperatures and discharge pressures defined by the dashed area.

If the compressor over time will operate outside the dashed area, it can cause early defects in the compressor.

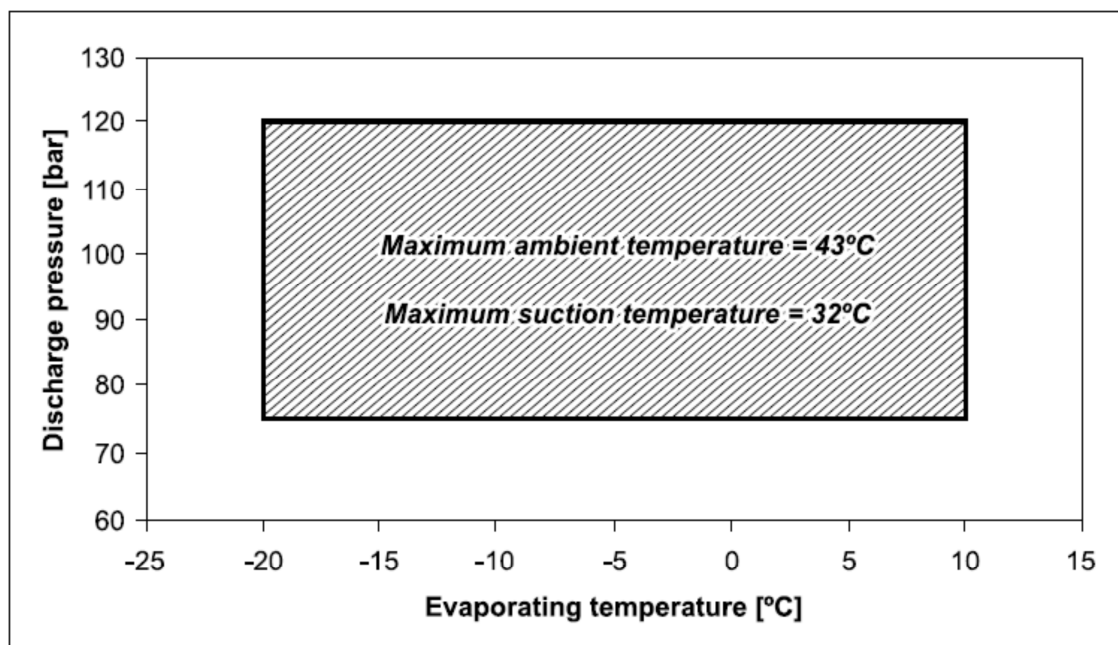


Figure 2.2-3 Compressor working envelope

Compressor power factor

The power factor by definition is the ratio between the power consumed doing work divided by the apparent power in volt-amperes. If the voltage and the amperage are in phase, the power is equal to the voltage multiplied with the amps. However if the voltage and the amperage are out of phase the product is “apparent power” measured in volt-amperes, while the actual power is of a smaller value. How much smaller the actual power is determined from how much the current and voltage is out of phase. In direct current circuits, since there are no reversal of current or voltage the power factor is always unity. In alternating current circuits with lagging current caused by inductive loads the power available is the product of the volts and ampere multiplied with the power factor.

Equation 2.2-1 shows how to calculate the power, P; with I as the current, R as resistance and PF as the power factor.

$$P = I^2 R \cdot PF$$

Equation 2.2-1 Power factor for single phase

All inductive devices such as motors, transformers and solenoid coils require magnetizing current to create the magnetic field for a device to operate. This magnetizing current is reactive and does not produce usable power, but the effect of the magnetic field is to cause the current drawn from the power line to lag the voltage. This is resulting in reactive power which is the product of reactive current and operating voltage. The great this reactive current, the greater are the reactive power and this reduces the power factor. (Copeland Corporation , 1994)

The motor to the compressor provided by Embraco will be tested for the power factor with a Hioki 3166 Clamp on Hitester. This instrument will also show the exact frequency and the power consumption of the compressor.

2.2.2. Heat exchangers

By designing the tube-finned heat exchangers both sides must be considered; the refrigerant side and the air side. For the air side the convective and the conductive heat transfers must be considered. The thermal resistance for the air include convective surface resistance and the fin surface to fin base conductive resistance. The conductivity depends on the geometrical design of the fin; mainly the thickness and the thermal conductivity of the material.

The heat exchangers used in this application will be a multipass cross-flow arrangement, but it will assume to be a perfect counter-flow heat exchanger.

The finned-tube heat exchangers have been designed using HXsim 2007 which is SINTEF produced software for heat exchanger simulation. The software consider several critical factors for the optimal design of heat exchangers, these include specific data on the fin and tube configuration.

The nature of this drying process with the increasing temperature through the cycle is a limitation of the software. The input data is static and the same is the analysis, thus the full development of temperature and humidity in the cycle cannot be modelled directly. To solve this best possible, air data from the R134a cycle has been applied in some reference points to find different critical conditions.

The heat exchangers include an evaporator, main gas cooler and an external gas cooler. It was performed simulations based on data results from the R134a system presented in Figure 5.1-1 and Figure 5.1-2, where the air temperature and the humidity are shown respectively. During the drying cycle will the air temperature at the outlet of the gas cooler or the inlet of the drum increase while the relative humidity will decrease. Due to the constant change of temperature and humidity in the air cycle, the optimal design point of the cycle will not maintain through the cycle. The simulation software has been applied for many set points during the drying period to find a design that will be as optimal as possible.

2.2.2.1. Main gas cooler

The main gas cooler will heat the air that has been dehumidified in the evaporator. In the beginning of the drying cycle the air inlet conditions will be low temperature and high relative humidity. During the drying cycle the moisture will be extracted from the fabric and the inlet temperature will increase.

Table 2.2-7 Main gas cooler geometrical data

Main gas cooler				
Main dimensions	unit	Tube bundle and lamellas		Unit
Core length	0,302 m	Tube diameter(s)	7,00/5.00	mm
Finned tube length	0,248 m	Fin thickness	1,2	mm
Core height	0,085 m	Fin spacing	2,69	mm
Core depth	0,204 m	Fin material	Aluminium	
Air side area	2,91 m ²	Tube material	Copper	
Tube inner area	0,351 m ²	Tube arrangement	Staggered up	
Area ratio	10,37 -	Number of vertical tubes	6	
		Vertical tube pitch	13	mm
Total tube length	24,74 m	Number of horizontal tubes	12	
		Horizontal tube pitch	17	mm

The heat exchanger has been tested with pressures from 80-120 Bara with varying inlet temperatures depending on the discharge pressure. The temperatures have been estimated with a compressor isentropic efficiency of 50% and evaporating temperature of 10 °C with 5 K overheat. The internal air flow in the simulations is the same as for the R134a system; 0.051 m³/s.

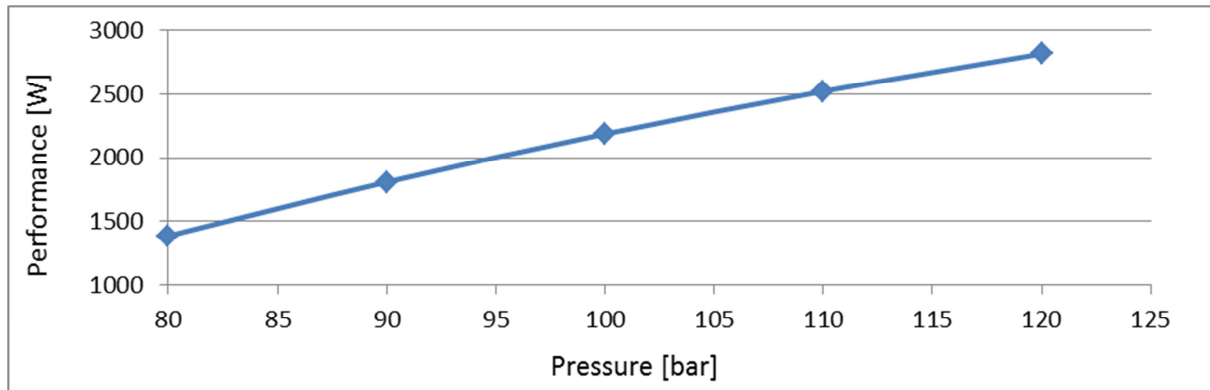


Figure 2.2-4 Gas cooler simulated performance

With a high gas cooler pressure and thus a high temperature the performance of the gas cooler will increase due to the increased heat energy in the refrigerant.

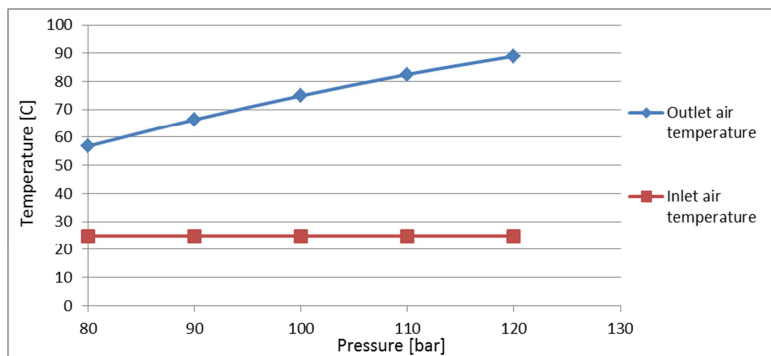


Figure 2.2-5 Gas cooler inlet and outlet air temperatures

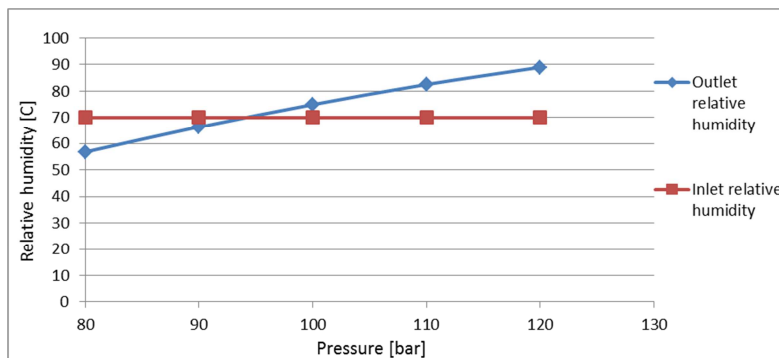


Figure 2.2-6 Gas cooler inlet and outlet relative humidity

With increasing pressure the gas cooler air outlet temperature will increase while the relative humidity will decrease. Air with higher temperature will be able to contain more humidity than colder air; however there are limitations on how hot the air can be due to damage to the fabric.

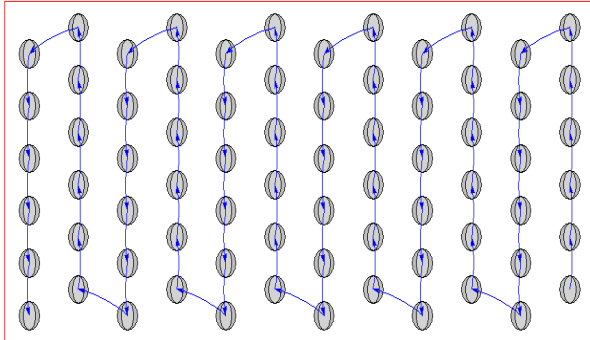


Figure 2.2-7 Main gas cooler flow distribution

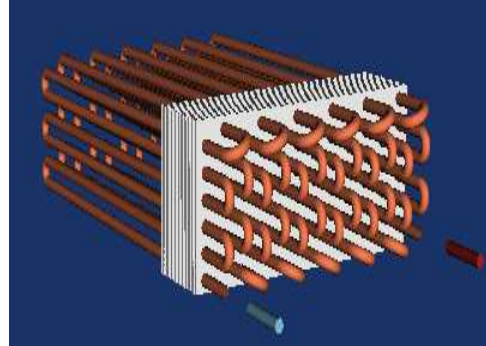


Figure 2.2-8 Gas cooler HXsim 2007 visualisation

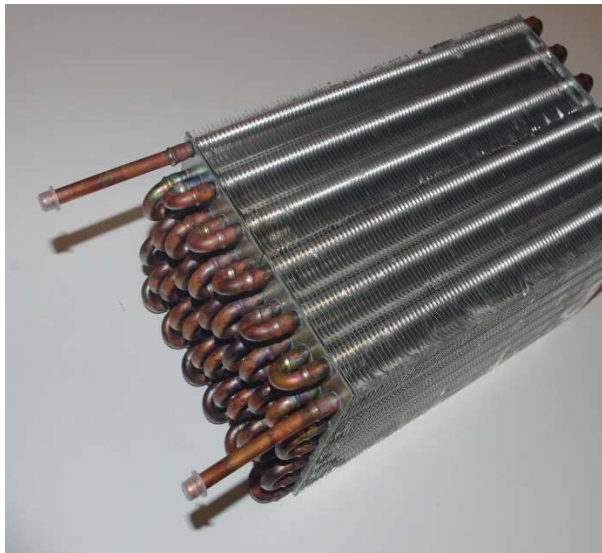


Figure 2.2-9 Main gas cooler #1



Figure 2.2-10 Main gas cooler #2

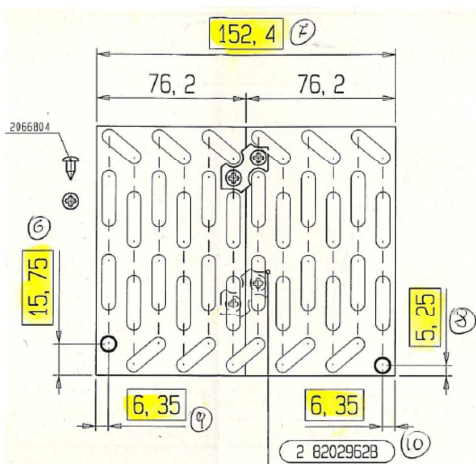


Figure 2.2-11 Main gas cooler manufacturer data #1

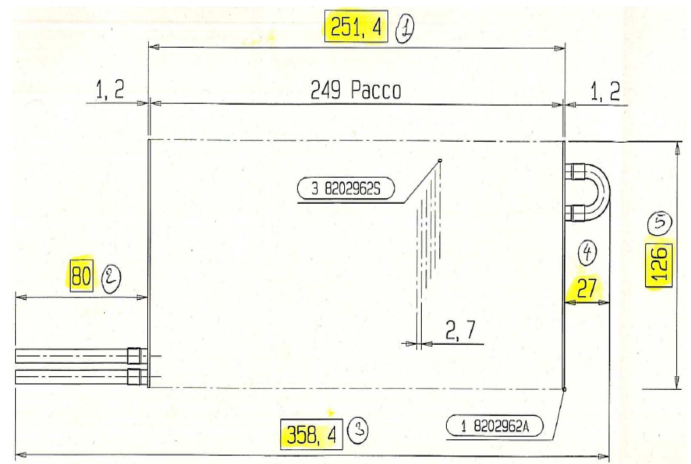


Figure 2.2-12 Main gas cooler manufacturer data #2

2.2.2.2. External gas cooler

The external gas cooler installed in the system will be placed after the main gas cooler to optimize the cooling of the refrigerant. The heat exchanger is placed close to the cabinet wall and ambient air will cool the refrigerant to decrease the throttling losses in the cycle. Figure 2.2-13 shows how the effect of the external gas cooler will decrease the temperature before throttling. The solid line represents a throttling temperature of 35 °C and the dotted line 40 °C. The extra Δh will increase the capacity and thus the COP of the system.

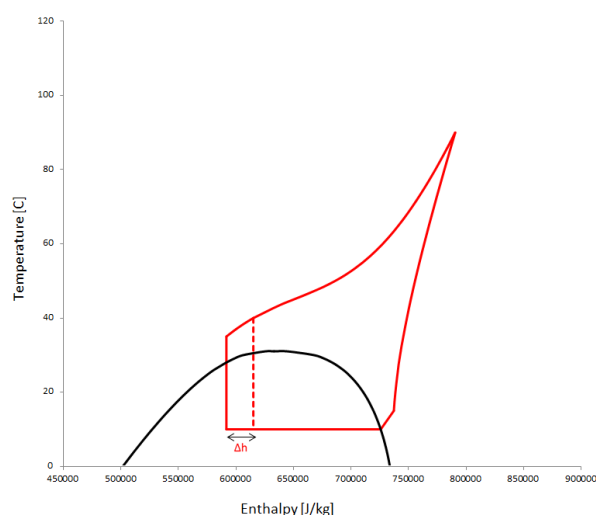


Figure 2.2-13 External gas cooler effect

Table 2.2-8 External gas cooler geometry

External gas cooler					
Main dimensions		unit	Tube bundle and lamellas		Unit
Core length	0,169	m	Tube diameter(s)	7,00/5.00	mm
Finned tube length	0,117	m	Fin thickness		0,12 mm
Core height	0,084	m	Fin spacing		2,8 mm
Core depth	0,051	m	Fin material	Aluminium	
Air side area	0,35	m ²	Tube material	Copper	
Tube inner area	0,051	m ²	Tube arrangement	Staggered down	
Area ratio	11,83	-	Number of vertical tubes	4	
			Vertical tube pitch	21	mm
Total tube length	2,7	m	Number of horizontal tubes	4	
			Horizontal tube pitch	12,7	mm

The figure below indicates how the heat exchanger will behave related to the operating pressure. The ambient conditions are set to 23 °C and a relative humidity of 55 %, the results obtained from the simulation will be compared to the results from the experiments.

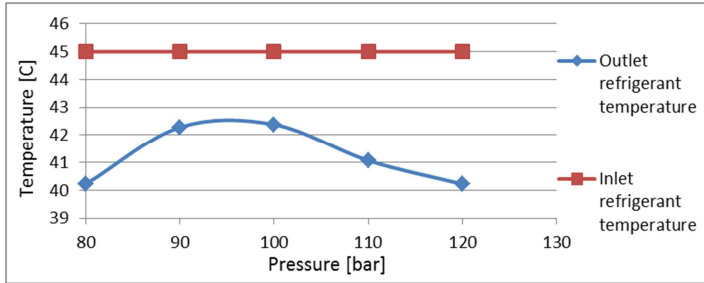


Figure 2.2-14 External gas cooler inlet and outlet refrigerant temperature

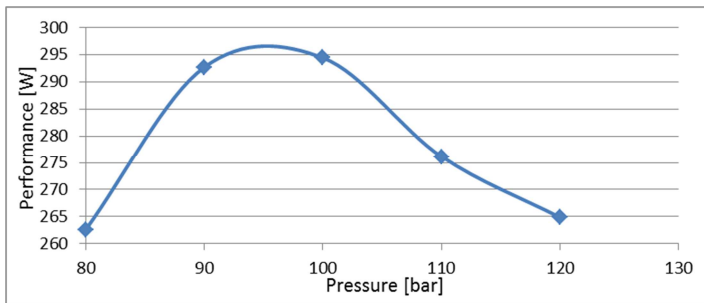


Figure 2.2-15 External gas cooler performance

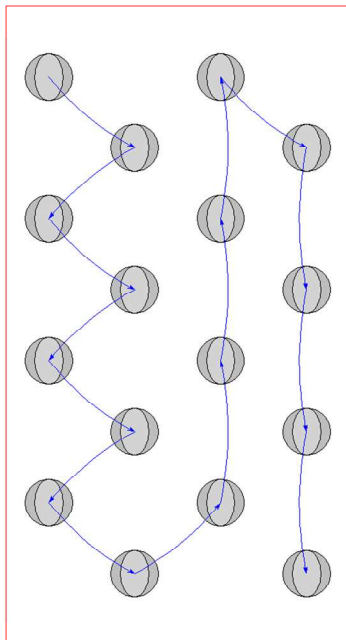


Figure 2.2-16 Gas cooler HXsim 2007 flow distribution

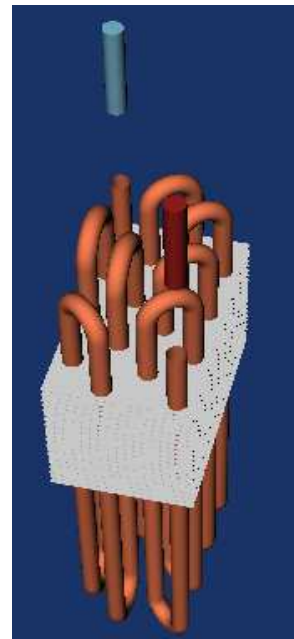


Figure 2.2-17 Gas cooler HXsim 2007 visualisation



Figure 2.2-18 External gas cooler #1

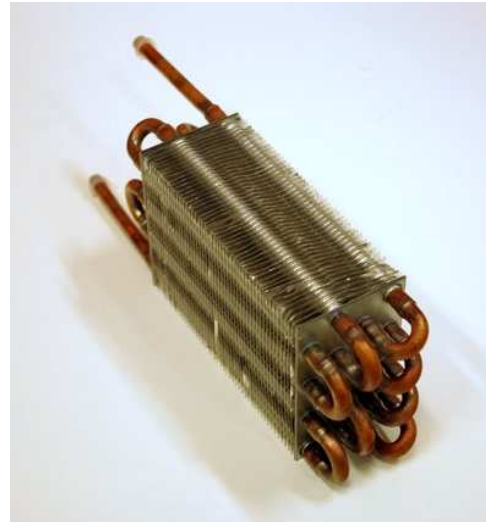


Figure 2.2-19 External gas cooler #2

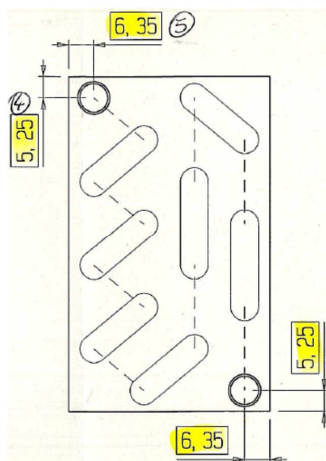


Figure 2.2-20 External gas cooler manufacturer data #1

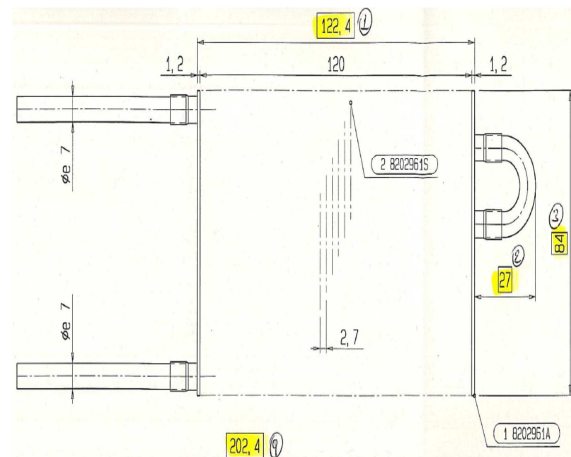


Figure 2.2-21 External gas cooler manufacturer data #2

2.2.2.3. Evaporator

The evaporator where the refrigerant should evaporate inside the tubes need to be designed carefully. Since the CO₂ has a high density compared to traditional refrigerants, this means a smaller mass flow for the same capacity. The flow pattern in the tubes for carbon dioxide will be different than the traditional refrigerants. It is important that the surface in the evaporator is wet so a good heat transfer coefficient can be obtained. In the evaporator the annular flow pattern is usually the preferred flow pattern where the velocity of the fluid will cover the inside of the tube surface.

If a traditional evaporator with larger tube diameter is used the flow pattern will be less ideal, the liquid CO₂ will move like a river in the bottom of the tube and less of the surface will be wet thus a

smaller heat transfer coefficient. For this prototype a special designed evaporator is used; the tubes are smaller than the R134a evaporator and the velocity will therefore increase to a more preferred level.

The main fan blows the humid air flow from the wet clothes and through the fins of the evaporator. When the air encounters with the cold fins of the evaporator the water in the air will condense on the surface of the fins. To improve the water drainage away from the evaporator a hydrophobic coating covers the surface of the aluminium fins. This will make the water to form drops on the fin surface instead of water film. The drops will easily be drained away from the fins to be pumped to the water storage.

A challenge of the design of the evaporator for a dryer application is that the system will not be in equilibrium during the cycle. When the temperature of the air that leaves the drum increase, more of the surface will be dried out, i.e. the evaporators' efficiency will decrease. The amount of refrigerant charge is important to determine correctly, so the overheat temperature do not vary too much.

With the constant pressure drop through the capillary tube and the increasing temperatures of the CO₂, it will cause both the evaporation and gas cooler pressure to increase during the drying cycle.

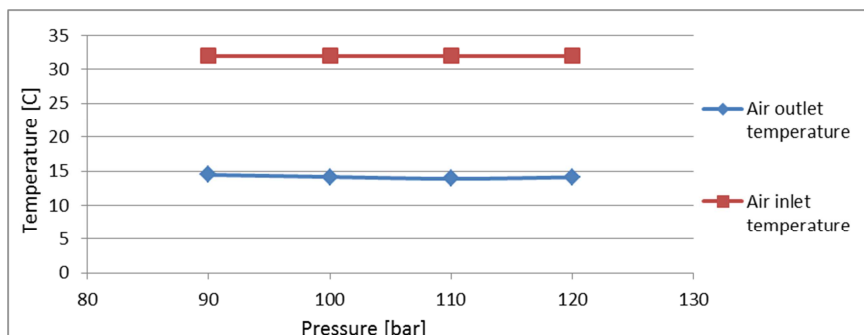


Figure 2.2-22 Evaporator air temperature

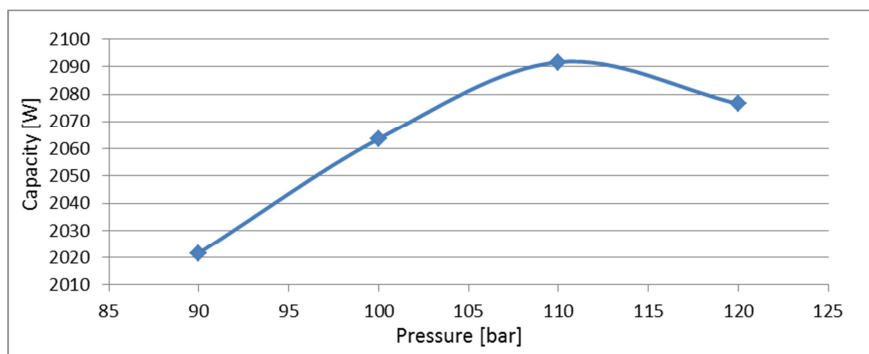


Figure 2.2-23 Evaporator capacity

Table 2.2-9 Evaporator geometry

Evaporator				
Main dimensions	unit	Tube bundle and lamellas		Unit
Core length	0,302 m	Tube diameter(s)	7,00/5.00	mm
Finned tube length	0,25 m	Fin thickness	0,15	mm
Core height	0,095 m	Fin spacing	2,69	mm
Core depth	0,136 m	Fin material	Aluminium(coated)	
Air side area	2,3 m ²	Tube material	Copper	
Tube inner area	0,245 m ²	Tube arrangement	Staggered down	
Area ratio	12,19 -	Number of vertical tubes	6	
		Vertical tube pitch	15,75	mm
Total tube length	14,5 m	Number of horizontal tubes	8	
		Horizontal tube pitch	17	mm

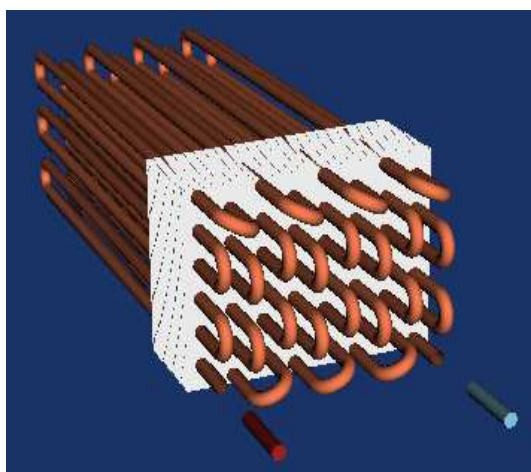


Figure 2.2-24 Evaporator HXsim 2007 visualisation

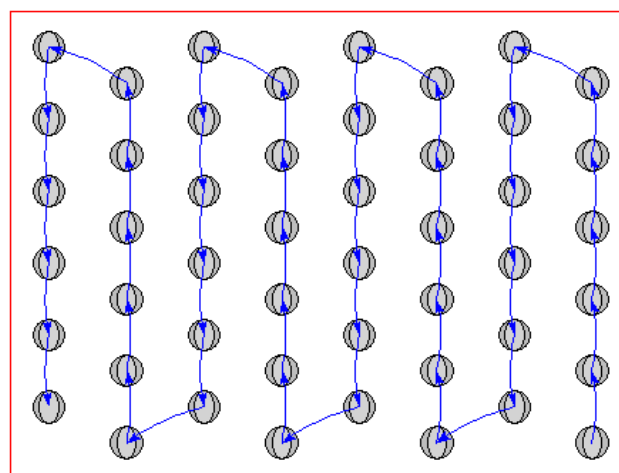


Figure 2.2-25 Gas cooler HXsim 2007 flow distribution

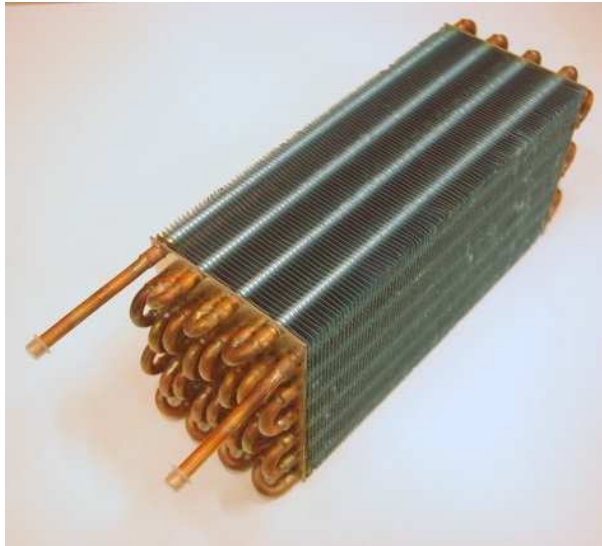


Figure 2.2-26 Evaporator #1



Figure 2.2-27 Evaporator #2

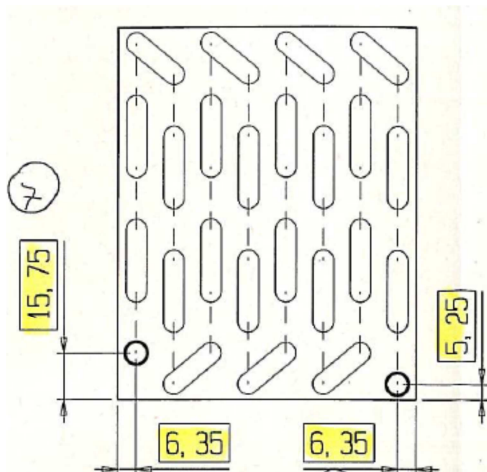


Figure 2.2-28 Evaporator manufacturer data #1

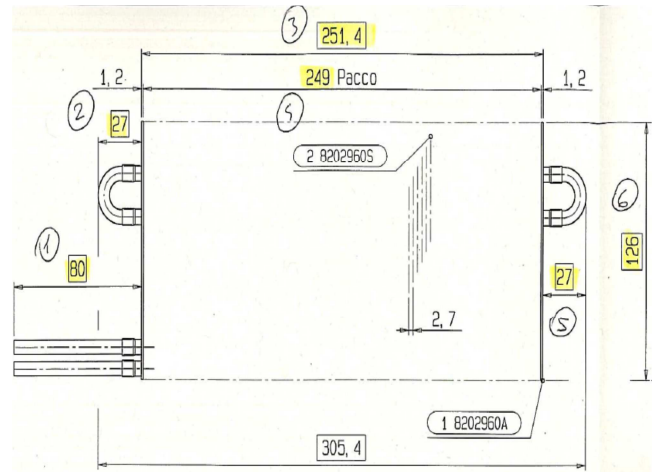


Figure 2.2-29 Evaporator manufacturer data #2

2.2.3. Expansion devices

In a traditional heat pump the condenser pressure is directly linked with heat transfer characteristics of the condenser and the temperature of the fluid it rejects heat to. In a transcritical cycle the upper cycle pressure depends mainly on the balance between the compressor capacity and the flow resistance in the throttling valve.

When evaporating temperature maintains constant the COP of the system will depend on the upper cycle pressure. This means that the throttling valves' job is to feed the evaporator with sufficient amount of refrigerant for optimal energy efficiency.

2.2.3.1. Manual throttling valve

When sizing the throttling valve the most important factor to consider is the flow that the valve can provide. The valve is sized from a correlation given in (Swagelok, 2007) which helps to determine the required size of the valve compared to the flow.

The correlation which is applied is designed for air with ideal gas properties; where temperature, volume and pressure are proportional. All the formulas are adapted from ISA S75.01.

For a fixed orifice it is a simple calculation including the size and shape of the orifice, the diameter of the pipe and the fluid density. With this information it is an easy calculation to determine the pressure drop across the orifice shown in Figure 2.2-30.

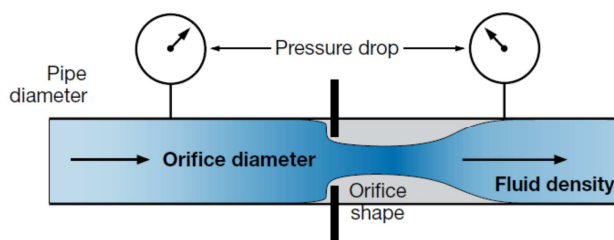


Figure 2.2-30 Flow rate through a fixed orifice

However to determine the pressure drop across a valve the flow pattern will adjust to be slightly more complex. The changes of angle and size in the valve will influence the flow; therefore we need to know the dimensions of the valve as well. The calculations have been simplified by applying the flow coefficient, C_v , which combines the effect of all flow restrictions in the valve into a single number.

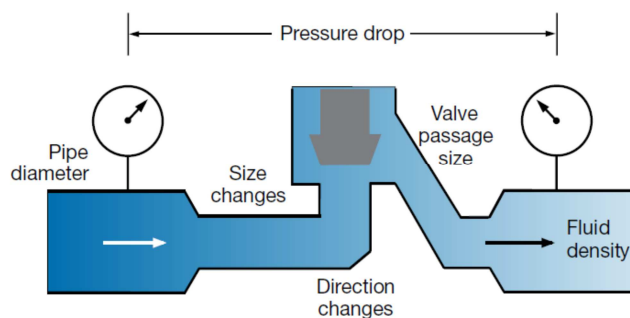


Figure 2.2-31 Valve flow rate calculations

To determine a valve for gas flow, the calculation must be considered for high and low pressure drop flow.

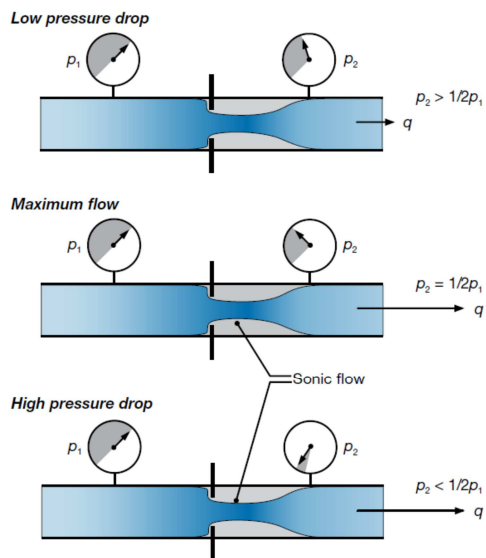


Figure 2.2-32 High and low pressure drop flow

The basic orifice meter illustrates difference in flow conditions for high and low pressure drops. A low pressure drop is defined as where the outlet pressure is greater than half of the inlet pressure. The outlet pressure restricts flow through the orifice: as outlet pressure decreases, flow and velocity of the fluid leaving the orifice increases.

To determine the flow coefficient the following values have been applied.

Table 2.2-10 Flow calculation symbols

Symbols used in flow calculations	Applied value	Units
C_v = flow coefficient	Table 2.2-12	
q = flow rate	Table 2.2-12	Std L/min
p_1 = inlet pressure (absolute pressure)	80-100 bar	Bar
p_2 = inlet pressure (absolute pressure)	45 bar	Bar
Δp = pressure drop ($p_1 - p_2$)		Bar
G_g = gas specific gravity (air = 1.0)	1.57	
N_1, N_2 = Constants for units	6950	
T_1 = Absolute temperature	313	K

For low pressure drop flow the following equation is used, where the C_v -value is obtained to find a suitable expansion valve.

$$q = N_2 C_v p_1 \left(1 - \frac{2\Delta p}{3p_1}\right) \sqrt{\frac{\Delta p}{p_1 G_g T_1}} \quad p_2 > 1/2 p_1$$

Equation 2.2-2 Low pressure drop flow

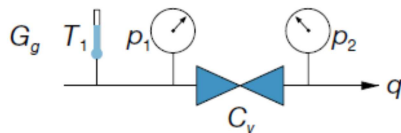


Figure 2.2-33 Low pressure drop flow

When the outlet pressure is decreased to the half of the inlet pressure, the gas leaves the orifice at the speed of sound, which is its maximum velocity. This flow condition determines the maximum flow rate, which also is known as the choked flow or the critical flow. A further reduction in the outlet pressure will not increase the velocity of the flow; thus high pressure drop flow only depends on the inlet pressure and not the outlet pressure.

To calculate the high pressure drop flow the equation will be a bit simpler because the flow only depends on the inlet pressure and temperature, flow coefficient and the specific gravity of the gas.

$$q = 0.471 N_2 C_v p_1 \sqrt{\frac{1}{G_g T_1}} \quad p_2 < 1/2 p_1$$

Equation 2.2-3 High pressure drop flow

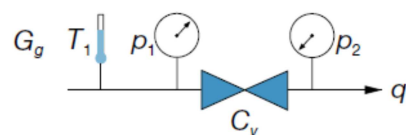


Figure 2.2-34 High pressure drop flow

For this system the pressure drop will be both low and high, therefore both correlations have been considered to determine the correct throttle valve.

The unit of the flow rate is given in standard L/min, ideal gas law has been applied manipulate the kg/s to the suitable unit. A mole weight of CO₂ of 44.01 g/mole is used in the calculation.

Table 2.2-11 Ideal gas law input data

Constant/variable	Value	Unit
Ideal gas constant, R	0.08257	Latm./moleK
Temperature	298	K
Pressure	1	Atm.
# Mole	27.2109	mole

$$PV = nRT$$

Equation 2.2-4 Ideal gas law

From the ideal gas law and the given values above the standard volume flow of CO₂ is calculated, and thus the C_v-value is estimated.

Table 2.2-12 Flow coefficient, C_v-calculations (p₁ = 100 bar, p₂ = 45 bar)

High pressure drop flow		
Mass flow	Volume flow	Flow coefficient, C _v
kg/s	std L/min	
0,015	499,0433367	0,033361874
0,016	532,3128925	0,035585999
0,017	565,5824482	0,037810124
0,018	598,852004	0,040034248
0,019	632,1215598	0,042258373
0,020	665,3911156	0,044482498

The chosen valve is a metering valve produced by Swagelok for medium-flow systems, which is designed for a C_v value up to 0.04. A consideration of the applicability of the valve will be considered in the result section.



Figure 2.2-35 Swagelok SS-31RS4

Table 2.2-13 Swagelok SS-31RS4

General information Swagelok SS-31RS4	
Body material	316 Stainless steel
Connection 1 size	¼ in.
Connection 1 type	Swagelok® Tube Fitting
Maximum flow	$C_v - 0.04$

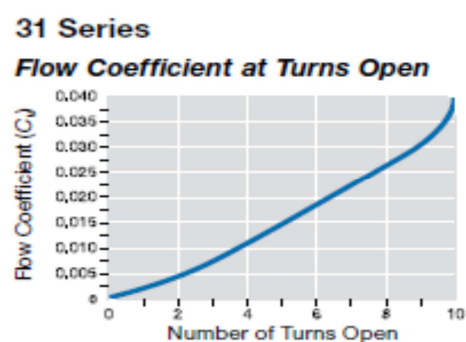


Figure 2.2-36 Flow coefficient vs. turns to open

2.2.3.2. Capillary tube dimensioning

The capillary tube are the most common throttling device for low capacity systems, it is cheap, simple and reliable. A capillary tube is not able to vary its flow factor and thus the equilibrium between the flow rate through the compressor and the capillary tube can only be reached due to self-adjusting action of the refrigeration system. There is a similarity of the traditional system to the transcritical one; the new equilibrium mainly relies on the variation on the fluid amount in the condenser or the gas cooler. The effect in a subcritical cycle is a flooding of the condenser, while in the transcritical process the upper cycle pressure will increase. When the fluid temperature at the outlet of the gas cooler increase, the capacity of the capillary tube tends to decrease and thus the gas cooler pressure will increase. The advantage that the capillary tube makes the system to be self-adjusting is in its favour to improve energy efficiency, however there is no certainty that the operating conditions remain close to the optimal ones.

The dimensioning of the capillary tube is based on an article from (Madsen, et al., 2005). For an optimal sizing of the capillary tube, it should be performed in a laboratory following an appropriate procedure, in order to obtain the best working conditions and to avoid the return of liquid to the compressor.

It is not recommended from the compressor manufacturer to apply capillary tubes with an internal diameter smaller than 0.6 mm.

Throttling with capillary tubes have been used for a long time for low pressure systems, but according to (Madsen, et al., 2005) with their study on capillary tubes for transcritical CO₂ it is not the case. They based their study on theoretical calculations from Friedel's and Colebrook's correlations on pressure drop and experimental tests that the capillary tubes. The capillary tubes was especially interesting when the evaporation pressure is stable and the gas cooler pressure varies no more than +-10 K from the design condition.

To estimate the required length of the capillary tube (Madsen, et al., 2005) procedure will be followed. The length of the capillary tube must be calculated by dividing it for one and two-phase flow, and finally sum up.

The friction factor of the capillary tube is calculated from Equation 2.2-5; this is assumed for single phase flow.

$$f_{SP} = -2.0 \left[\log \left(\frac{\varepsilon/d_i}{3.7} + \frac{5.74}{Re^{0.9}} \right) \right]^{-2}$$

Equation 2.2-5 Miller's friction factor correlation

Mean velocity is used to find the Reynolds number of the pressure drop, this is found from the mass flow, cross section area and the density of the flow.

$$\Delta L_{SP} = 2 \cdot d_i \cdot \Delta P \cdot \frac{1}{f_{SP} \cdot V^2 \cdot \rho}$$

Equation 2.2-6 Capillary tube length

To take into account for the change in properties of the CO₂ the pressure difference between the high pressure after the gas cooler, and the pressure on the saturation line is divided into 100 steps. For each step, the length of the tube is calculated and finally summed up.

$$L_{SP} = \sum_{i=0}^{100} \Delta L_{SP}$$

Equation 2.2-7 Sum of tube intervals

Design conditions for the capillary tube in the single phase region show that the

When the flow enters the two phase region another calculation must precede.

$$M_{ref} = \frac{\dot{m}_{ref}}{A} = \frac{4\dot{m}_{ref}}{\pi \cdot d_i^2}$$

Equation 2.2-8 Mass flux

$$f_l = 0.25 \left[\log \left(\frac{\varepsilon/d_i}{3.7} + \frac{5.74}{Re_l^{0.9}} \right) \right]^{-2}$$

Equation 2.2-9 Liquid friction factor

$$f_g = 0.25 \left[\log \left(\frac{\varepsilon/d_i}{3.7} + \frac{5.74}{Re_g^{0.9}} \right) \right]^{-2}$$

Equation 2.2-10 Gas friction factor

$$\Phi^2 = G + \frac{3.21 \cdot F \cdot H}{Fr_h^{0.045} \cdot We_h^{0.035}}$$

Equation 2.2-11 Multiphase flow coefficient

Where the coefficients G, F and H are represented in the three equations below:

$$G = (1 - x)^2 + x^2 \frac{\rho_l f_g}{\rho_g f_l}$$

$$F = x^{0.78} (1 - x)^{0.224}$$

$$H = \left(\frac{\eta_g}{\eta_l} \right)^{0.91} \left(\frac{\eta_g}{\eta_l} \right)^{0.19} \left(1 - \frac{\eta_g}{\eta_l} \right)^{0.7}$$

$$\rho_h = \frac{1}{\left(\frac{1}{\rho_g} + \frac{1 - x}{\rho_l} \right)}$$

$$Fr_h = \frac{M_{ref}^2}{g \cdot d_i \cdot \rho_h^2}$$

Equation 2.2-12 Froude number

$$We_h = \frac{M_{ref}^2 d_i}{\sigma \cdot \rho_h}$$

Equation 2.2-13 Weber number

$$\Delta L_{TP} = \frac{\Delta p \cdot 2 \cdot \rho_l \cdot d_i}{f_l \cdot M_{ref}^2 \Phi^2}$$

Equation 2.2-14 Two phase throttling length

$$L_{TP} = \sum_i^{80} \Delta L_{TP}$$

Equation 2.2-15 Sum of two-phase throttling length

When the length of the tube for the single and the two-phase region has been calculated, they are summed up to make the total length of the capillary tube.

From the calculations based on Equation 2.2-5 to Equation 2.2-15 the length of the capillary tube has been estimated. The system is designed for a flow rate of 0.015 kg/s and a pressure drop from 100 Bara in the gas cooler to 45 Bara in the evaporator.

By altering the flow rate through the system the effect on the length of the capillary tube is rather large. By increasing the flow rate from 0.015 kg/s to 0.020 kg/s the length will decrease by 28%. Another important factor the estimation of the length of the capillary tube is the relation inner diameter to the surface roughness. If the inner diameter is changed from 0.9 mm to 1 mm inner diameter the length will be changed with 33 %. The capillary tube used in the first prototype will be based on the numbers in the table below.

Table 2.2-14 Capillary tube data

Input variables	value	Unit
Inlet pressure	100	bar
Outlet pressure	45	bar
Mass flow	0,015	kg/s
Tube inner diameter	0,0009	m
Inlet temperature	40	°C
Surface roughness	0,0000005	m
Calculated values		
Flow area	6,36E-07	m ²
Enthalpy	615131,408	J/kgK
Surface tension/diameter	0,000556	
Mass flux	23578,51009	kg/m ² s
Tube total length	0,647087297	m
Single phase length	0,177499539	m
Two-phase length	0,469587758	m

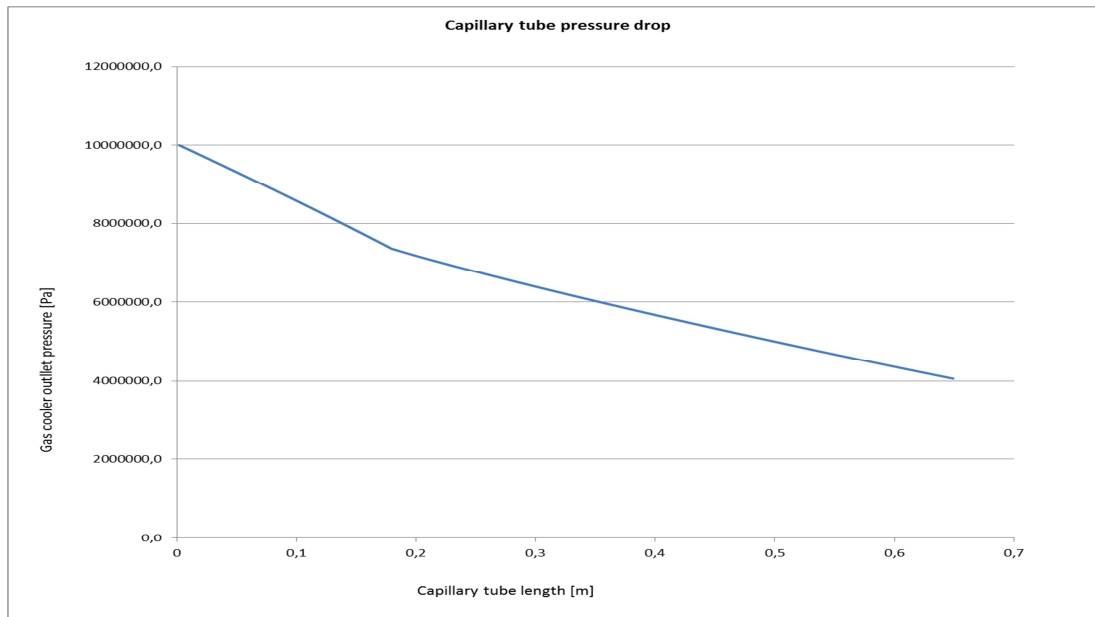


Figure 2.2-37 Capillary tube pressure drop

2.2.4. Tubes and fittings

The system is built with ¼ inch outer diameter tubes where the components are connected with brazing and with Swagelok fittings. The inner diameter will be estimated on the base of the outer diameter and the wall thickness.

$$d_i = d_o - 2\delta_w$$

Equation 2.2-16 Inner diameter

With ¼ inch is 6.35 mm and a wall thickness of 1 mm, thus the inner diameter will be 4.35 mm.

During the brazing of the connectors on the compressors copper plated steel tubes; two important notes must be followed.

- Do not allow the torch flame to reach the housing during the welding of the compressor tubes, in order to avoid overheating, damages to welding, and oil carbonization on the compressor internal walls.
- Do not allow the torch flame to approach the hermetic terminal in order to avoid the cracking of the glass insulating material of the three pins and subsequent gas leaks.

The tube connections to the compressor and to the heat exchangers will be welded with 38% silver content welding material. To limit internal contamination by de-oxidizing flux, it is suggested by Embraco to apply small quantities of de-oxidizer on the connection tube after connecting it to the

compressor tube. Also to avoid formation of oxides it is recommended to blow nitrogen through the tubes while welding.

All connections must be welded by professionals and be checked for leakages. CO₂ do have larger risk of leakages than other refrigerants due to its low molecular size and the high working pressures. Procedures suitable for the system will be performed to obtain any leakages in the system.

Leakage control

To keep the system running normal for a lifetime great attention to must be paid to installation. One of the most important factors is the absence of leakages. Estimations say that a 10% leakage during a period of 10 years will still allow for proper running of the refrigeration system. Since the system is a prototype the running lifetime will not be as long as for a commercial product. However to be able to obtain reliable results it is important that the system does not leak.

All of the heat exchangers have been tested by the manufacturer with 183 Bara and leakages proven in all tube connections.

First the system with the compressor disconnected was tested with pressures up to 160 Bara; this revealed some leakages in connections which were replaced, and the system was pressurized to the same pressure again.

The system with all components included was filled with nitrogen at 100 Bara; during the first hour the pressure decreased to 99 Bara, and for the next 14 hours to 98 Bara.

Reasons for the pressure drop can be:

- High pressure nitrogen mixes with the oil charge in the compressor.
- Minor leakages

However the small change in pressure is at a satisfying level.

3. Instrumentation and plan for experimental tests

During the experiments process' COP, SMER and total energy use the value should be calculated; therefore it must be measurements both for the CO₂ cycle and the air cycle. Additionally the input power to the system will be monitored. The signals from the instrumentation will be processed and then visualized in LabView. All of the instruments' signal wires are collected into a locker containing all electrical connections. This way it is easy to keep order and track of the signals, and a source of measurement error can be eliminated.



Figure 2.2-1 Electrical connections and instrumentation locker

3.1. Instrument overview

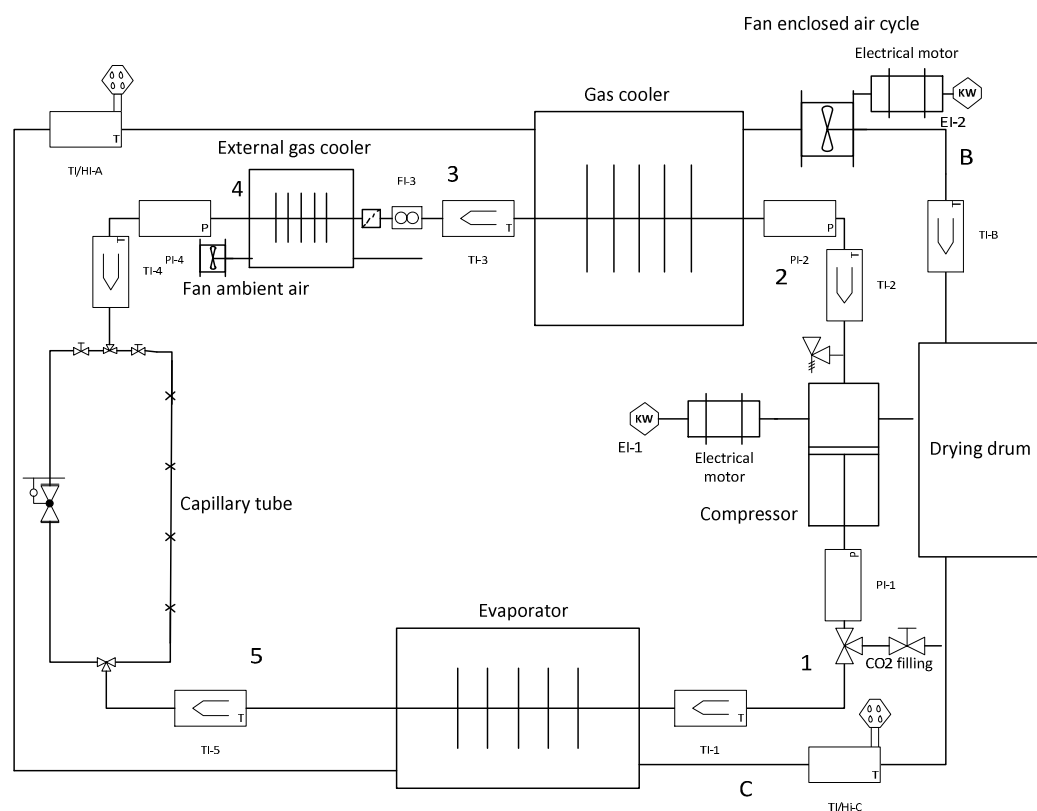


Figure 3.1-1 Instrument overview

Table 3.1-1 Instrument list

Instrument List					
Displayed Text	Description	Connection Type	Output signal	Manufacturer	Model
FI-3	Coriolis Mass flowmeter with fast response	8 mm	4-20 mA	RHEOINK	RHM04
PI-1	Pressure sensor	(1/8)"	0.4-2.0 V	Druck	PTX 1400
PI-2	Pressure sensor	(1/8)"	0.8-4.0 V	Druck	PTX 1400
PI-4	Pressure sensor	(1/8)"	4-20 mA	Druck	PTX 510-00
TI-1	Thermocouple	Outer tube surface		National instruments	9211
TI-2	Thermocouple	Outer tube surface		National instruments	9211
TI-2a	Thermocouple	In air cycle		National instruments	9211
TI-3	Thermocouple	Outer tube surface		National instruments	9211
TI-4	Thermocouple	Outer tube surface		National Instruments	9211
TI-5	Thermocouple	Outer tube surface		National Instruments	9211
TI/Hi-A	Temp and humidity transmitter	In air cycle		KIMO	AMI 300
TI/Hi-C	Temp and humidity transmitter	In air cycle		Vaisala	HMP235
EI-1	Wattmeter	Compressor	4-20 ma	M-system CO Ltd	LWT-24A1-H
EI-2	Wattmeter	Drum power supply	4-20 mA	M-system CO Ltd	LWT-24A1-H

3.1.1. Temperature measurement

The temperature at the CO₂ will be measured with thermocouple elements; these will be wound around the copper tube, outside a thin layer of electrical insulation tape to avoid electrical contact points. Outside the thermocouple wire aluminium tape maintain the connection of the wire along

the tube surface, to obtain as accurate measurements as possible. A layer of thermal insulation taped outside the thermocouple wire to avoid any effect from the ambient temperature.

The thermocouple wire applied is T-type (copper-constantan) and is suited for measurements in the range from -200 to 350 °C of range. Type T-thermocouples have a sensitivity of about 43 $\mu\text{V}/^\circ\text{C}$.

(Thermometrics - Precision Temperature Sensors)



Figure 3.1-2 T-type thermocouple

Key features

- High accuracy/performance
- Built-in-signal conditioning for direct connection to sensors and industrial devices
- LabVIEW compatible

Table 3.1-2 Thermocouple specifications

Detailed specification	
Input characteristic	
Number of channels	4 thermocouple channels, 1 internal autozero channel, 1 internal cold-junction compensation channel
ADC resolution	24 bits
Type of ADC	Delta-Sigma
Voltage measurement range	± 80 mV
Temperature measurement ranges	Works over temperature ranges defined by NIST (J, K, T, E, N, B, R, S thermocouple types)
Conversion time	70 ms per channel; 420 ms total for all channels including the autozero and cold-junction channels
Channel-to-COM	± 1.5 V
COM-to-earth ground	± 250 V

Overvoltage protection	±30 V between any input and COM
Differential input impedance	20 MΩ
Input current	50 nA
Gain error	0.05% max at 25 °C, 0.06% typ at -40 to 70 °C, 0.1% max at -40 to 70 °C
Offset error (with autozero channel on)	15 μV typ, 20 μV max
Gain error from source impedance	Add 0.05 ppm per Ω when source impedance >50 Ω
Offset error from source impedance	Add 0.05 μV typ, 0.07 μV max per Ω source impedance >50 Ω
Cold-junction compensation sensor accuracy	
0 to 70 °C	0.6 °C typ, 1.3 °C max
Temperature Measurement Accuracy	
Measurement sensitivity¹	
With autozero channel on	
Types J, K, T, E, N	<0.07 °C
With autozero channel off	
Types J, K, T, E, N	<0.05 °C

¹ Measurement sensitivity represents the smallest change in temperature that a sensor can detect. It is a function of noise. The values assume the full measurement range of the standard thermocouple sensor according to ASTM E230-87.



Figure 3.1-3 4-Channel, 14 S/s, 24-Bit, ±80 mV C Series Thermocouple Input Module NI 9211

To calibrate the thermocouple measuring devices one wire will be implemented in a batch of melting ice in water, which maintains a stable temperature of 0 °C. The other wires measuring around the

cycle will apply this reference point to output the correct measured temperature. This method is cheap, simple and accurate.

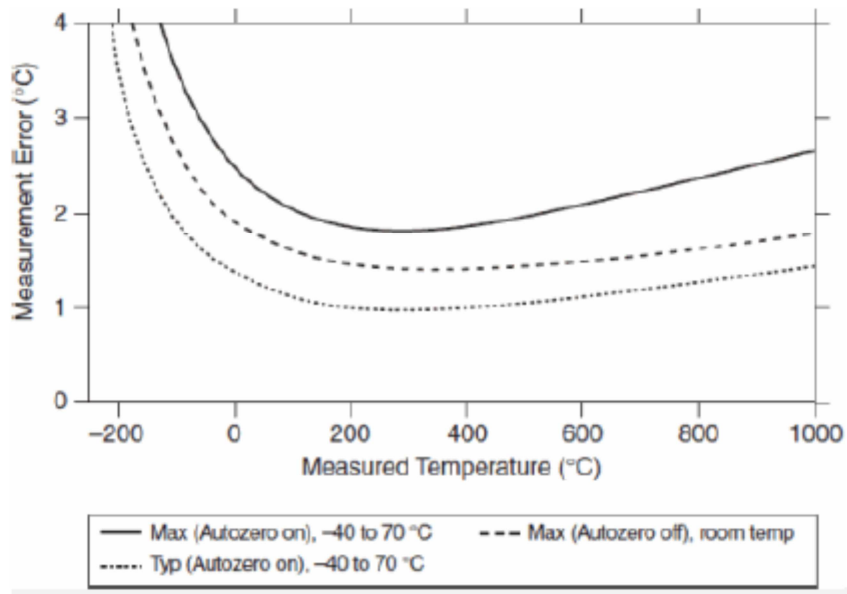


Figure 3.1-4 T-type maximum error using NI9211

3.1.2. Pressure measurement

The pressure measurements will be performed by pressure transmitters from Druck PTX series. In the system two of the sensors are PTX 1400 and one PTX 510.

Druck PTX 510



Figure 3.1-5 Druck PTX-510

The Druck PTX 510 combines micro machined silicone diaphragms with fully welded stainless steel and Hastelloy pressure ports to provide a highly accurate, stable pressure transmitter with materials and environmental protection required for industrial applications.

Table 3.1-3 Druck PTX-510 Specifications

Specifications Druck PTX-510	
Number of units	1
Maximum allowable pressure	100 bar
Temperature range – process media	-29°C to 122°C
Output signal	4-20 mA
Accuracy	Combined non-linearity, hysteresis and repeatability: $\pm 0.15\%$ typical, $\pm 0.25\%$ maximum best straight line (BSL) definition
Long term stability	0.2% FS range per annum typical
Temperature effects	For ranges of 5 psi and above the output will not deviate from room temperature calibration by more than <ul style="list-style-type: none"> • 1 % F.S. over -10 °C to 50 °C • 2 % F.S over -21 °C to 79.4 °C For ranges below 5 psi these values will increase pro-rata with calibrated span
Cable	For gauge pressures below 60 bar the PTX 510 requires vented cable

Druck PTX-1400



Figure 3.1-6 Druck PTX 1400

The Druck PTX-1400 is a stainless steel isolation diaphragm and fully welded stainless steel pressure module ensures excellent media compatibility without compromising the performance.

Integral electronics provide a three-wire 4-20 mA output proportional to applied pressure. Integral non-interactive zero and span controls ensure system interchange ability and easy of calibration.

Table 3.1-4 Druck PTX-1400 Specifications

Specifications Druck PTX-1400	
Number of units	2
Maximum allowable pressure	130 and 160 bar
Temperature range	-20°C to 80°C
Output signal	4-20 mA
Accuracy	Combined non-linearity, hysteresis and repeatability: $\pm 0.15\%$ typical, $\pm 0.25\%$ maximum best straight line (BSL) definition
Long term stability	0.2% FS range per annum typical
Temperature effects	Total error band (TEB) 1.5% FS typical, 2% FS maximum, -20°C to 80°C.

Measurement type

The most common pressure reference used is gauge pressure, which means the pressure measured minus the atmospheric pressure. Of the gauge type measurement, there are two types; sealed gauge (sg) or vented gauge (g or vg). The one on this application is the sealed gauge type.

The vented gauge will allow atmospheric air into the negative side of the device, and thus show zero pressure when the process pressure are held open to the air.

The sealed gauge reference type is similar except that the atmospheric pressure is sealed on the negative side of the diaphragm. This is the common application for high pressure ranges such as hydraulics where atmospheric pressure changes will have negligible effect on the accuracy of the measurement.

Another sealed gauge reference is a high vacuum seal on the reverse side of the sensing diaphragm. Then by adjusting the electronics the output signal is offset by 1 bar so the pressure sensor reads close to zero when measuring atmospheric pressure.

A sealed gauge reference pressure transducer will never read exactly zero because atmospheric pressure is always changing and the reference in this case is 1 bar. (©2011 SensorsONE Ltd)

3.1.3. Mass flow measurement – Rheonik RHM 04 – Coriolis mass flow meter



Figure 3.1-7 Rheonik RHM 04 - Coriolis Mass Flow meter with fast response

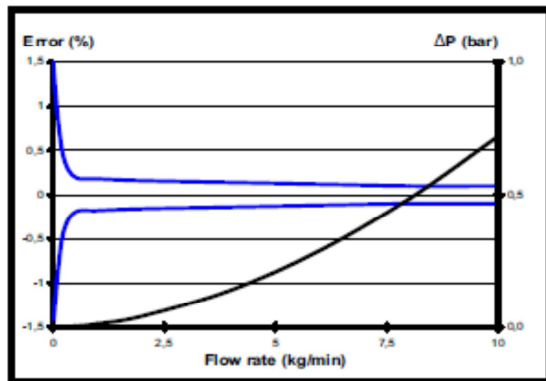
The RHM 04 can measure flow rates from 0.1 kg/min to 10 kg/min, with minimal flow as low as 0.02 kg/min. The devices' response time is 60 ms and better and with excellent repeatability. The RHM 04 has been in production in 10 years and has been optimized for applications that require high accuracy and fast response. The accuracy of this flow meter is better than 0.1% with a repeatability of 0.05%.

Rheonik uses the patented Omega tube design with increased signal to noise ratio, which provides excellent performance and reliability. Rheonik uses the patented torsion swinger with the omega shape which results in high accuracy measurement independent of pressure even at very low velocities.

The model used in the system has been adjusted to a minimum and maximum flow rate of 0.2 kg/min to 2 kg/min; this will increase the accuracy and repeatability of the flow meter.

The flow meter is based on the Coriolis-effect and is possible to apply for almost all fluids with a very high level of accuracy. The principal of Coriolis is based on vibrations in the omega-tube in the flow meter; these vibrations will be registered to find the mass flow through the tube very accurately.

Standard Models



Gold Line Models

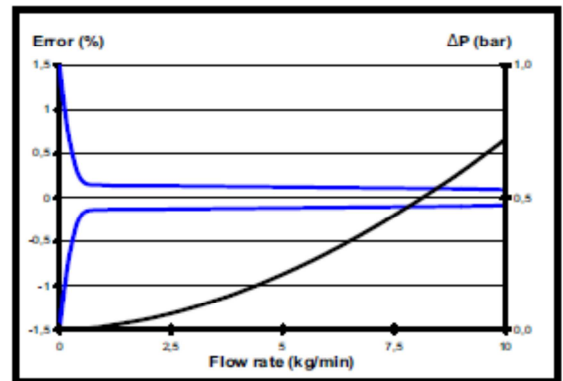


Figure 3.1-8 Flow meter error



Figure 3.1-9 Rheonik RHE 08 Advanced transmitter

To log the signal provided from the RHM 04 Coriolis flow meter, the RHE 08 advanced Rheonik transmitter has been applied.

Table 3.1-5 Rheonik RHE 08 - Advanced transmitter

General specifications RHE 08	
Pressure rating	150 bar @120 °C
Power consumption	<15 W
Digital output	0/4 - 20/22 mA
Housing	Aluminium
Power supply	230 VAC ±10%
Installation	

- Rapid temperature fluctuations must be avoided
- Do not exceed maximum allowable pressure – be aware of pressure peaks
- Abrasive media can reduce the wall thickness and thus reduce the allowable maximum pressure.
- Check the tubes for corrosion before installation.
- The sensor RHM, as well as the measuring cable must be installed as far away from sources of electrical interference (transformers, high tension switching components, large electrical motors, frequency converters etc.) as possible.

3.1.4. Air temperature and humidity measurement

In the air cycle it is necessary to obtain results on temperature and humidity at two points to determine the efficiency of the air cycle. The instruments applied to measure the humidity and temperature is the Vaisala HMP235 and a KIMO AMI 300. There will be one sensor between the evaporator and the gas cooler and the other one after the drum. Data on humidity and temperature in these locations will be able to tell us how much water that is condensed in the evaporator and when the clothing is finished drying.

These transmitters have been designed for applications where the measurement of humidity is important, this include drying processes, air-conditioning as well as storage and warehouse areas. They are also an application suitable for lab experiments.

Both sensors have limits well above the temperatures the air will experience in the drying cycle. The readings of the values from the air cycle is performed every 5th minute during the drying cycle. This is considered to be sufficient due to the relatively slow changes in air temperature and humidity.



Figure 3.1-10 Vaisala HMP 235 Temperature and humidity transmitter



Figure 3.1-11 KIMO AMI 300 Temperature and humidity transmitter

Table 3.1-6 Vaisala HMP 233

Vaisala HMP 235	
Temperature range	-40 °C to 180 °C
Mixing ratio	0 to 500 g/kg d.a
Wet bulb temperature	0 °C to 100 °C
Absolute humidity	0 to 600 g/m ³
Enthalpy	-40 to 1500 kJ/kg
Outputs	
• Two analogue	0 to 20 mA
• Selectable and scalable	4 to 20 mA
	0 to 1 V
	0 to % V
	0 to 10 V
Typical accuracy of analogue (20 °C)	+/- 0.05% of full scale
Measured	Relative humidity
	Temperature
Calculated	Dew point temperature
	Mixing ratio
	Absolute humidity
	Wet bulb temperature
	Enthalpy
Operating voltage	230 VAC

Table 3.1-7 KIMO AMI 300 Temperature and humidity transmitter

KIMO AMI 300	
Temperature range	-20 °C to 80 °C
Relative humidity	5 to 95 %
Temperature accuracy	0.1 °C
Relative humidity accuracy	0.1 % RH

3.1.5. Electrical power measurement

To determine the energy use input of the system the effect used in the compressor and the main motor running the drum and fan will be monitored during the whole drying cycle. During the cycle different factors will affect the load of these two electrical components, thus the value obtained from these measurements will be related to the clothing load and compressor running conditions. Except from the pump draining water from the system all of the components will run continuous through the whole drying process. The pump will be alternated to run for 20 seconds every 3rd minute.

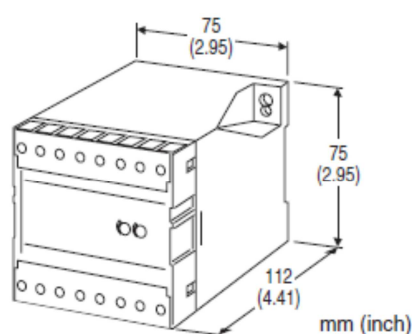


Figure 3.1-12 L-unit LWT Watt Transducer

To measure the power consumption the L-unit LWT watt transducer will be used. Specifications listed in Table 3.1-8.

Table 3.1-8 L-unit LWT Watt transducer

General specifications	
Construction	Stand-alone, terminal access at the front
Housing material	Flame resistant resin (black)
Isolation	Voltage output to current input DC output to pulse output to power
Computation	Time division multiplication
Over range output	-10 – +120 % at 1 – 5 V
Zero adjustment(DC output)	-5 to + 5 % (front)
Span adjustment(DC output)	95 to + 105 % (front)
Input specifications	
Frequency	50/60 Hz
Voltage input	
• Operational range	0-120% of rating
• Overload capacity	1000% of rating for 3 seconds, for 10 seconds 120 %
Output specifications	
DC current	-10 – /+ 20 mA DC
Load resistance	Output drive 12 V maximum; 10 V for +/- output

3.2. Uncertainly analysis

According to Richard P. Feynman modern science is characterized by uncertainty. All scientific data measured in the experiments do have a relevant amount of uncertainty. Data which are not accounted for uncertainty cannot be relevant scientifically.

All of the instruments used in the experiments have a certain level of uncertainty, to be able to obtain plausible results all of these must be accounted for.

Firstly it is of course important to reduce the magnitude of the error, by doing the measurement correctly. There are two different types of measurements; directly and indirectly. The directly measured data will be the most correct data, but in many cases the quantity is only possible to obtain indirectly. In highly evolved sensors and detectors many measurements are conducted indirectly, i.e. physical properties such as temperature, pressure and mass flow will be converted to electrical or optical signals that easily can be measured. To read these signals linear conversion or conversion curves are used to transform the signal into desired dimension.

During an experiment there are two basic uncertainty sources connected with measurements to concern; random and systematic uncertainties.

Random: are those uncertainties where repeating the measurement gives a randomly different result each time in a unpredictable way. The more measurements performed the better estimate for the correct value is possible to obtain.

Systematic: this uncertainty type include where the same factor will affect the measurement time after time in a predictable way. The reason for the uncertainty does not have to be known and therefore different methods or calculations must be used to recognize the systematic error.

For the random error calculation it is necessary to determine a distribution of the results for the measurements. When the number of data reaches a certain point, the distribution becomes a probability distribution. For values surrounding a mean value it is common to consider the Gaussian normal distribution. This model is frequently used in statistics, easy to handle and can describe many processes.

The average of a series of measurements is calculated from Equation 3.1-1, this value will be the base to determine the “correct” result. During this process the air will be in constant change and will never reach steady state during the measurements in this experiment. This is due to the removal of the moisture from the air, the temperature will increase and the relative humidity in the air will decrease. This will affect the CO₂ cycle to always be changing during the cycle. There will not be any

values logged from the instruments that are comparable to make a series for the normal distribution. Since the X_i -value always will be changing, amount of measurements in a series N will be always being equal to 1.

$$\bar{X} = \frac{1}{N} \sum_{i=1}^N X_i$$

Equation 3.1-1 Measured series average

To be able to specify how correct the series are, the standard deviation is obtained by applying the calculated average value of the series in Equation 3.1-2. In each series the standard deviation will be the same for all values in the specific series; this implies that some of the measured values may deviate more and some deviates less. As it can be seen from Equation 3.1-2 with $N=1$, it is not possible to consider the random error deviation in the Gaussian normal distribution.

$$S(\bar{X}) = \sqrt{\frac{\sum_{i=1}^N (X_i - \bar{X})^2}{N - 1}}$$

Equation 3.1-2 Standard deviation

From the equation introduced above the definition of the Gaussian distribution is shown in Equation 3.1-3, the formula is based on the population value X , standard deviation σ and average population μ .

$$f(x) = \frac{1}{\sigma\sqrt{2\pi}} e^{-\frac{(X-\mu)^2}{2\sigma^2}}$$

Equation 3.1-3 Gaussian normal distribution

The uncertainty that will be considered for this experiment will be the systematic uncertainty, since the random uncertainty not will be applicable for the experiments.

Total uncertainty

For an experiment it is useful to determine the total uncertainty, this includes the random and the systematic uncertainty. To determine the systematic uncertainty referred to as the bias, the value given from the manufacturer on the specific instrument will be applied. In the instruments there are two factors to consider; the measurement and the controller uncertainty. Since it not will be any comparable values for the random errors; this analysis will be based on the measurement uncertainty from the instruments given from the manufacturers. To merge the measurement and controller errors the total uncertainty is obtained by Equation 3.1-4.

$$\delta X_i = \sqrt{S_{\bar{X}} + S_{Measurement}^2 + S_{Controller}^2}$$

Equation 3.1-4 Total uncertainty

The $S_{Measurement}$ will contain the uncertainty for the measured value, while the $S_{Controller}$ will contain the value for the controller. From this formula it is possible to obtain the systematic errors produced in the instruments.

Compounded error analysis

To find the total error deviation in the measurements; the errors from the instruments have been examined and the heat and COP_{HP} have been calculated to see the effect. The values considered will be obtained from the data in one of the experiments to get the real relation between them. To calculate the enthalpy to find the heat transferred in the heat exchangers RnLib will be used with pressure and temperature as input. To find the heat exchanged in the heat exchangers; the calculations will depend on the enthalpy at the inlet and outlet as well as the mass flow. The measured pressure, temperature and mass flow will all have a certain grade of uncertainty that will affect the final calculation of the heat.

Table 3.1-9 Total uncertainty estimation

Measure point								
Measured values	Measured value	Measurement error	Controller error	δX	High value	Low Value	Percentage difference	Unit
p1	45,268	0,113	0,10	0,151	45,419	45,117	0,665 %	bar
p2	90,587	0,226	0,10	0,248	90,835	90,339	0,545 %	bar
p4	90,315	0,226	0,10	0,247	90,562	90,068	0,545 %	bar
t1	12,662	0,500	0,50	0,707	13,369	11,955	10,578 %	°C
t2	62,040	0,500	0,50	0,707	62,747	61,333	2,254 %	°C
t3	39,375	0,500	0,50	0,707	40,082	38,668	3,528 %	°C
t4	36,990	0,500	0,50	0,707	37,697	36,283	3,752 %	°C
t5	12,822	0,500	0,50	0,707	13,529	12,115	10,453 %	°C
t_amb	23,299	0,500	0,50	0,707	24,006	22,592	5,891 %	°C
m_flow	0,0147	0,0001	0,00	0,0001	0,0148	0,0146	1,980 %	kg/s
Watt motor	214,027	0,107	0,00	0,107	214,134	213,920	0,100 %	W
Watt compressor	717,333	0,359	0,00	0,359	717,692	716,974	0,100 %	W
Calculated values								
h1	731476,846				732631,034	730301,495	0,318 %	J/kg
h2	749128,327				750336,755	747904,674	0,324 %	J/kg
h3	635456,613				642545,062	628758,239	2,146 %	J/kg
h4	613505,282				618452,231	608998,635	1,529 %	J/kg
h5	613505,282				618452,231	608998,635	1,529 %	J/kg
Q Gas cooler	1993,659				2098,447	1883,921	10,223 %	W
Q Evaporator	1734,182				1835,570	1627,742	11,322 %	W
COP	2,779				2,927	2,625	10,313 %	-

In Table 3.1-9 the total uncertainty from a selected point is shown as well as the calculated values of the heat in the gas cooler and evaporator and the COP of the heat pump. From the calculated value of the COP it is noticed that with measurement errors it can vary from around 2.625 to 2.927, a deviation on 10.313 %.

4. Plan for experiments

The goal of the testing procedure is to compare the measured results with the obtained results from the R134a cycle. The two systems will be compared based on the COP, SMER, energy use and drying time.

Throughout the experiments it should be considered the effect of the external gas cooler. The fan that draws the ambient air through the fins of the external gas cooler is possible to turn ON/Off with a switch on the instrumentation locker. To determine the effect; two cycles with the same load will be performed, one with the fan running and one without. Thermocouple elements are connected outside the tube both in front and after the external gas cooler, so any heat rejection from the tubes to the ambient will be logged.

By weighing the water it is possible to determine leakages from the enclosed air cycle; since the chassis for the dryer is of prototype material it is not optimized towards leakages. Thus the clothing will be weighed at dry state, wet state and final state, and the water removed from the cycle and pumped into the water storage will be measured at the end of the cycle.

The energy use of the process will be logged by using a reference experiment with full load; this is 6.316 kg of cotton fabric. The cycle will end when the humidity is removed from the cotton; this can be noticed from the measurements of temperature and humidity while running the cycle. The fabric will be humidified first in a washing machine with a centrifuge, to distribute the water well in all of the fabric. The fabric will be weighed before and after it is loaded into the drum, the mass will vary between 9.5-10 kg in wet condition.

The second part of the experiments includes finding the optimal point for the capillary tube as expansion device. First experiment will try out the theoretical design of the capillary tube at 900 mm, if the chosen length results in a too large or a too small pressure drop it will be altered to find a more optimal solution in the next experiment. The external fan will also be considered for the experiments using the capillary tube.

Due to some leakages during the first test runs it caused some oil and CO₂ to leave the system there is no precise control of the mass CO₂ filled in the system. Before start-up the standstill pressure will be checked to be below the saturated pressure at the ambient temperature to be sure of how much of the refrigerant is liquid. During the cycle the mass flow of the CO₂ will be monitored and logged so the refrigerant charge can be estimated.

4.1. Experiment overview

Experiment 1 and 2 will be used to check how the performance of the external gas cooler is and how the design of the throttling devices behaves during a drying cycle. The first 2 experiments will have an evaporator pressure of 40-50 Bara and a gas cooler pressure of 85-100 Bara. By applying the manual throttle valve it will be flexible to find the best set point for the system. After the first set of experiments it there will be a conclusion of the efficiency of having the external fan running through the cycle.

The next part of the experiments will be used to find the optimal length and design point of the capillary tube. Since this will be the expansion method for the final product it will be important to find the best set point; both for the heat pump performance and the drying cycle. The first experiment will use a length of the capillary tube longer than the calculated one in section 2.2.3.2; this is due to practical reasons when adjusting the length. When a suitable length has been obtained the further experiments will find a refrigerant charge with and without the external fan turned on.

- Experiment 1: Manual throttling valve, no external fan
- Experiment 2: Manual throttle valve, external fan on
- Experiment 3: Capillary tube, external fan, 900 mm capillary tube
- Experiment 4: Capillary tube, external fan, adjusted length of the capillary tube. (740 mm)
- Experiment 5: Capillary tube, no external fan, adjusted length of the capillary tube. (660 mm)
- Experiment 6: Capillary tube, no external fan, adjusted length of the capillary tube. (660 mm), reduced refrigerant charge
- Experiment 7: Capillary tube, no external fan, adjusted length of the capillary tube. (660 mm), increased refrigerant charge
- Experiment 8: Capillary tube, external fan, adjusted length of the capillary tube. (660 mm)

5. Measuring performance data of the drying cycle

5.1. R134a results

The construction and experimenting of the CO₂ dryer has been performed with the base in the results from the R134a cycle. Temperature and humidity have been directly input for the simulation software used in the design phase of the project.

During testing of the R134a system an energy use of $0.27 \text{ kWh/kg}_{\text{Dry fabric}}$ is a key number that the new CO_2 system should be compared to. The dry batch of fabric used during these experiments have a mass of 6.316 kg , thus the total energy use during a drying cycle cannot exceed 1.705 kWh in total. For this reference number to be valid the fabric must be at completely dry state when removed from the drum.

In Figure 5.1-1 and Figure 5.1-2 the air data of an R134a cycle are shown; these show the temperature and the humidity at the drum inlet and outlet and the evaporator outlet. The temperature at the inlet of the drum is steadily increasing until it reaches its maximum after around 4000 seconds of $56 \text{ }^\circ\text{C}$. It is also noticed that after the same time the humidity content of the air is starting to get lower. Due to water droplets coming onto the sensor head of the measuring equipment the values at the drum outlet will vary quite much. However it is still possible to see a trend of how the temperature and humidity behave through the cycle.

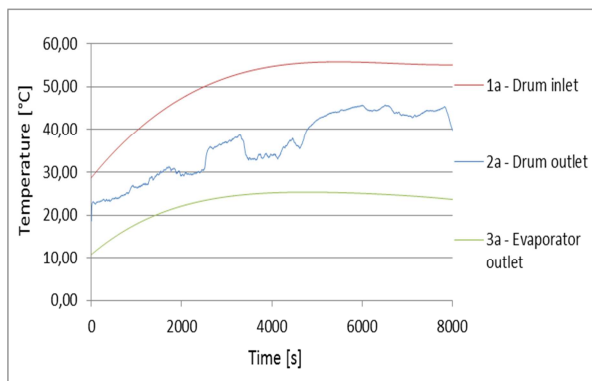


Figure 5.1-1 Drying cycle air temperature

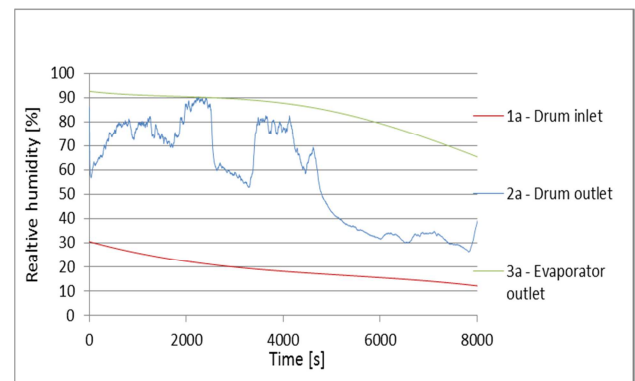


Figure 5.1-2 Drying cycle air relative humidity

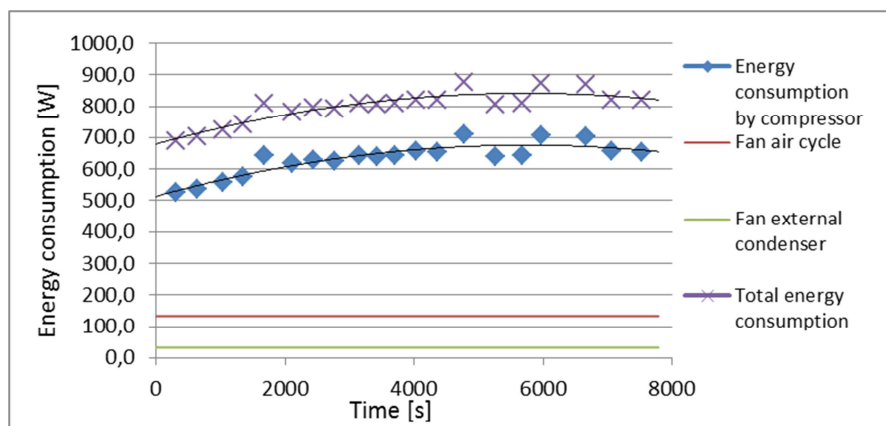


Figure 5.1-3 R134a energy consumption

The energy consumption for this presented data is shown for a cycle with 3 kg dry material with 1.77 kg water when loaded in the drum. Thus the energy use of the motor running the main fan and the drum will be smaller than for full load, this can be seen in the figures presenting the energy use of the CO₂ system.

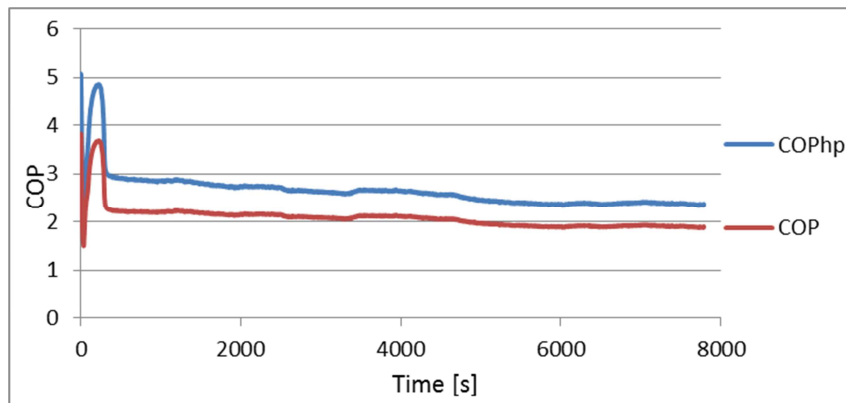


Figure 5.1-4 R134a cycle COP

Figure 5.1-4 shows the development of the COP of the R134a cycle. Looking at the COP for the system including the motor running the drum and the main fan for the air cycle the average COP is just above 2, implies an energy saving of about 50 %.

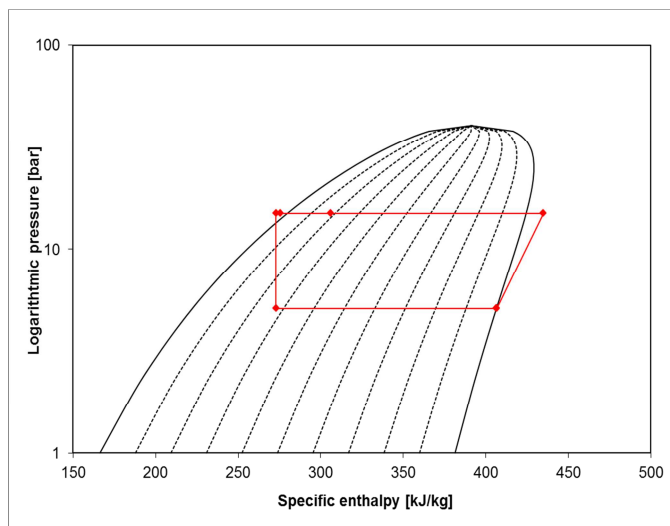


Figure 5.1-5 Log-ph-diagram of the R134a system

Visualizing the difference of the two cycles, the R134a cycle is as shown in Figure 5.1-5 a subcritical cycle with both evaporating and condensing processes. This cycle is shown with an evaporating pressure of 5 Bara and condensing pressure of 15 Bara which represent the former process.

5.2. Experiment 1: Manual throttle valve, no external fan

This experiment will evaluate the effect of applying the external fan for the external gas cooler; the expansion process is performed by the manual throttle valve. Locations of the temperatures shown in Figure 5.2-1 is explained in the instrument overview in Figure 3.1-1. The external fan will not be applied during this experiment.

The fabric used in the experiment was weighed to be 6.316 kg dried up, it was then moistened and centrifuged and weighed again to become 9.500 kg. This implies that the amount of water in the fabric loaded to the drum is 3.184 kg. After the drying cycle ends the clothing and the water removed is weighed again – now it is possible to determine the specific moisture extraction rate and the leakage ratio from the system. After the drying process the discharge temperature measured with the thermocouple, T_2 seemed to be too low, thus the isentropic efficiency based on the real electrical input to the compressor is used to find the discharge temperature. The figure shows a rather large deviation from the measured value of the discharge gas temperature.

The calculated temperature from the real electrical input will be used during the presentation and discussion of the results.

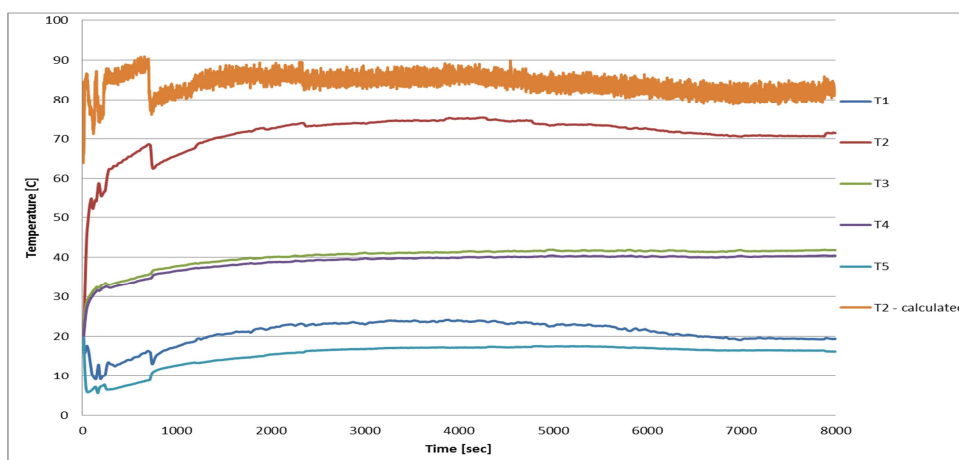


Figure 5.2-1 Measured temperatures CO₂ circuit

As the process stabilises after 1500 seconds the evaporating pressure is between 45-50 Bara while the gas cooler pressure is stable around 95 Bara.

Temperature measurement T_3 and T_4 shows the temperature before and after the external gas cooler, the temperature drop along the tubes is averagely 1.3 K during the cycle. This corresponds to a capacity of 230 W of calculated with enthalpy values from RnLib. Values calculated for the external gas cooler will be compared to the experiment with the external fan connected.

During the full cycle the average overheat-temperature was around 7.7 K, which is a bit high, and the evaporator capacity will thus be reduced a slightly. It is reduced due to the dry surface at the end of the evaporator which results in a not as preferable heat transfer coefficient.

Once the mass drying cycle has stabilized it will have a continuous value of around 0.0145 kg/s, the evaporator effect will start off around 1750 W and decrease down to 1500 W, while the average performance of the main gas cooler is 2400 W.

The energy use of the motor and compressor are monitored and logged through the cycle; the motor running the fan and the drum will run stable at roughly 200 W after 500 seconds, while the compressor will take around 1000 seconds to stabilize its value around 750 W.

The coefficient of performance and the energy savings have been deduced from the values of the gas cooler and evaporator performance and the electrical consumption. Thus the efficiency of the heat pump will start off at a COP at 3.7 and slightly decrease until it reaches 3.2 at the end of the drying period. The COP including the motor will have the same pattern, but will start off at 2.7 and decrease to 2.5. This represents an average energy saving of 60% compared to an appliance not applying heat pump.

During the drying period the CO₂ cycle will start off in a subcritical process, before the pressure in the gas cooler adjust to the air side conditions. In Figure 5.2-2 and Figure 5.2-3 and the process is shown in case of a T-h and a P-h diagram respectively. It can be seen from the figure that the overheat temperature is a bit high compared to the optimal model. This will cause the suction temperature for the compressor to become a bit higher than optimal and thus the discharge temperature will increase. It will also affect the heat transfer surface of the evaporator since the heat transfer coefficient will be decreased compared to annular flow with wet surface.

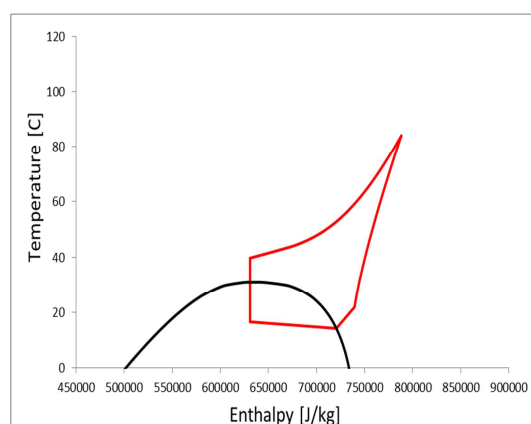


Figure 5.2-2 T-h diagram average value 1000-8000 seconds

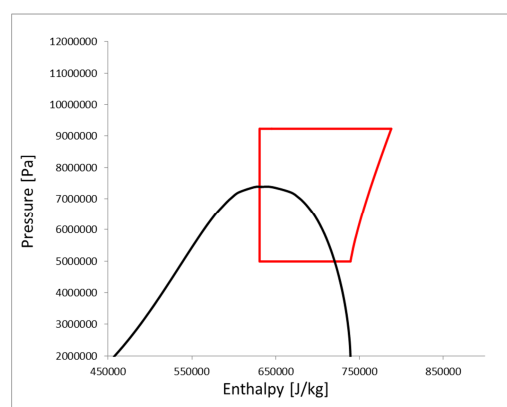


Figure 5.2-3 P-h diagram average value 1000-8000 seconds

From the same time span some values have been deduced from the logged data, these values are shown in Table 5.2-1.

Table 5.2-1 Average CO₂ values : 1000-8000 seconds

Effect compressor	722,211	W
Effect motor	211,533	W
Total effect	933,744	W
Mass flow	0,0148	kg/s
COP – Heat pump	3,263	
Energy savings	69,35 %	
Gas cooling effect	2355,32	W
Evaporator effect	1633,13	W
Energy use 100 minutes	1,55	kWh

Exploring the air graphs of the drying cycle it is noticed that from 6000 seconds the temperature at the evaporator inlet is increasing and the relative humidity is decreasing drastically. This indicates that almost all of the moisture has been removed from the fabric.

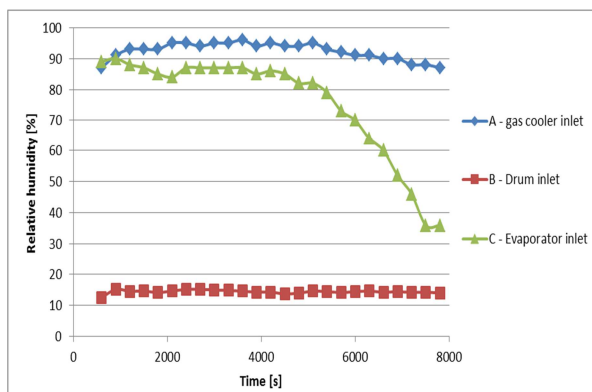


Figure 5.2-4 Air relative humidity

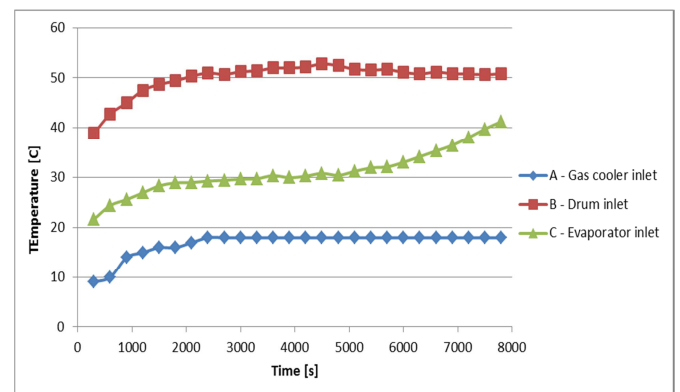


Figure 5.2-5 Air temperatures

The temperature of the air at the drum inlet is reaching its stable value at just over 50 °C after around 2000 seconds and this value remains throughout the cycle. It is noticed after 5000 seconds that the temperature at the evaporator inlet is drastically increasing towards the temperature at the drum inlet; this indicates that the moisture has been removed from the surface and the drying period 2 is imminent. The drying cycle is finished when the relative humidity into the evaporator is around 30 %. With an average temperature around 50 °C into the drum the drying time is 7600 seconds and has consumed a total of 1.96 kWh.

During the first 100 minutes of the cycle 1.696 kg had been removed from the cycle in the evaporator and pumped away to the water storage. When the drum was opened after 125 minutes the water drained away had increased to 1.970 kg. The fabric was removed from the drum and the mass was 6.316 kg i.e. all of the moisture had been removed from the fabric. The measured energy use related to the removed moisture from the fabric is calculated to be 0.612 kWh/kg_{water}.

The suction temperature, T_1 during the experiment started below 20 °C and peaked at around 24 °C and ended up at 20 °C in the end of the process, while the average evaporating temperature represented by T_5 was 17 °C. Looking Table B-1 where the dew point temperature for different air temperatures and relative humidity are shown. The air inlet conditions to the evaporator enter at the warmest point in the evaporator. When the temperature is 24 °C at the peak of suction line, the inlet conditions of the air are 85% RH and 30 °C and the dew point temperature is 27.8 °C. Since the warmest temperature at the evaporator is lower than the dew point the area of overheat will also be effective for condensation of water.

Table 5.2-2 Water and fabric

	Mass [kg]
Dry fabric	6.316
Wet fabric - loaded	9.500
Water (100 min)	1.696
Water (125 min)	1.970
Fabric at end (125 min)	6.316
Leaked water	1.214

Looking at the leakage ratio from the system with 1.214 kg leaked out during the drying process this represents a leakage ratio of 38%.

The SMER value based on the effect of the compressor alone and for the total system has been calculated. The figure shows the relation between the water removed in the evaporator to the effect used in the system. The SMER-value is determined for three values through the cycle, and has its peak in the middle of the cycle.

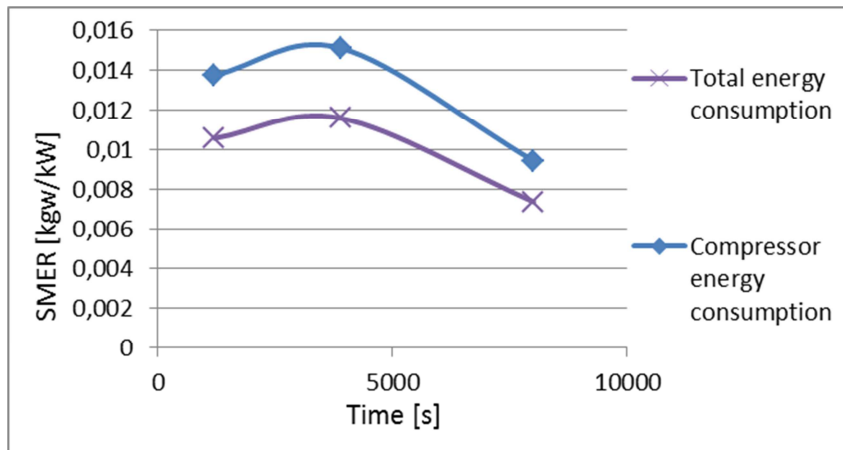


Figure 5.2-6 SMER-value

More graphs from experimental results can be found in [appendix A – Experiment 1](#).

5.3. Experiment 2: Manual throttling external gas cooler fan connected

During this experiment the external fan is turned on and the manual throttling valve has been used. By applying the fan to the external gas cooler it will decrease the temperature of the CO₂ further before throttling and thus improve the transcritical CO₂ process. The goal is to see if the enthalpy gained by cooling the refrigerant further before the throttling process exceeds the extra energy required by the fan.

The load of fabric is the same as for experiment 1; 6.316 kg dry fabric containing water to become 9.500 kg wet fabric. During the cycle the gas cooler pressure was observed to be around the same as in experiment 1, while the evaporating pressure was a bit lower.

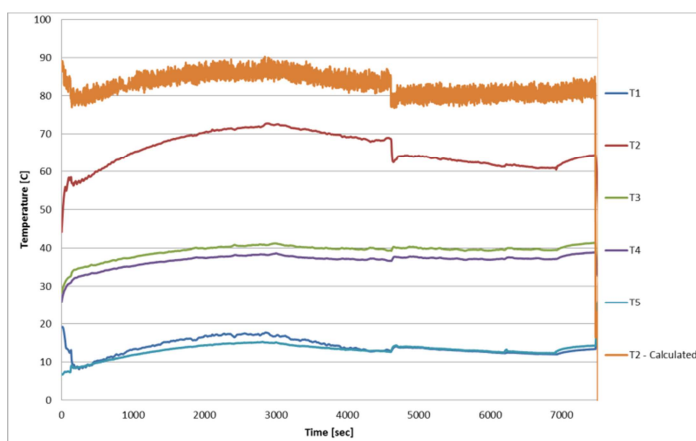


Figure 5.3-1 Measured temperatures CO₂-cycle

The temperatures shown in Figure 5.3-1 visualises the same pattern as for the experiment without the external fan turned on. However it should be noticed that the compressor suction temperature is quite much lower in this experiment.

The average refrigerant mass flow in experiment 2 is calculated to be 0.0142 kg/s, which is a bit smaller than in experiment 1. The mass flow has been changed due to some small leakages in the system that was discovered and fixed. However the change in the mass flow is low and will not affect the heating or cooling performance crucially. The gas cooler capacity will quickly reach 2500 W performance and maintain this effect throughout the process; the evaporator however will start at 2000 W have a small reduction to 1750 W and stay at this level throughout the drying time.

The energy consumption will increase by the energy use of the fan to the external gas cooler; this is not significant, but will have a constant load of 33.4 W which has been added to the total consumption. Calculating the average enthalpy difference over the external gas cooler it will during the full cycle have an effect of 305 W.

The performance of the process with the external fan turned on will give more or less the same efficiency as without. The COP for the heat pump will start around 3.7 and throughout the cycle be reduced to 3.4, correspond to an average energy saving potential of 73%. While the COP including energy from the motor and external fan will start at 2.7 and be reduced to 2.5, an energy saving of 62%. The results obtained here are very equal to the results obtained in experiment 1. The performance of the external gas cooler will increase, but with increasing ambient temperatures the effect of the fan will be limited.

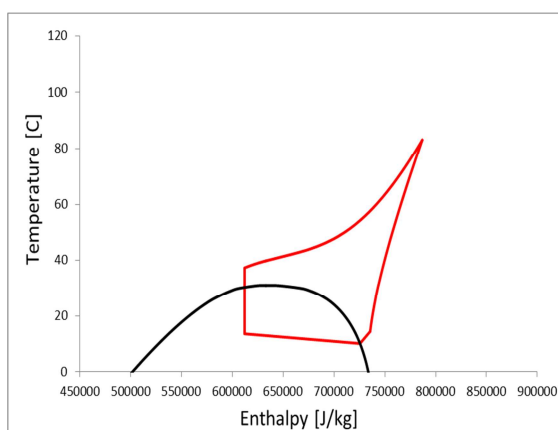


Figure 5.3-2 T-h diagram 1000-7000 seconds

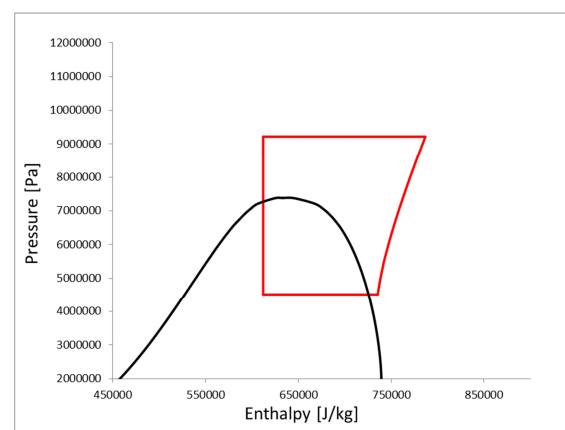


Figure 5.3-3 p-h diagram 1000-7000 seconds

For the same time span as for Figure 5.3-2 and Figure 5.3-3 average values for the CO₂ cycle have been calculated.

Table 5.3-1 Average CO₂ values: 1000 – 7000 seconds

Effect compressor	729,632	W
Effect motor	216,552	W
Total effect	946,184	W
Mass flow	0,0142	kg/s
COP – Heat pump	3,431	
Energy savings	70,85 %	
Gas cooler effect	2502,610	W
Evaporator effect	1772,978	W
Energy use (100 min)	1,632	kWh

From the table it can be seen that the total effect has increased compared to experiment 1 due to the extra effect of the fan. However the average gas cooler effect has increased with 200 W and the evaporator with 140 W.

The air conditions in the process are also very equal to experiment 1, the temperature at the inlet of the drum will decrease a bit, while the drying time has slightly decreased.

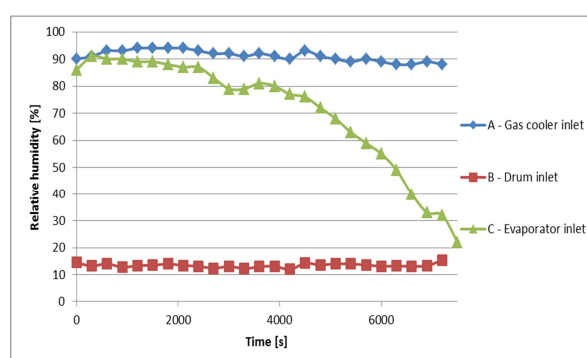


Figure 5.3-4 Air relative humidity

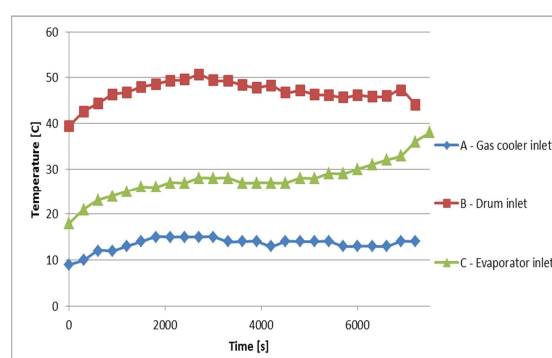


Figure 5.3-5 Air temperatures

Looking at the temperature at the drum inlet in Figure 5.3-5, it is below 50 °C throughout the process, and is unable to absorb large amounts of moisture in the drum.

The average temperature suction temperature in this experiment is around 15 °C; this means that all of the area of the evaporator will be effective for condensing water on the surface.

Table 5.3-2 Water and fabric

	Mass [kg]
Dry fabric	6.316
Wet fabric - loaded	9.500
Water (100 min)	1.733
Water (115 min)	1.938
Fabric at end (115 min)	6.326
Leaked water	1.246

In this experiment 1.246 kg water did not end up in the water storage this means that as much as 39% of the water in the fabric has leaked from the system. The average high pressure of the system is just under 95 Bara, which implies a lower gas cooler temperature. After 115 minutes the relative humidity at the drum inlet is around 30 % and the fabric is dry and the total energy consumption is around 1.99 kWh. The estimated consumed energy related to the removed water content is 0.625 kWh/kg_{water}.

In Figure 5.3-6 the SMER-value is shown for the experiment at three points, the water removed is large from the start and to the middle of the drying cycle, but decrease towards the end of the cycle.

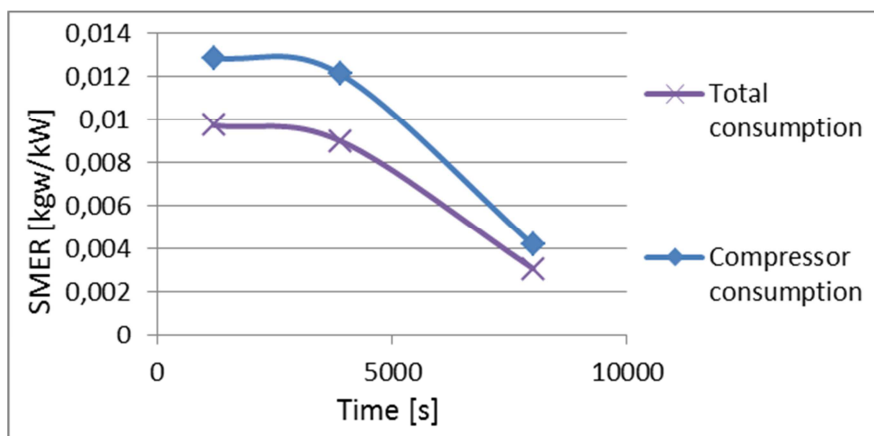


Figure 5.3-6 SMER-value

More graphs from experimental results can be found in [appendix A – Experiment 2](#).

5.4. Experiment 3: Capillary tube (900 mm), external fan

This experiment was performed to see the required length of the capillary tube in a drying process. From calculations presented earlier in the report the length was calculated to be below 700 mm; however this value deviates a lot if the mass flow, inner diameter or inner surface roughness is not perfect designed. For this first experiment with capillary tube a length of 900 mm is used. The external fan has been used throughout the whole experiment.

Related to the large water leakages the drum was removed and all connections in the air cycle were overlooked to determine if there were any large air leakages in the enclosed air cycle. Tape was used to close the cycle as much as possible.

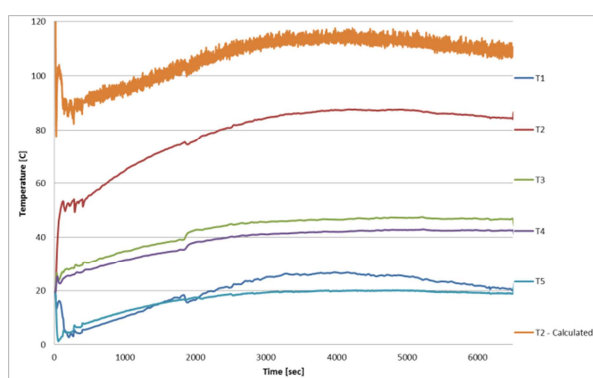


Figure 5.4-1 CO₂ Temperatures

The logged temperatures from the cycle were a bit higher compared to experiment 1 and 2. This is caused by a higher pressure ratio. The first test with the capillary tube showed that the pressure drop is too large; thus the capillary tube is too long. It will be performed some new calculations to determine the adjusted length for the next experiment.

During the cycle the high pressure was stable around 120 Bara and the low pressure was at 45-50 Bara, this causes the pressure ratio to be too high and the compressor has to work extra hard.

The mass flow stabilised at 0.0134 kg/s and the performance of the gas cooler reached 2900 W after 500 seconds and slowly decreased throughout the drying period and ended up at 2600 W. The evaporators' performance started at 2100 W and ended up at 1700 W at the end of the cycle.

The compressors energy consumption reached an average value from 1000-6000 seconds of almost 900 W with the current pressure level. This results in a reduced value for the coefficient of performance for the total process. The average COP for the total system is around 2.5, while it is 3.1 for the heat pump alone, these values correspond to energy saving values of 60% and 68% respectively.

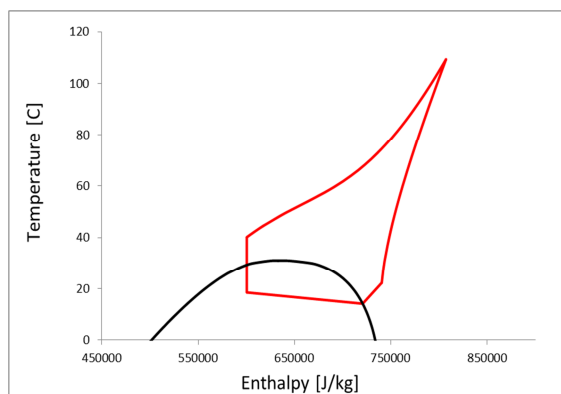


Figure 5.4-2 T-h diagram of average values 1000-6000 seconds

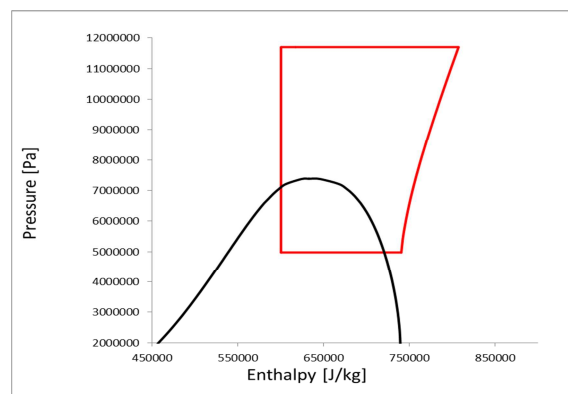


Figure 5.4-3 p-h diagram of average values 1000-6000 seconds

Table 5.4-1 CO₂ average values: 1000-6000 seconds

Effect compressor	898,469	W
Effect motor	204,260	W
Total effect	1102,728	W
Mass flow	0,0135	kg/s
COP - Measured	3,112	
Energy savings	67,86 %	
Gas cooler effect	2791,787	W
Evaporator effect	1893,319	W
Energy use (100 minutes)	1,896	kWh

For the air cycle the process air experienced an increased temperature at the inlet of the drum, thus more humidity could be absorbed in the air flow into the drum. This resulted in a drying time shorter than in experiment 1 and 2. When the air humidity at the evaporator inlet is reduced to 30% relative humidity, the fabric is dry. In this process the fabric is dry after 100 minutes, which is around 20 minutes shorter than the previous experiments. However with a higher pressure ratio and thus higher energy consumption from the compressor the total energy use of the system will still be high.

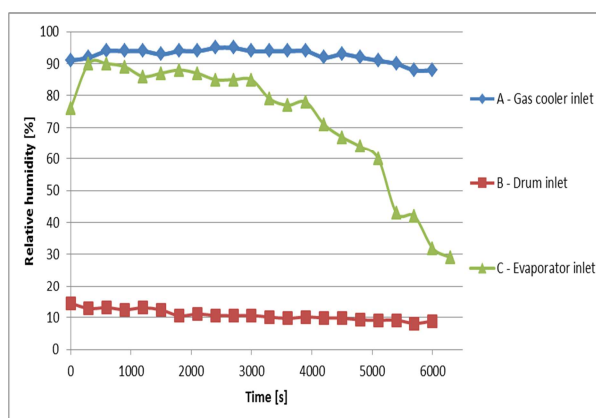


Figure 5.4-4 Relative humidity

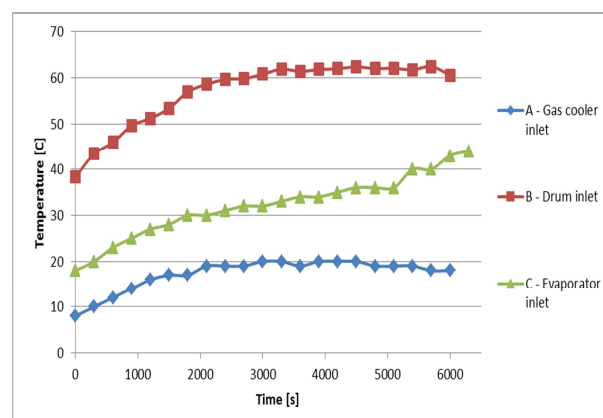


Figure 5.4-5 Air temperatures

Figure 5.4-4 and Figure 5.4-5 show the relative humidity and temperature levels for the air cycle. The air temperature at the drum inlet reaches a stable value above 60 °C after 2000 seconds, the high temperature results in shorter drying time.

The evaporating temperature is stable at 20 °C during most of the drying cycle, while the overheat temperature at the compressor suction line peaks at 28 °C after 4000 seconds. However after 4000 seconds the air humidity is still around 80% to a temperature of 33 °C, thus a dew point temperature of 29.1 °C. This means that the overheated area in the evaporator will still be effective for condensing water.

Table 5.4-2 Fabric and water

	Mass [kg]
Dry fabric	6.316
Wet fabric - loaded	9.500
Water (100 min)	2.246
Fabric at end (105 min)	6.315
Leaked water	0.938

After the work on the connections in the air cycle, some improvements of the leakages was noticed, the leakage ratio in this experiment has sunken to 29%. Better, but still high. For this cycle the process finished after 100 minutes and the total energy used during the cycle is 1.89 kWh. Energy consumed related to the water removed is 0.593 kWh/kg_{water}.

The SMER-value calculated for the experiment show a significant high amount of water removed in the middle of the drying process. Due to that the fabric is still moist at the surface and the air temperature into the drum has reached its maximum value.

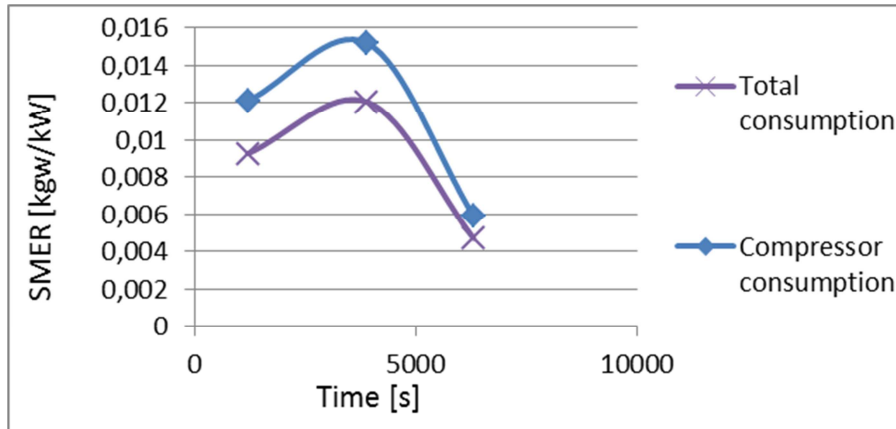


Figure 5.4-6 SMER-value

More graphs from experimental results can be found in [appendix A – Experiment 3](#).

5.5.Experiment 4: Capillary tube (740 mm), external fan

In experiment 3 with the first dimensioned capillary tube of 900 mm, a new length of the capillary tube was tried out. It was shortened to 740 mm to register the change in pressure drop over the capillary tube. Of course when altering the size of the capillary tube, the system is emptied for CO₂, evacuated and depressurized again. This means that the refrigerant charge will deviate from the previous experiment.

Due to a less efficient centrifuging process the fabric was 9.972 kg when loaded into the drum, this will of course increase the drying time of the system.

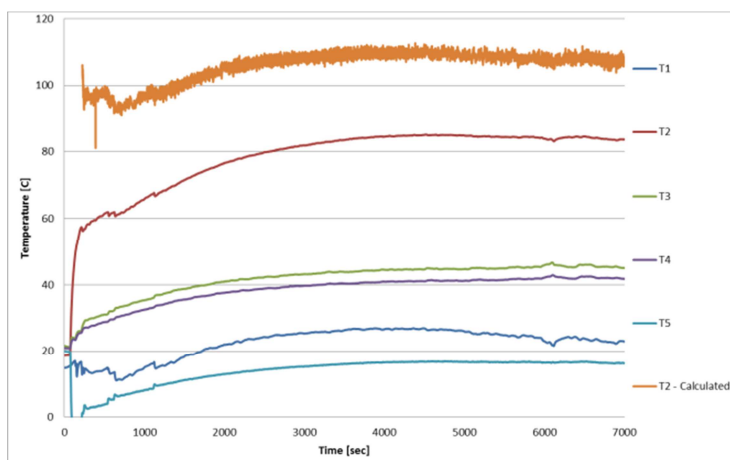


Figure 5.5-1 Measured CO₂ temperatures

The average discharge temperature of the compressor in the process is a bit lower due to a slightly smaller refrigerant charge. For the stable drying period in this experiment the pressure was around 110 Bara and discharge temperature close to 110 °C. The evaporator overheat temperature is all through the cycle from 8 to 13 K which is a bit too high, and will lower the capacity of the evaporator and increase the suction temperature of the compressor.

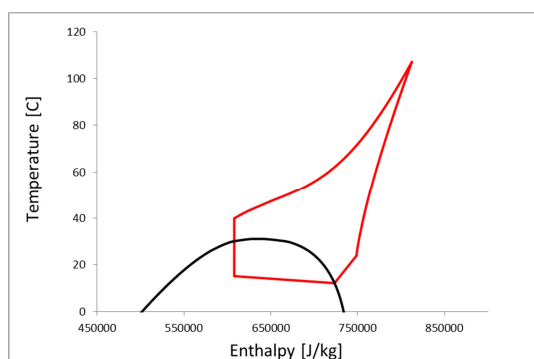


Figure 5.5-2 T-h diagram CO2 average 1000-7000 seconds

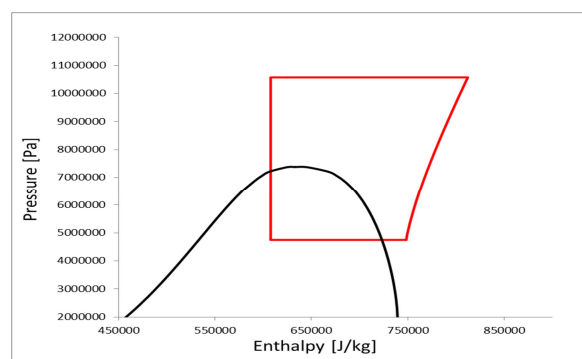


Figure 5.5-3 p-h diagram CO2 average 1000-7000 seconds

Table 5.5-1 Average values CO2: 1000-7000 seconds

Effect compressor	805,4912907	W
Effect motor	208,0392017	W
Total effect	1013,530492	W
Mass flow	0,012604501	kg/s
COP - Measured	3,220195561	
Energy savings	68,95 %	
Gas Cooler effect	2589,172802	W
Evaporator effect	1783,547262	W
Energy use	1,805308338	kWh

It is noticed that the average effect of the compressor in this experiment is 100 W less than in experiment 3, due to the lowered pressure ratio for the compressor. On the contrary with a lower pressure the temperature of the discharge gas is lower and thus the temperature in the drum is lower and the drying time is increased. The performance of the gas cooler rises up to 2600 W during the first 1000 seconds; and finishes at 2500 W at the end of the drying cycle, while the average evaporating capacity is just under 1800 W.

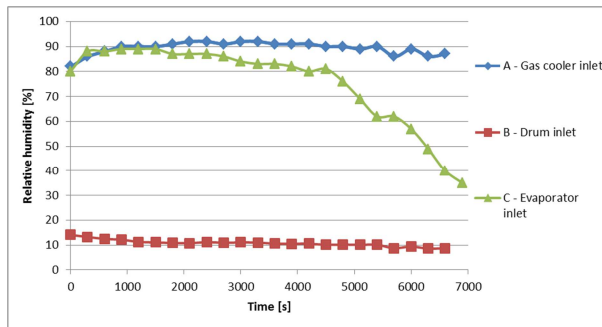


Figure 5.5-4 Relative humidity

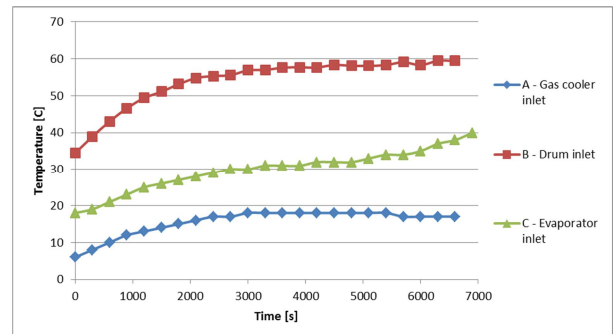


Figure 5.5-5 Air temperatures

With a drying time at 7000 seconds the energy used for the full cycle will be approximately 2.0 kWh.

An evaporating temperature stable below 20 °C and maximum overheat temperature at the compressor suction is 27-28 °C, these temperatures compared to the air conditions into the evaporator will result in water condensing throughout the drying process.

Table 5.5-2 Fabric and water

	Mass [kg]
Dry fabric	6.316
Wet fabric - loaded	9.972
Water (100 min)	2.536
Fabric at end (105 min)	6.328
Leaked water	1,120

The leakage ratio from the system is still high; in this experiment it is around 30%, which should be reduced to optimize the product further. The water content in the fabric was almost 0.5 kg higher in this experiment compared to the previous ones; this resulted in a longer drying time. The specific energy consumption is 0.548 kWh/kg_{water}.

The SMER-value calculated in the drying cycle show that the highest value is found halfway into the drying process where the drum temperature is high and the fabric surface is still moist.

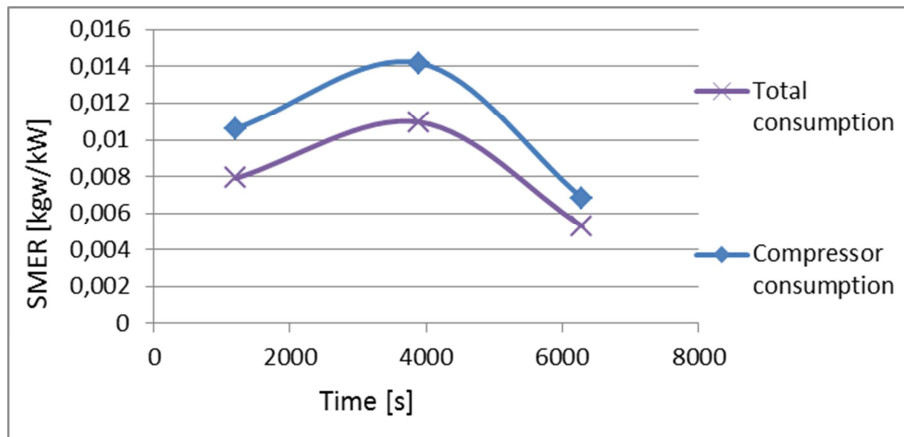


Figure 5.5-6 SMER-value

More graphs from experimental results can be found in [appendix A – Experiment 4](#).

5.6. Experiment 5: Capillary tube (660 mm), no external fan

Before starting the operation the standstill pressure in the system was stable at 53 Bara. The saturation pressure at the ambient temperature in the lab of 21 °C is 58.5 Bara which mean that the total volume of CO₂ is in gaseous state. The mass of the wet fabric loaded into the drum is 9.500 kg.

During the drying period the average discharge temperature was 110 °C with a peak towards 115 °C. The high discharge temperature is caused by a high suction temperature shown in T1. The large difference between T1 and T5 after throttling shows that the overheat temperature is relatively large.

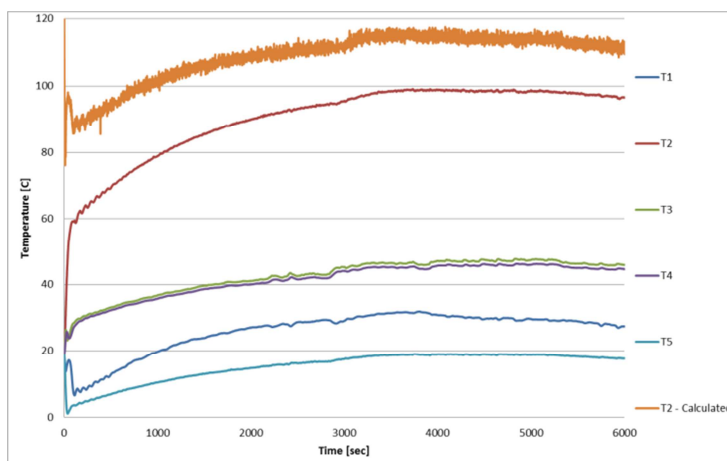


Figure 5.6-1 Measured CO₂ temperatures

The gas cooler pressure is around 110 Bara at stable operation while the evaporator is around 50 Bara throughout the cycle.

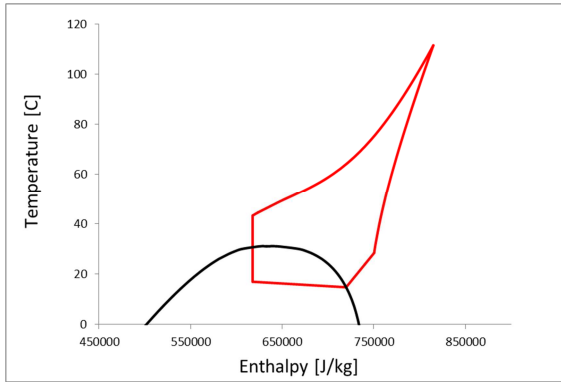


Figure 5.6-2 T-h diagram CO2 average 1000-6000 seconds

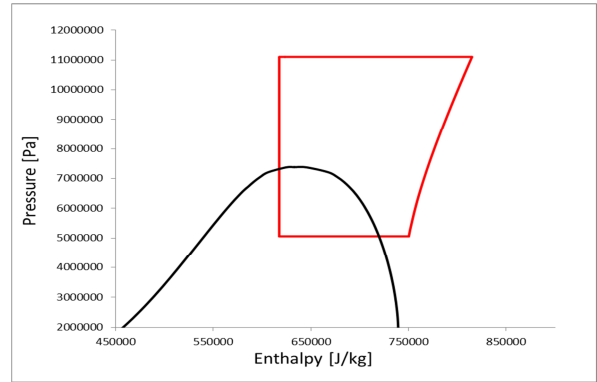


Figure 5.6-3 p-h diagram CO2 average 1000-6000 seconds

The overheat temperature for this experiment is also too high, with a evaporating temperature of 15 °C and a suction temperature of 30 °C, the conditions for the evaporator and the compressor are not optimal.

Table 5.6-1 Average CO2 values 1000-6000 seconds

Effect compressor	848,0494359	W
Effect motor	218,3773799	W
Total effect	1066,426816	W
Mass flow	0,013101845	kg/s
COP - Measured	3,07261219	
Energy savings	67,45 %	
Gas cooler effect	2597,654185	W
Evaporator effect	1749,604749	W
Energy use (100 minutes)	1,802692437	kWh

With the relative high gas cooler pressure the energy use of the compressor will be quite high. Gas cooler capacity will be at an average level around 2600 W while the evaporating capacity is stable at 1750 W.

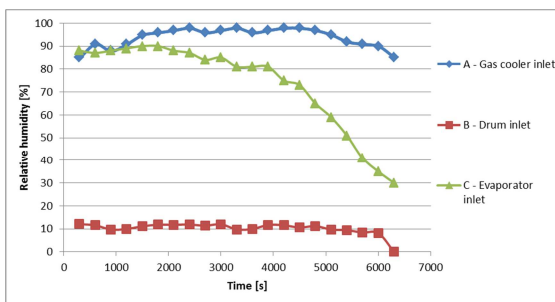


Figure 5.6-4 Relative humidity

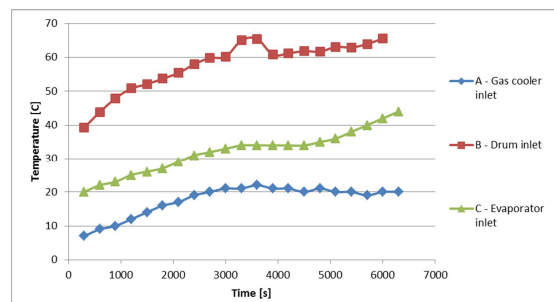


Figure 5.6-5 Air temperatures

Suction temperature above 30 °C around 4000 seconds compared to air conditions at the same time show that the dew point temperature will be lower than the surface temperature which means no effective condensing on the overheated surface.

When the process finishes after 105 minutes the total energy use in the system is 1.83 kWh, the specific energy use during the process is calculated to be 0.576 kWh/kg_{water}.

Table 5.6-2 Fabric and water

	Mass [kg]
Dry fabric	6.316
Wet fabric - loaded	9.500
Water (100 min)	1.618
Fabric at end (100 min)	6.323
Leaked water	1.566

The leakage of water is still high during a drying cycle, with above 1.5 kg not ending up in the drum there are severe air leaks in the system. This corresponds to a leakage ratio of as much as 49 %. Since previous experiment the system has been opened, covers and drum removed, this might be the reason why the leakage ratio is this large.

The SMER-value is increasing towards the highest point halfway into the drying process, when the clothes are getting dry less water is removed, while the electrical consumption is fairly stable.

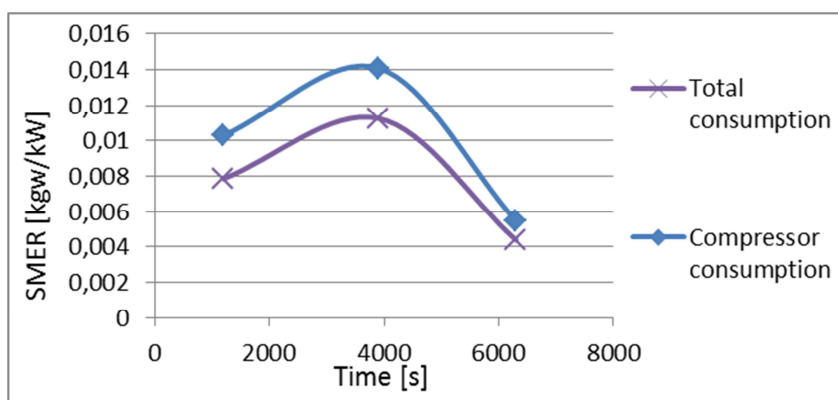


Figure 5.6-6 SMER-value

More graphs from experimental results can be found in [appendix A – Experiment 5](#).

5.7.Experiment 6: Capillary tube (660 mm) no external fan – reduced refrigerant charge

Before starting the compressor the standstill pressure in the system is reduced to 50 Bara to see how the process will react to this change.

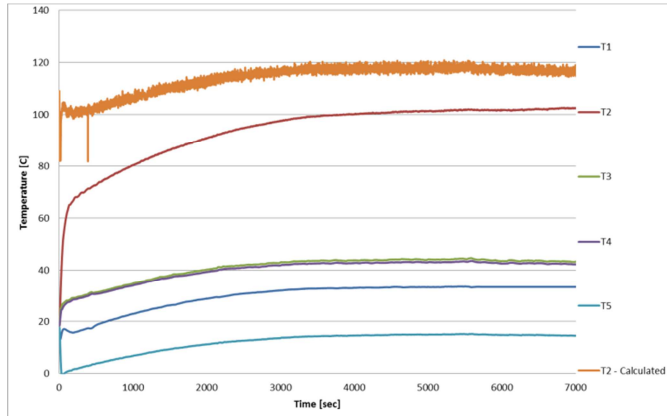


Figure 5.7-1 CO2 temperatures

With the reduced refrigerant charge the overheat temperature and thus the running conditions for the compressor will not be optimal. The energy used in the compressor will be larger than necessary.

Figure 5.7-2 Measured CO₂ temperatures

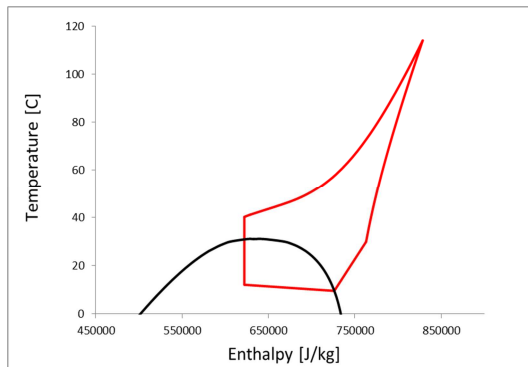


Figure 5.7-3 T-h diagram average value 1000-4000 seconds

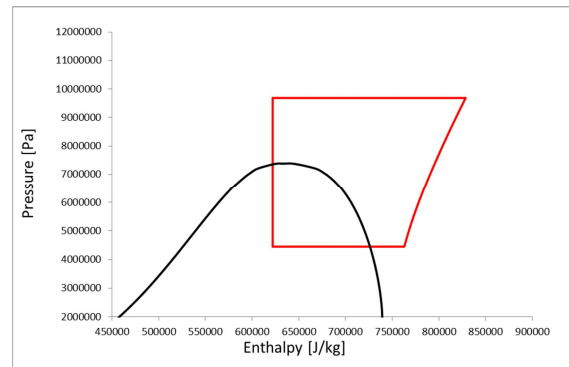


Figure 5.7-4 p-h diagram average value 1000-4000 seconds

From the Table 5.7-1 it is noticed that the effect of the compressor is reduced by over 100 W, due to the decreased mass flow. On the contrary the gas cooler effect has been decreased with 250 W and the evaporator effect with 130 W. Despite the larger decrease in the effect in the heat exchangers the COP of the heat pump has increased by 1.1 % due to the smaller energy consumption.

During the process as expected with a smaller refrigerant charge the overheat temperature was increased compared to the previous experiment. The compressor datasheet shows a maximum suction temperature limit of 32 °C, the logged data this experiment was stable around this value.

Table 5.7-1 CO₂ average values: 1000-4000 seconds

Effect compressor	741,4640374	W
Effect motor	225,1616511	W
Total effect	966,6256886	W
Mass flow	0,011303478	kg/s
COP - Measured	3,187069432	
Energy savings	68,62 %	
Gas cooler effect	2358,883142	W
Evaporator effect	1617,419105	W
Energy use (100 minutes)	1,634238037	kWh

The process finishes after 7000 seconds with the relative humidity in the evaporator inlet to be close to 30 %, and the clothing is dry. The total energy consumed during the drying process is 1.87 kWh.

During stable operation will the compressor suction temperature be around 32 °C, compared to the measured values in the air entering the evaporator and the Table B-1 Dew point table it shows that the inlet of the evaporator will not very effective for water condensation. Yet the evaporation temperature is stable at 16 °C so water will condense further in the evaporator.

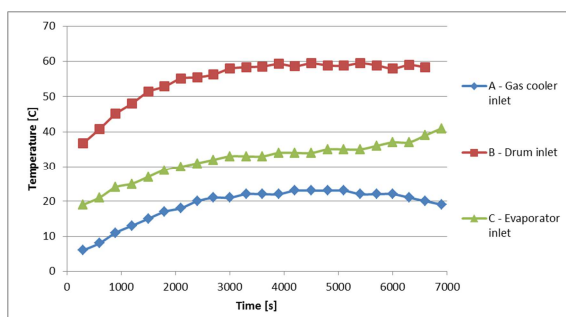


Figure 5.7-5 Air temperatures

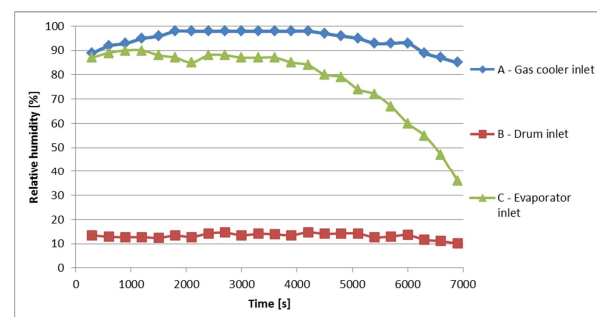


Figure 5.7-6 Air relative humidity

The estimated consumed energy related to the removed water content is 0.527 kWh/kg_{water}, while the value corresponding to the dry mass of fabric is 0.296 kWh/kg_{Dry fabric}.

Table 5.7-2 Fabric and water

	Mass [kg]
Dry fabric	6.316
Wet fabric - loaded	9.908
Water (100 min)	2.360
Fabric at end (100 min)	6.362
Leaked water	1.232

The leakage ratio from the process is still high with a percentage leak of 34% from the system.

The calculated SMER-value is low in the start and increasing towards the highest point in the middle of the drying process. At the end of the process the SMER-value is decreased below the start-up level.

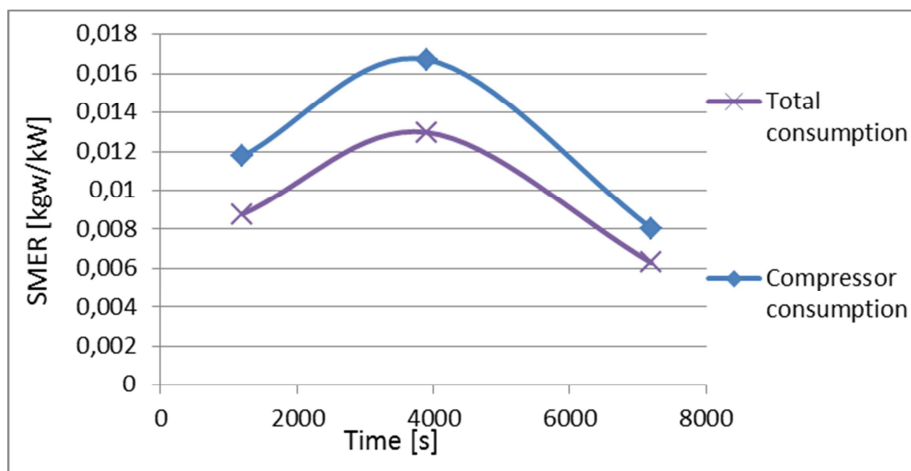


Figure 5.7-7 SMER-value

More graphs from experimental results can be found in [appendix A – Experiment 6](#).

5.8. Experiment 7: Capillary tube (660 mm) no external fan – increased refrigerant charge

To reduce drying time and the overheat temperature the refrigerant charge has been increased to a standstill pressure of 58 Bara. The drying cycle was performed with no fan to the external gas cooler and the fabric load was 9.500 kg.

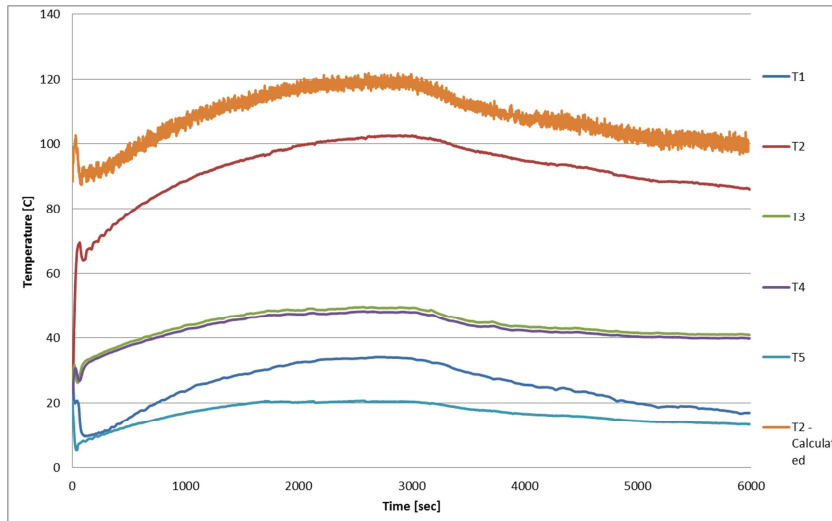


Figure 5.8-1 CO₂ temperatures

After the cycle had run for 2000 seconds the system was stabilizing at a gas cooler pressure at 120 Bara and an evaporator pressure at 50 Bara. Figure 5.8-1 shows the temperatures of the CO₂ through the drying cycle. The maximum discharge temperature during the process is just over a 120 °C, this is caused by the suction temperature above 30 °C.

The high temperature before throttling in this experiment is visualised in Figure 5.8-2, thus the gas cooler and evaporating capacity will be reduced and the throttling losses increased.

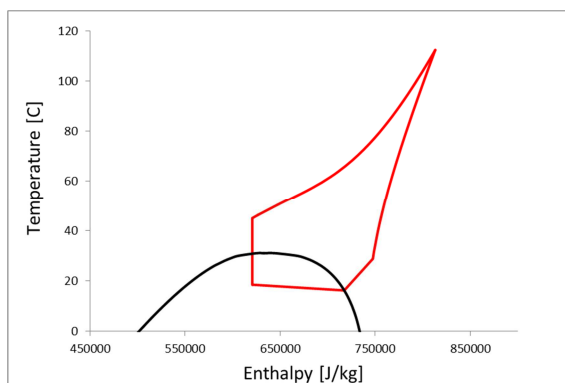


Figure 5.8-2 T-h diagram: 1000-5000 seconds

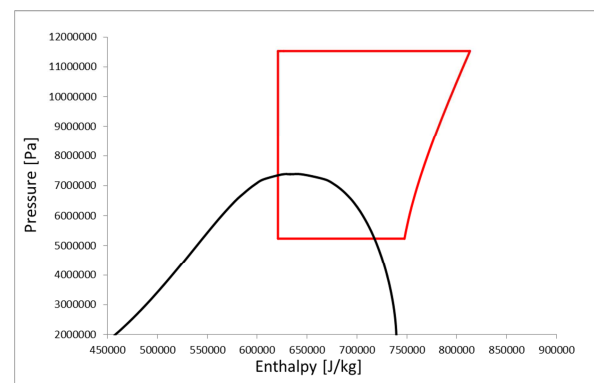


Figure 5.8-3 P-h diagram: 1000-5000 seconds

Relative high energy use of the compressor due to the extra refrigerant charge, other data of average values from 1000-5000 seconds can be found in Table 5.8-1.

Table 5.8-1 Average values 1000-5000 seconds

Effect compressor	884,5076108	W
Effect motor	216,0980716	W
Total effect	1100,605682	W
Mass flow	0,013478529	kg/s
COP - Measured	2,951811834	
Energy savings	66,12 %	
Gas cooler effect	2606,539539	W
Evaporator effect	1722,031928	W
Energy use (100 minutes)	1,696473846	kWh

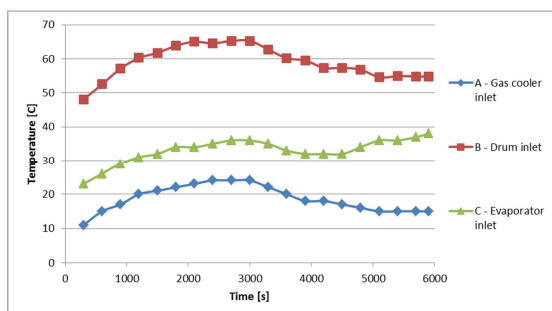


Figure 5.8-4 Temperature

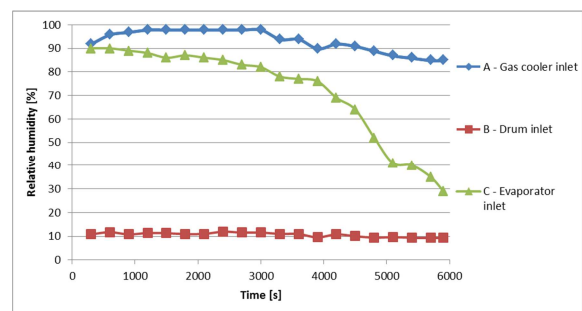


Figure 5.8-5 Air relative humidity

With the high pressure in the gas cooler the temperature at the inlet of drum peaks at close to 70 °C, with the high temperature into the wet fabric the change in absolute humidity over the drum is increased and thus the drying time is decreased to 6000 seconds. The high inlet temperature due to the high pressure will also rapidly increase the air temperature into the evaporator.

Table 5.8-2 Water and air values

	Mass [kg]
Dry fabric	6.316
Wet fabric - loaded	9.500
Water (100 min)	1.988
Fabric at end (100 min)	6.325
Leaked water	1.187

The amount of leakage from the system is still above the acceptable level with its 37% and must be reduced. The specific energy consumed related to the water content is calculated to be 0.534 kWh/kg_{Water}, while it corresponds to exact to the reference value of R134a at 0.27 kWh/kg_{Dry fabric}.

The calculated SMER-value starts low and is increasing towards the halfway of the drying process; at the end of the process it reaches its minimum value.

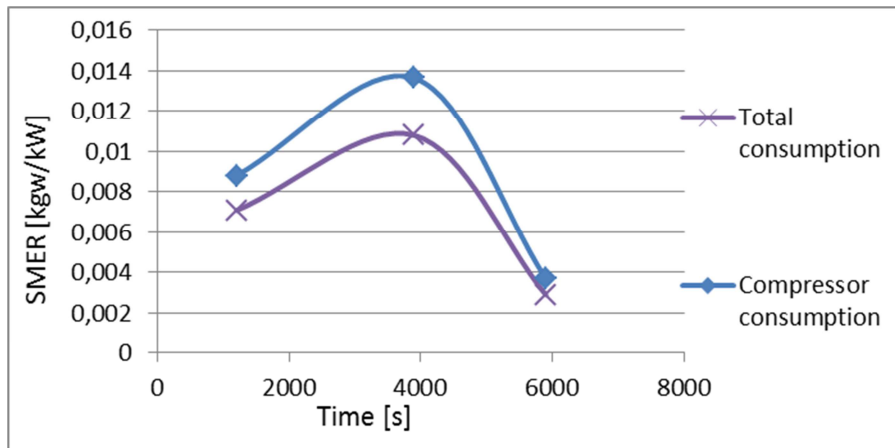


Figure 5.8-6 SMER-value

5.9.Experiment 8: Capillary tube (660 mm) external fan connected

The system standstill pressure before the drying cycle commenced is 54 Bara, which is under the saturation pressure at 20 °C. During the drying cycle the pressure stabilized after around 2000 seconds at 100 Bara, thus a temperature at the drum inlet at an average of 50 °C. The external fan was turned on during this experiment to register if there would be any positive change.

The drying drum was loaded with 9.810 kg of wet fabric, due to an inefficient centrifuge process, this is expected to increase the drying time compared to experiment 7.

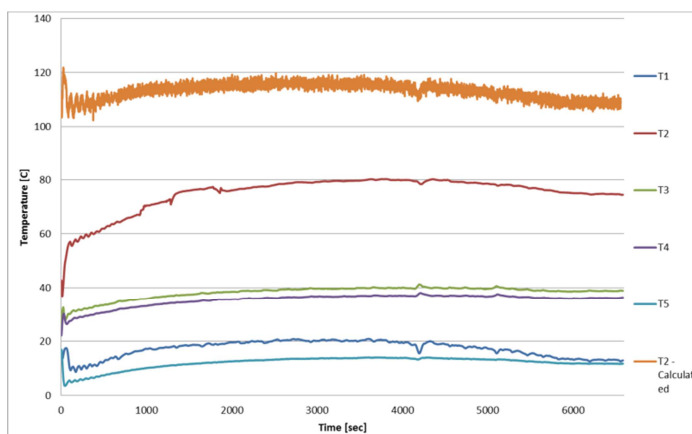


Figure 5.9-1 CO2 Temperature values

The temperature levels of the CO₂ are at average around 115 °C, which is a bit lower than the previous experiment. Evaporating temperature has stable operation at 45 Bara, and with a gas cooling pressure around 100 Bara.

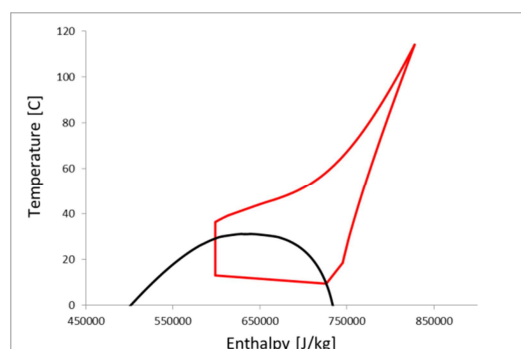


Figure 5.9-2 T-h diagram 1000-6000 seconds

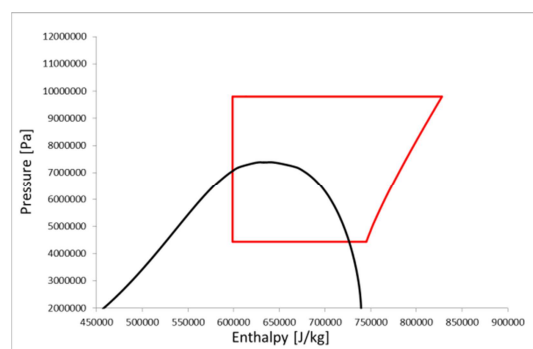


Figure 5.9-3 P-h diagram 1000-6000 seconds

The average temperature value at the outlet of the external gas cooler was 36 °C in average, in experiment 7 not using the external fan it was well above 40 °C. This leads to a larger capacity in the evaporator and gas cooler, despite a smaller flow rate. Due to the extended cooling of the refrigerant the gas cooler capacity is 240 W larger, while the evaporating capacity is over 100 W larger. With a smaller refrigerant charge as well, the electrical power consumption of over 100 W lower for experiment 8.

Table 5.9-1 Average CO₂ values 1000-6000 seconds

Effect compressor	761,498	W
Effect motor	230,494	W
Total effect	991,992	W
Mass flow	0,0124	kg/s
COP - Measured	3,744	
Energy savings	73,29 %	
Gas cooler effect	2849,416	W
Evaporator effect	1824,023	W
Energy use (100 minutes)	1,646	kWh

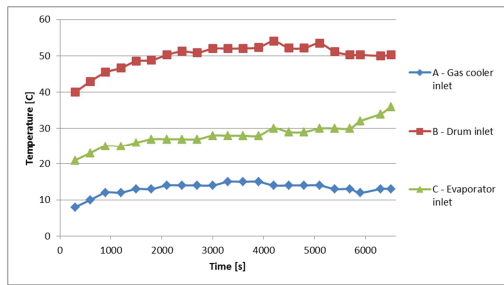


Figure 5.9-4 Air temperatures

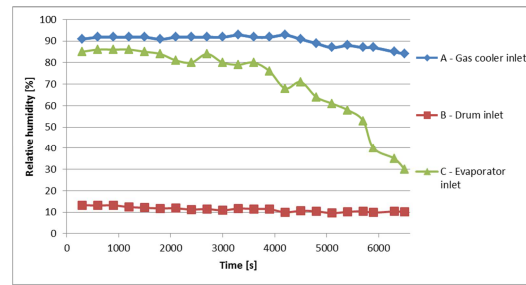


Figure 5.9-5 Air relative humidity

Looking at the temperature into the drum it shows that it is just over 50 °C, experiences from previous operations tells us that it leads to an extended running time. The experiment was ended after 110 minutes with all of the moisture extracted from the fabric and an accumulated energy use during the process of 1.85 kWh. The specific energy consumption during operation is 0.532 kWh/kg_{Water}, lower than in experiment 7.

The suction from the compressor during this drying cycle was below 20 °C and thus no problems with the dew point temperature at the inlet of the evaporator.

Table 5.9-2 Water and air values

	Mass [kg]
Dry fabric	6.316
Wet fabric - loaded	9.810
Fabric at end (110 min)	6.332
Leaked water	1.384

The leakage ratio for this experiment is as much as 39% and a focus to reduce this is important.

The SMER-value start at a relative high value and is being decreased towards the end of the cycle when the fabric is dry.

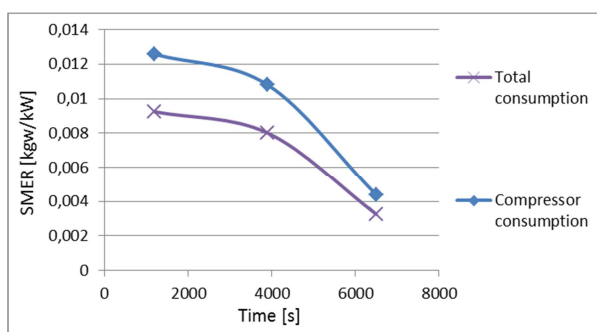


Figure 5.9-6 SMER-value

6. Discussion of initial theoretical and experimental data

The dependence on a low temperature outlet from the gas cooling process in the CO₂ transcritical process is important. To visualize this, the COP and the energy savings are shown in Figure 5.9-1 and Figure 5.9-2 respectively. Figures are based on data from Table 5.9-1 Assumptions COP calculations and CO₂ calculations have been performed with RnLib add-on in Excel. The enthalpy at the compressor outlet have been calculated with definition from (Moran, et al., 2006) shown in Table 5.9-1. And from the enthalpy the temperature has been deduced.

Table 5.9-1 Assumptions COP calculations

Assumptions		
Factor	Value	Unit
Evaporation temperature	15	°C
Superheat	5	K
Compressor isentropic efficiency	0,5	-

Calculated with RnLib software the COP and energy savings for a CO₂ cycle have been deduced, pressures from critical pressure to 125 Bara have been considered.

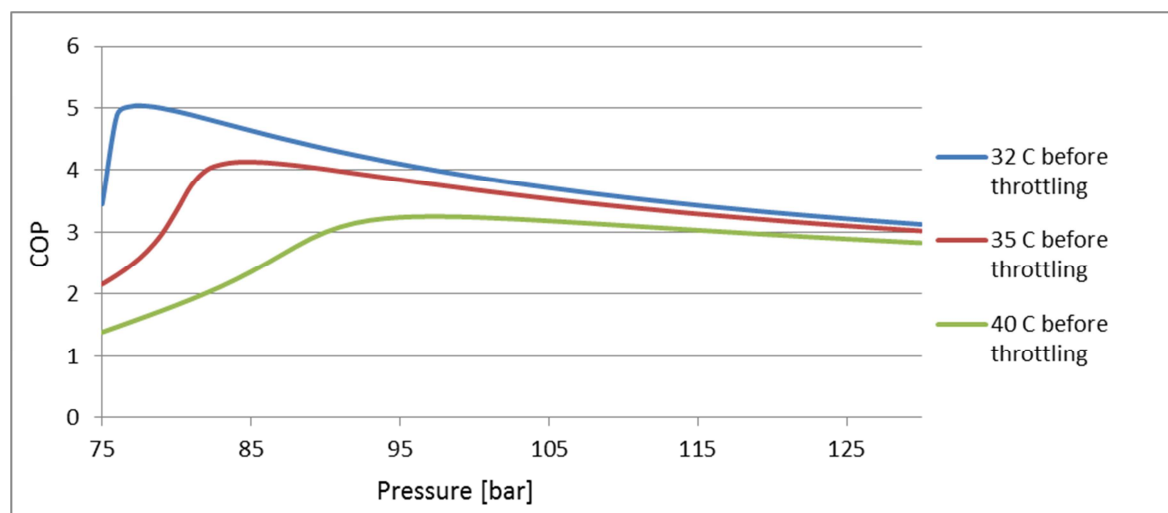


Figure 5.9-1 COP varying gas cooler outlet temperature

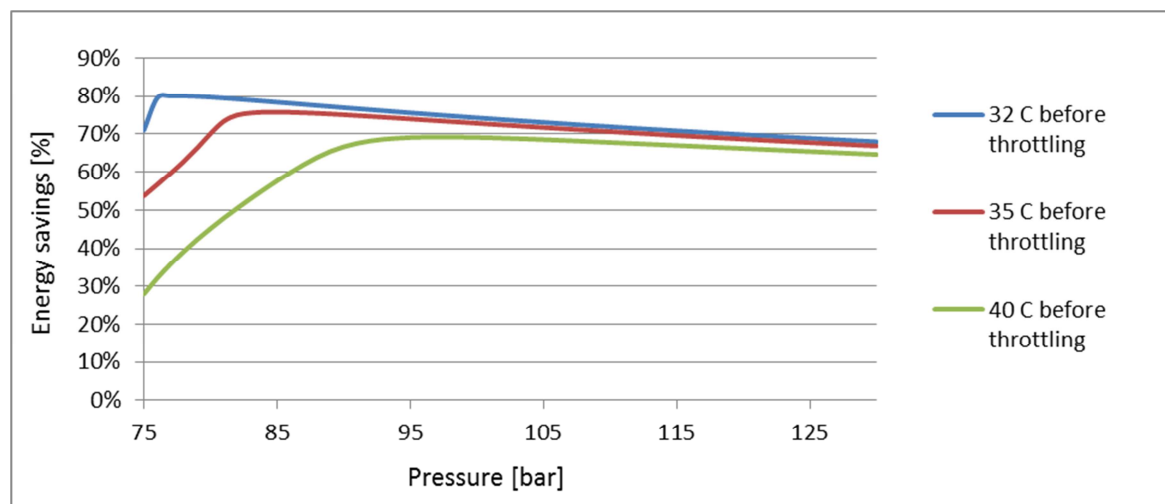


Figure 5.9-2 Heat pump energy savings, with varying gas cooler outlet temperatures

The relation between the COP and the energy savings can easily be seen in Figure 5.9-1 and Figure 5.9-2, the figures shows that the COP reaches a maximum value at a certain gas cooler pressure when the throttling temperature is fixed. For increasing pressures above the optimal the COP will slowly be reduced, on the other hand when the pressure is decreasing from the optimal point the COP will then reduce with a steep slope. Looking at 40°C before throttling around 95 Bara gas cooling the COP is around 3.2 and the energy savings will be close to 70 %. If the COP is increased to 4, the energy saving will only increase to 75%, however if the COP drops to 2.4 the energy savings will be 58%. This shows that the COP value will influence the energy savings much more at lower values than on higher COP values.

Discussion of experimental values

During the experiments different throttling devices have been used, change in the refrigerant charge, altered length of the capillary tube and inclusion of the external fan. By changing the factors in the experiments the measured pressure and temperatures of the CO₂ have varied with a large margin. When the pressure in the gas cooler is rising the temperature of the CO₂ at the compressor outlet will rise and so will the air into the drum. The pressure level in experiment 2 where the average gas cooler pressure is at 95 Bara is the temperature of the inlet air into the drum is just above 50 °C. While the total drying time is 115 minutes and 1.90 kWh consumed. Looking at experiment 7 with a gas cooler pressure just above 120 Bara the air temperatures rises above 65 °C and the drying time is reduced to under 100 minutes. With the high pressure in the gas cooler a higher pressure ratio, thus more energy needed for the compressor, but the gain from the reduced drying time gives a total consumption of 1.70 kWh in experiment 7.

Continue to look at the COP-value of experiment 2 and 7 the average value with high pressure is 2.4 while it is 2.6 for low pressure for the total consumption. During the process the heat pump under high pressure will not operate as efficient as for the low pressure operation, however the slight difference in performance during the first 100 minutes does not cover the extended drying time at experiment 2.

The process in experiment 2 has an average total effect of 974 W, which means every minute in extra drying time will add 0.016 kWh. If the system runs for another 15 minutes it consumes almost 0.25 kWh additionally, thus a focus to reduce drying time is important.

Comparing experiment 7 and 8; where in experiment 7 the pressure is high and no external fan is used and in experiment 8 where the fan is used and the pressure is lower. As presented earlier in the report the importance of the cooling of the refrigerant before throttling. This will be represented with a small example from the results. The average temperature before throttling in experiment 7 is 42.5 °C while it is 35.5 °C in experiment 7. With a ΔT of 7 K increased temperature before throttling in experiment 8 it will correspond to a decreased gas cooler capacity from 2850 W to 2367 W, while the evaporating capacity goes from 1720 W to 1350 W. This shows that by operating a process that is able to cool down the refrigerant sufficiently is very important. The extended capacity in the evaporator is the most important because this will be applied directly in the air process to decrease the drying time. While a great deal of the extra capacity in the gas cooler will only be disposed to the ambient air.

During the experiments the dew point temperature has been discussed at the inlet of the evaporator. Generally through the experiment it is observed that if the suction temperature is below 30 °C, there will not be any problems with non-condensing evaporator surfaces. However with high suction temperatures when the humidity content is reduced to around 60 %, the air temperature needs to be higher than 40 °C for the surface to still be effective.

Generally speaking of the experiences during the testing of the system is that the drying time is really important to maintain the energy use at an acceptable level. The most energy efficient experiment was number 7, where the pressure was above 120 Bara and thus a high temperature of the air into the drum. With operations with gas cooler pressures below 100 Bara the temperature is too low and drying time is increased close to 2 hours. The measured COP of the process in experiment 7 with the high gas cooler pressure is below 3, due to the high energy use in the process. The process in experiment 7 has a COP of the heat pump above 3.7 which imply over 73% in energy savings. In experiment 8 the fabric load was almost 0.5 kg higher than in experiment 7, this is a

reason why the energy used here are higher. In further testing of the prototype more experiments on gas cooler pressures around 115-120 Bara should be performed, since this seems to be the most energy effective set-point. As for the R134a cycle the process air into the drum should be around 55 °C, and with CO₂ as refrigerant this is made really easy by increasing the gas cooler pressure.

The experiments has shown that the potential of drying a 10 kg batch of wet clothes during 100 minutes is absolute possible. None of the experiments have a leakage ratio less than 29%, even though the connections were fixed to improve this value it was not possible to reduce it further.

The refrigerant charge calculations in the theoretical part of the process indicated that the total charge should be just above 0.200 kg, but when the system was started up a charge above 0.400 kg was required to get high enough pressures. However during all operation there was no standstill pressure above the saturation pressure for the current temperature in the laboratory, thus no risk of liquid slug to the compressor.

Compressor

The compressor used in the experiments is an Embraco EK6214CD built for R744. The compressor is running very smoothly and does not produce a large amount of noise. In this result section the compressors power factor, isentropic and volumetric efficiency are presented.

During an experiment the Clamp on Hitester was connected to the compressor source. The system was running on 120 Bara in the gas cooler and 50 Bara in the evaporator. From the display on the instrument the power factor was stable between 92-94%, which is very good for such small motor.

Throughout the experiments all data on pressures and energy consumption have been logged every second running the system. The logged values are based on different mass flows since they are obtained from 8 different experiments. One dot on the figure is calculated as the average value over 500 seconds from each experiment, then the results was sorted based on the pressure ratio and presented as seen below.

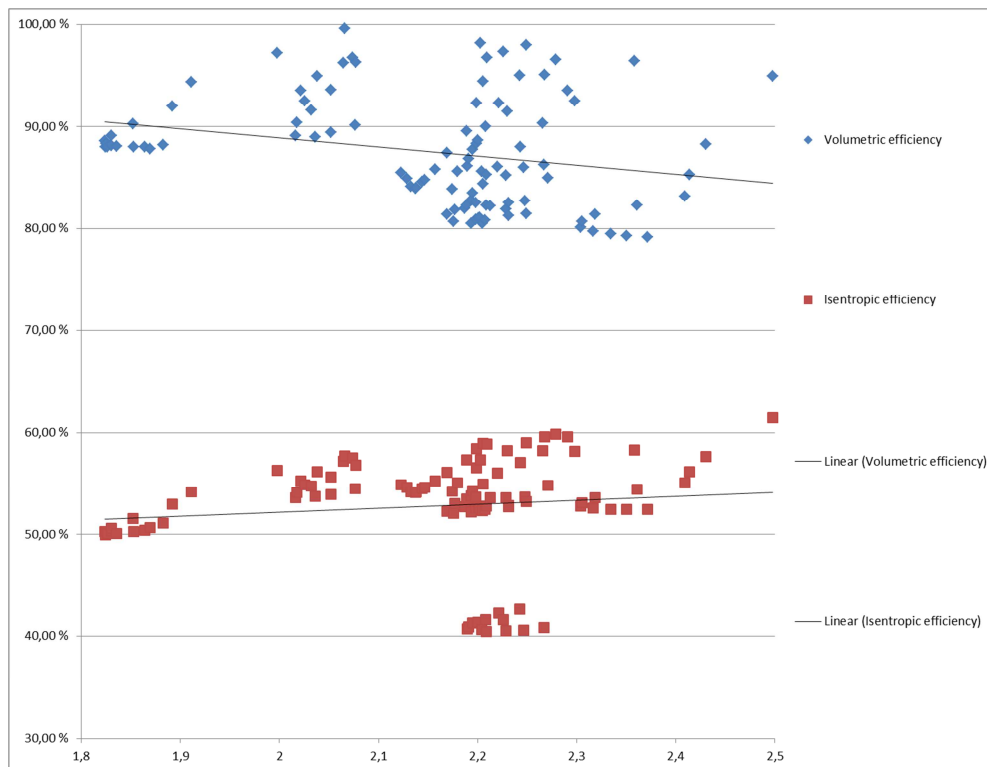


Figure 5.9-3 Isentropic and volumetric efficiency Embraco EK6214CD

It is seen in the figure that the volumetric efficiency of the compressor is very large; an average value around 85%, and decreasing for higher pressure ratio. The isentropic efficiency has an average registered value of 53%. The low values of the isentropic efficiency around a pressure ratio of 2.2 are all from experiment 8; the gas cooler pressure in this experiment was on average around 100 Bara, but the temperature at compressor discharge close to 120 °C. The relative high temperatures compared to the gas cooler pressure might be related to lubrication of the compressor. During operation of the system there have been several occasions with oil leaking from the system along with CO₂. With a less efficient lubrication the compressor will have to work harder than optimal.

These values are important for this specific prototype, but for the next prototype a new compressor that will fit in the system should be applied.

Heat exchangers

In [section 2.2.2](#) the performance of the heat exchangers have been discussed from the data obtained in HXSIM Basic 2007. The refrigerant side of the main gas cooler has been visualised for pressures from 80 to 120 Bara in Figure 2.2-4. With a constant refrigerant flow of 0.015 kg/s, the performance is fairly linear from 1400 W at 80 Bara and reaches 2800 W for 120 Bara. Comparing these results with experiment 1 at 95 Bara shows a performance of around 2400 W with a mass flow of 0.0143 kg/s. This shows that for 95 Bara the simulation software will return a smaller value in the

simulation compared to the gas cooler in the prototype. Looking at experiment 4 with a gas cooler pressure of 110 Bara, the performance of the main gas cooler is measured to be 2600 W with a refrigerant flow of 0.0127 kg/s. The simulated values for 110 Bara and 0.015 kg/s show a performance of 2500 W, thus roughly equal values. For 120 Bara the performance from the simulations are 2800 W, this is also the value at the same gas cooler pressure in experiment 7 with a mass flow of 0.0141 kg/s. The air side of the gas cooler is also deviating with a large margin. While the air temperature in the experiments will be around 50 °C when the pressure is 95-100 Bara and up to 65 °C for pressures around 120 Bara, the air temperatures from the simulations are much higher. Only at gas cooler pressures at 80 Bara will the simulated air temperature be below 60 °C, while for 120 Bara the temperature was close to 90 °C.

From the first two experiments it was looked at the performance of the external gas cooler with the external fan turned on or off. The fan has an effect of 33.4 W which will consume 0.056 kWh during a cycle of 100 minutes. The average performance of the external gas cooler during the process without the fan running is 240 W with 0.0145 kg/s mass flow. For experiment 2 with the fan running is the performance of the heat exchanger increased to 300 W with an average mass flow of 0.0140 kg/s. Linearly scaled to a mass flow of 0.0145 kg/s the performance will be 310 W. Comparing these results to the performance simulations they vary between 260 W and 290 W with a mass flow of 0.015 kg/s. Consequently the results of the gas cooler performance with the fan running will be up to 50 W larger in the prototype than for the simulated values.

Another consideration for the external gas cooler is the increased evaporating capacity with the increased cooling of the high pressure gas. This results in a 5 minutes shorter drying time than for the experiment not using the fan. Experiment 1 without the fan finishes after 7500 seconds with a total consumption of 1.96 kWh, while experiment 2 finishes after 7200 seconds with a total consumption of 1.99 kWh.

The evaporator performance with the simulation software shows an average performance from 2000 W to 2100 W with gas cooler pressures varying from 80 to 120 Bara. Results from the experiments show that the performance of the evaporator while in the most stable operation of the drying cycle will vary from 1700 W to 2100 W. These values will be slightly difficult to compare when the overheat temperature at the evaporator outlet will vary with a large margin; while the simulated overheat temperature is constantly 5 K. Also the evaporating pressure during the experiments will deviate from the constant value of 45 Bara in the simulation.

Expansion devices

During the experiments both the manual expansion device and the capillary tube have been applied. The first two experiments were performed using the manual expansion valve while the rest of the experiments used the capillary tube of varying length.

In [section 2.2.3.1](#) the flow coefficient or the Cv-value for the chosen valve is calculated to determine the relation between the turns to open and close to the mass flow. It was observed during the first two experiments that when the valve was turned towards open or closed it had an instant effect on the heat pump cycle. During the first two experiments the chosen valve seemed to behave exactly how it was foreseen. The valve is sized for a Cv-value up to 0.04 and looking in Table 2.2-12 for calculated Cv-values for different flow rates; the theoretical calculations are correct.

The remaining experiments have been performed to find a set-point for the heat pump with a correct length of the capillary tube. The first chosen length of the tube was 900 mm; this was chosen based on calculations in [section 2.2.3.2](#). With small inner diameter as for the capillary tube of 0.9 mm, and with running conditions that would vary with the refrigerant charge the capillary tube was over dimensioned for the for the first experiment. This was performed due to the practical aspect of cutting the tube in contrast to add more length to the tube. When the capillary tube was removed for adjusting; the system was emptied, the adjusted tube length was installed and a vacuum pump applied to remove air from the system. When the refrigerant was refilled into the system some deviations in the measured mass flow was observed. However in Figure 5.9-4 the pressure ratio for a specific mass flow is shown, it shows that the pressure ratio is much higher for the 900 mm tube than for the 660 mm tube. The average value for the 900 mm capillary tube is 2.47, while for 740 mm it is 2.28 and 2.18 for the 660 mm tube. With a smaller pressure ratio the compressor work is lowered and the COP is increasing.

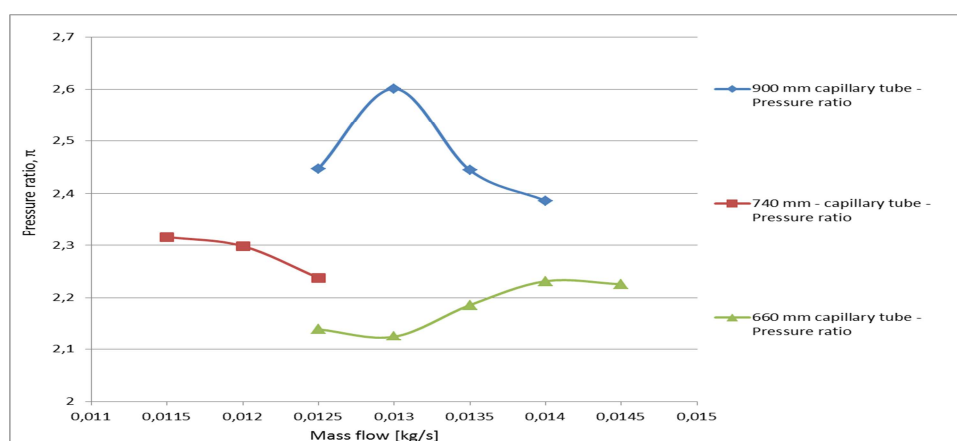


Figure 5.9-4 Capillary tube pressure ratio

7. Evaluation of control strategies

A regular tumble dryer is a cheap investment, but high in energy use, thus operational costs will be high. For a heat pump dryer the investment will be increased, but a potential energy saving of 70% will reduce the operational costs a great deal. The average consumer looks first at the investment cost of an appliance then to the reduced operational costs and then to environmental aspects. Therefore an economical focus on the components for the system is important; there are not room financially to invest in components to vary the compressor load or a thermostatic throttling valve.

The simple design of the current prototype will have a certain size of the compressor to determine the capacity, a certain length of the capillary tube to determine the pressure drop and a certain refrigerant charge to determine the pressure levels and the overheat. Thus there are no possibilities in the prototype for any other operation than a start-up and a turn off when finished. The procedure used in the experiments has been to use the relative humidity measured at the evaporator inlet to know when the fabric is dry. However to find a humidity transmitter that will be robust and cheap enough for a market model will be tough.

A control of the temperature at the inlet of the drum is directly dependent by the gas cooler pressure and the isentropic efficiency of the compressor. The chosen refrigerant charge will determine the gas cooler pressure for operation, thus the temperature levels. If the drying fabric is sensitive to high temperatures and there is a demand of lower temperatures it will affect the drying time and thus the energy use. By applying the fan to the external gas cooler the temperature will be reduced, however not by a large margin. Moving the external gas cooler in front of the main gas cooler can be an alternative to more directly control the temperature of the drum inlet air. However by reducing the temperature of the air into the drum will affect the drying time and increase the energy used. The external fan could also have a possibility of being controlled by the maximum temperature into the drum. A control like this would preserve the quality of clothes that have maximum temperature limits.

An easy way to control the system will be to have a time control for the drying cycles based on clothing load. With sufficiently experiments with varying clothing loads on the chosen system configuration it will be possible to determine an average time to dry a certain clothing load.

The most important for a control system is that it will do its purpose and not reduce the energy efficiency of the system by a large manner. If new components like temperature and humidity sensors will be used it is important that the components installed are robust and do not reduce the lifetime of the dryer.

8. Conclusion

Heat pumps in are for sure a way to optimize drying appliances, by making it possible to use both the heating capacity and the cooling capacity in the drying process it is very advantageous. When it comes to choosing CO₂ as refrigerant for this small appliance there are solely a great potential. The energy used during a drying process will vary from 1.70 kWh to 2.0 kWh while the drying time will be varying from under 100 minutes for high gas cooler pressures to 130 minutes for lower pressures.

To get the best operation with the largest energy savings and the shortest drying time it can be concluded that by running the compressor at a pressure that forces the temperature at the drum inlet to become 55 °C and above will increase the drying rate at a large manner. This will result in a decreased drying time of the operation. This requires normal compressor operation gas cooler pressures at 110 Bara and above.

The evaporating pressure should be kept from 45-50 Bara to experience an optimal condensation of water on the surface. While the suction temperature of the compressor should be kept below 25 °C at any point to assure that the total area of the evaporator will be used to condense water.

The use of the external fan showed the increased evaporating capacity will improve the evaporating capacity sufficiently. This is recommended to continue to use for further prototypes, as well as the effect of different ambient temperatures.

The system has been operated using the capillary tube without any problems during operation, the oil return and the heat transfer conditions in the evaporator and the gas cooler was unproblematic. This shows that the flow speed in the external gas cooler is high enough to return the oil to the compressor which seemed to be a potential problem initially due to the top to down flow distribution.

The unproblematic operation is also an indication that the system does not need expensive controlling to maintain the overheat temperature fixed or frequency control of the compressor. The compressor runs very smoothly without large amounts of noise, even at tough working conditions.

It is recommended in this first stage to continue to use the chosen capillary tube of 660 mm since this gave the largest energy savings and the shortest drying time. With a new smaller core size compressor placed inside the chassis and a new dryer to place the CO₂ system inside the results can be more exact. Comparing the specific energy use in Appendix C and D with data from both CO₂ and R134a respectively; it shows that the R134a system will use 0.31 kWh/kg_{dry fabric} while the best

experiment from the testing with CO₂ showed a specific energy use of 0.36 kWh/kg_{dry fabric}. These values are corrected from EN 61121:2005.

9. Suggestion of further work

To optimize the drum dryer it should from the start of the project be based on an economic aspect, this means that the components and the running of the system should be designed to be as simple and stable as possible.

For the optimal operation of the system also based on the financial aspects of the total system the expansion process should be working as simple as possible. This means that the system should be optimized with a capillary tube as throttling device. To optimize the capillary tube the length and the refrigerant charge of the system must be in a correct balance. The capillary tube will determine the pressure drop over the heat exchangers. The further optimizing of the system should be based on results presented in this report.

The capacity of the compressor used in this first prototype is correct dimensioned related to displacement volume, however the outer dimensions of the compressor is too large to fit within the chassis. To further optimize the system for a sales purpose it must of course be with a compressor that fulfils the capacity demands and fits within the chassis. Therefore more work should be done contacting manufacturers of small displacement compressors for CO₂ purposes. Before commencing more experiments with the current compressor, the oil ratio should be evaluated. The compressor was delivered with 150 cm³ oil, but due to leakages and several procedures to empty the system the content has been reduced extensively.

Further work should be on the external gas cooler capacity; this report only tests the external gas cooler for a single ambient temperature. The results registered from the external gas cooler is positive; by applying it the evaporation capacity will be increased extensively and this will decrease the drying time of the total system. In the laboratory the registered temperature was from 19-22 °C fairly stable and experiences with the simulation results says that with lower ambient temperatures will the effect of the external gas cooler be increased a great deal. It is therefore suggested to test the system in controlled ambient temperatures to see how large effect it will have to place the system in a location with lower temperature.

Unfortunately the measured temperature at the discharge of the compressor seems to have a rather large deviation from the value it was supposed to have. The error in this was not found so the temperature was calculated from the values of the isentropic efficiency calculated from the electrical consumption. A suggestion can be to drill a hole in the copper tube and insert the

thermocouple in the high pressure stream, this was considered during the building procedure, but was found to be unnecessary due to the good heat conduction in the copper tube.

For the next prototype the model should be implemented into a new cabinet to find source of the air leakages. Through extensively work on air tightening of all connections is has not been possible to get the value reduced enough. However the heat exchangers used in this first prototype seems to be working as they supposed to and should be used for further prototypes.

The results presented in this report should be used as a basis to do more experiments on the system, make the repeatability of the experiments better since this have not been the main focus in this report. Also due to the large errors in the measured temperature values discovered more experiments should be performed before publishing the results. An article draft will be presented in in the attachments of this report.

References

- ©2011 SensorsONE Ltd SensorsONE [Online] // Pressure Measurement Instrumentation. - 26 09 2011. - <http://www.sensorsone.co.uk/pressure-measurement-glossary/gauge-reference-pressure.html>.
- Bansal P. K., Braun J. E. and Groll E. A.** Improving Energy Efficiency of conventional tumbler clothes drying systems [Article] // International Journal of Energy Research. - [s.l.] : John Wiley & Sons Ltd., 2001. - Vol 25. - Issue 15 : Vol. 2001. - pp. 1315 - 1332.
- Bhattacharyya J., Gopal Ram M and Sarkar J** Optimization of a transcritical CO₂ heat pump cycle for simultaneous cooling and heating applications [Article] // International journal of refrigeration. - [s.l.] : Elsevier, 2004. - pp. 830-838.
- Bison Alberto, Fornasieri Ezio and Minetto Silva** Home laundry dryer [Report] : Patent document. - [s.l.] : World International property Organization, 2007. - WO 2009/065538.
- Colak Neslian and Hepbasli Arif** A review of heat pump drying: Part 1 – Systems, models and studies [Article] // Energy Conversion and management. - [s.l.] : Elsevier, 2009. - 50. - pp. 2180-2186.
- Colver Gerald M. and Bassily Ashraf M** Performance Analysis of An Electric Clothes Dryer [Article] // Drying Technology, 21. - [s.l.] : Taylor & Francis, 2003. - pp. 499-524.
- Copeland Corporation** Power Factor Correction [Journal]. - [s.l.] : Copeland, 1994. - Application Engineering Bulletin AE-1249-R9.
- Dekker Marcel** Handbook of industrial drying [Book]. - New York (USA) : Mujumdar AS, 1987.
- Dr. Drog Manfred** Dealing with uncertainties - guide to Error Analysis - 2ed [Book]. - [s.l.] : Springer-Verlag Berlin Heidelberg, 2009.
- Kim Man-Hoe, Pettersen Jostein and Bullard Clark W** Fundamental process and system design issues in CO₂ capor compression systems [Journal] // Progress in Energy and Combustion Science. - Trondheim, Norway : Elsevier, 2004. - Vol. 30. - pp. 119-174.
- Klöcker K, Schmidt E L and Steimle F** Carbon dioxide as a working fluid in drying heat pumps [Article] // International journal of refrigeration. - 2001. - 24. - pp. 100-107.
- Lambert J. D., Spruit F. P.M and Claus J** Modelling as a tool for evaluating the effects of energy-saving measures. Case study: A tumbler drier [Book]. - Eindhoven : Elsevier Science Publishers Ltd, 1991. - Vol. Applied Energy 38 : pp. 33-47.
- Li Minxia [et al.]** Analysis of CO₂ Transcritical Cycle Heat Pump Dryers [Article] // Drying Technology. - Tianjin, China : Taylor & Francis Group, LLC, 2009. - Thermal Energy Research Institute, Tianjin University : Vol. 27. - pp. 548-554.
- Madsen B Kenneth, Poulsen S. Claus and Wiesenfarth Maike** Study of capillary tubes in transcritical CO₂ refrigeration system [Journal]. - Århus : Elsevier, 2005. - International Journal of Refrigeration : Vol. 28.

Moran Michael J and Shapiro Howard N Fundamentals of Engineering Thermodynamics [Book]. - Southern Gate, Chichester, West Sussex : John Wiley & Sons Ltd, 2006. - 5 : p. 248. - Formula 6.50.

Schmidt E L [et al.] Applying the transcritical CO₂ process to a drying heat pump [Book]. - Essen, Germany : Elsevier, 1998. - Vol. International journal of refrigeration 21 : pp. 202 - 211.

Stene Jørn Varmepumper Grunnleggende Varmepumpeteknikk [Book]. - 1997. - 4. - 82-14-00397-0.

Strømmen Ingvald [et al.] Low temperature drying with heat pump new generations of high quality dried products [Journal]. - Trondheim : [s.n.], 2002. - 13th International drying symposium.

Swagelok Valve sizing - Technical Bulletin [Report]. - [s.l.] : Swagelok Company, 2007.

Thermometrics - Precision Temperature Sensors [Online] // ThermometricsCorp. - 26 09 2011. - <http://www.thermometricscorp.com/thertypt.html#>.

Valero Paolo, Zgliczynski Marek and Casamassima Renzo Heat pump laundry dryer: R134a and environmental friendly alternatives [Article] // The latest technologies in air conditioning and refrigeration industry. - 2009.

Table of figures

Figure 1.1-1 Heat pump and dryer cycle.....	3
Figure 1.3-1 Transcritical CO ₂ cycle, gas cooler pressure of 100 bar	7
Figure 1.3-2 Volumetric refrigeration capacity vs. temperature	9
Figure 1.3-3 Temperature loss vs. pressure loss.....	9
Figure 1.4-1 Carbon dioxide heat pump dryer (Klöcker, et al., 2001)	10
Figure 1.4-2 – h-x-Chart of the drying process; based on (Klöcker, et al., 2001)	12
Figure 1.4-3 Energy saving potential (ESP) vs. effectiveness (Klöcker, et al., 2001).....	13
Figure 1.4-4 Drying progress	14
Figure 2.1-1 Complete system – inside	16
Figure 2.1-2 Complete system - outside	16
Figure 2.2-1 Compressor outer dimensions.....	17
Figure 2.2-2 Compressor EK 6214CD	17
Figure 2.2-3 Compressor working envelope	23
Figure 2.2-4 Gas cooler simulated performance	26
Figure 2.2-5 Gas cooler inlet and outlet air temperatures	26
Figure 2.2-6 Gas cooler inlet and outlet relative humidity	26
Figure 2.2-7 Main gas cooler flow distribution	27
Figure 2.2-8 Gas cooler HXsim 2007 visualisation	27
Figure 2.2-9 Main gas cooler #1.....	27
Figure 2.2-10 Main gas cooler #2.....	27
Figure 2.2-11 Main gas cooler manufacturer data #1	27

Figure 2.2-12 Main gas cooler manufacturer data #2	27
Figure 2.2-13 External gas cooler effect	28
Figure 2.2-14 External gas cooler inlet and outlet refrigerant temperature	29
Figure 2.2-15 External gas cooler performance.....	29
Figure 2.2-16 Gas cooler HXsim 2007 flow distribution	29
Figure 2.2-17 Gas cooler HXsim 2007 visualisation	29
Figure 2.2-18 External gas cooler #1.....	30
Figure 2.2-19 External gas cooler #2.....	30
Figure 2.2-20 External gas cooler manufacturer data #1	30
Figure 2.2-21 External gas cooler manufacturer data #2	30
Figure 2.2-22 Evaporator air temperature.....	31
Figure 2.2-23 Evaporator capacity.....	31
Figure 2.2-24 Evaporator HXsim 2007 visualisation	32
Figure 2.2-25 Gas cooler HXsim 2007 flow distribution	32
Figure 2.2-26 Evaporator #1	33
Figure 2.2-27 Evaporator #2	33
Figure 2.2-28 Evaporator manufacturer data #1	33
Figure 2.2-29 Evaporator manufacturer data #2.....	33
Figure 2.2-30 Flow rate through a fixed orifice	34
Figure 2.2-31 Valve flow rate calculations.....	34
Figure 2.2-32 High and low pressure drop flow.....	35
Figure 2.2-33 Low pressure drop flow	36
Figure 2.2-34 High pressure drop flow	36
Figure 2.2-35 Swagelok SS-31RS4	38
Figure 2.2-36 Flow coefficient vs. turns to open	38
Figure 2.2-37 Capillary tube pressure drop	42
Figure 2.2-1 Electrical connections and instrumentation locker	44
Figure 3.1-1 Instrument overview	45
Figure 3.1-2 T-type thermocouple	46
Figure 3.1-3 4-Channel, 14 S/s, 24-Bit, ± 80 mV C Series Thermocouple Input Module NI 9211.....	47
Figure 3.1-4 T-type maximum error using NI9211.....	48
Figure 3.1-5 Druck PTX-510.....	48
Figure 3.1-6 Druck PTX 1400.....	50
Figure 3.1-7 Rheonik RHM 04 - Coriolis Mass Flow meter with fast response.....	52
Figure 3.1-8 Flow meter error.....	53
Figure 3.1-9 Rheonik RHE 08 Advanced transmitter	53
Figure 3.1-10 Vaisala HMP 235 Temperature and humidity transmitter	54
Figure 3.1-11 KIMO AMI 300 Temperature and humidity transmitter.....	54
Figure 3.1-12 L-unit LWT Watt Transducer.....	56
Figure 5.1-1 Drying cycle air temperature	63
Figure 5.1-2 Drying cycle air relative humidity	63
Figure 5.1-3 R134a energy consumption.....	63
Figure 5.1-4 R134a cycle COP	64
Figure 5.1-5 Log-ph-diagram of the R134a system.....	64
Figure 5.2-1 Measured temperatures CO ₂ circuit.....	65

Figure 5.2-2 T-h diagram average value 1000-8000 seconds	66
Figure 5.2-3 P-h diagram average value 1000-8000 seconds	66
Figure 5.2-4 Air relative humidity	67
Figure 5.2-5 Air temperatures.....	67
Figure 5.2-6 SMER-value	69
Figure 5.3-1 Measured temperatures CO ₂ -cycle	69
Figure 5.3-2 T-h diagram 1000-7000 seconds.....	70
Figure 5.3-3 p-h diagram 1000-7000 seconds	70
Figure 5.3-4 Air relative humidity	71
Figure 5.3-5 Air temperatures.....	71
Figure 5.3-6 SMER-value	72
Figure 5.4-1 CO ₂ Temperatures	73
Figure 5.4-2 T-h diagram of average values 1000-6000 seconds	74
Figure 5.4-3 p-h diagram of average values 1000-6000 seconds	74
Figure 5.4-4 Relative humidity	75
Figure 5.4-5 Air temperatures.....	75
Figure 5.4-6 SMER-value	76
Figure 5.5-1 Measured CO ₂ temperatures.....	76
Figure 5.5-2 T-h diagram CO ₂ average 1000-7000 seconds	77
Figure 5.5-3 p-h diagram CO ₂ average 1000-7000 seconds	77
Figure 5.5-4 Relative humidity	78
Figure 5.5-5 Air temperatures.....	78
Figure 5.5-6 SMER-value	79
Figure 5.6-1 Measured CO ₂ temperatures.....	79
Figure 5.6-2 T-h diagram CO ₂ average 1000-6000 seconds	80
Figure 5.6-3 p-h diagram CO ₂ average 1000-6000 seconds	80
Figure 5.6-4 Relative humidity	80
Figure 5.6-5 Air temperatures.....	80
Figure 5.6-6 SMER-value	81
Figure 5.7-1 CO ₂ temperatures	82
Figure 5.7-2 Measured CO ₂ temperatures.....	82
Figure 5.7-3 T-h diagram average value 1000-4000 seconds	82
Figure 5.7-4 p-h diagram average value 1000-4000 seconds	82
Figure 5.7-5 Air temperatures.....	83
Figure 5.7-6 Air relative humidity	83
Figure 5.7-7 SMER-value	84
Figure 5.8-1 CO ₂ temperatures	85
Figure 5.8-2 T-h diagram: 1000-5000 seconds	85
Figure 5.8-3 P-h diagram: 1000-5000 seconds	85
Figure 5.8-4 Temperature	86
Figure 5.8-5 Air relative humidity	86
Figure 5.8-6 SMER-value	87
Figure 5.9-1 CO ₂ Temperature values	87
Figure 5.9-2 T-h diagram 1000-6000 seconds.....	88
Figure 5.9-3 P-h diagram 1000-6000 seconds	88

Figure 5.9-4 Air temperatures.....	89
Figure 5.9-5 Air relative humidity	89
Figure 5.9-6 SMER-value	89
Figure 5.9-1 COP varying gas cooler outlet temperature	90
Figure 5.9-2 Heat pump energy savings, with varying gas cooler outlet temperatures.....	91
Figure 5.9-3 Isentropic and volumetric efficiency Embraco EK6214CD.....	94
Figure 5.9-4 Capillary tube pressure ratio	96
Figure A-1 Measured temperatures CO ₂ circuit.....	109
Figure A-2 Measured pressures	109
Figure A-3 Measured mass flow	109
Figure A-4 Gas cooler and evaporator performance	109
Figure A-5 Energy consumption.....	110
Figure A-6 Coefficient of performance	110
Figure A-7 Energy savings	110
Figure A-8 Air relative humidity	110
Figure A-9 Air temperatures	110
Figure A-10 Measured temperatures CO ₂ -cycle	111
Figure A-11 Measured pressures CO ₂ -cycle.....	111
Figure A-12 Measured mass flow CO ₂	111
Figure A-13 Gas cooler and evaporator performance	111
Figure A-14 Energy consumption.....	111
Figure A-15 Coefficient of performance	111
Figure A-16 Energy savings	112
Figure A-17 Air relative humidity.....	112
Figure A-18 Air temperatures	112
Figure A-19 CO ₂ Temperatures.....	112
Figure A-20 CO ₂ pressure measurements.....	112
Figure A-21 Mass flow.....	113
Figure A-22 Evaporator and gas cooler performance.....	113
Figure A-23 Energy consumption.....	113
Figure A-24 Coefficient of performance	113
Figure A-25 Energy savings	113
Figure A-26 Relative humidity.....	114
Figure A-27 Air temperatures	114
Figure A-28 Measured CO ₂ temperatures	114
Figure A-29 Measured CO ₂ pressures	114
Figure A-30 Measured mass flow	114
Figure A-31 Evaporator and gas cooler performance.....	114
Figure A-32 Energy consumption.....	115
Figure A-33 Energy savings	115
Figure A-34 Coefficient of performance	115
Figure A-35 Measured air temperatures	115
Figure A-36 Measured air relative humidity.....	115
Figure A-37 Measured CO ₂ temperatures	116
Figure A-38 Measured CO ₂ pressures	116

Figure A-39 Measured mass flow	116
Figure A-40 Evaporator and gas cooler performance.....	116
Figure A-41 Energy consumption.....	116
Figure A-42 Coefficient of performance	116
Figure A-43 Energy savings	117
Figure A-44 Measured air temperatures	117
Figure A-45 Measured air relative humidity.....	117
Figure A-46 Measured CO ₂ temperatures	117
Figure A-47 Measured CO ₂ pressures	117
Figure A-48 Measured CO ₂ mass flow.....	118
Figure A-49 Calculated CO ₂ performance	118
Figure A-50 Energy consumption.....	118
Figure A-51 Coefficient of performance	118
Figure A-52 Energy savings	118
Figure A-53 Air temperatures	118
Figure A-54 Air relative humidity.....	118
Figure A-55 Measured CO ₂ temperatures	119
Figure A-56 Measured CO ₂ pressures	119
Figure A-57 Measured CO ₂ mass flow.....	119
Figure A-58 Calculated CO ₂ performance	119
Figure A-59 Energy consumption.....	119
Figure A-60 Coefficient of performance	119
Figure A-61 Energy savings	119
Figure A-62 Air temperatures	120
Figure A-63 Air relative humidity.....	120
Figure A-64 Measured CO ₂ temperatures	120
Figure A-65 Measured CO ₂ pressures	120
Figure A-66 Measured CO ₂ mass flow.....	120
Figure A-67 Calculated CO ₂ performance	120
Figure A-68 Energy consumption.....	120
Figure A-69 Energy savings	120
Figure A-70 Coefficient of performance	121
Figure A-71 Air temperatures	121
Figure A-72 Air relative humidity.....	121
Figure C-1 - Experiment overview – CO ₂	123
Figure D-1 - Experiment overview - R134a	124

Table of tables

Table 1.3-1 Thermo physical properties of R134a and CO ₂ (Stene, 1997).....	8
Table 1.4-1 Equipment list	15
Table 1.4-2 Valve and pipeline list	15
Table 2.2-1 Refrigerant purity degree specs.....	18
Table 2.2-2 Inconvenience caused by moisture in the system	18
Table 2.2-3 System volume calculations.....	19
Table 2.2-4 Refrigerant charge calculations	20
Table 2.2-5 Refrigerant standstill saturated state conditions	21
Table 2.2-6 Compressor boundary conditions.....	23
Table 2.2-7 Main gas cooler geometrical data.....	25
Table 2.2-8 External gas cooler geometry	28
Table 2.2-9 Evaporator geometry	32
Table 2.2-10 Flow calculation symbols	35
Table 2.2-11 Ideal gas law input data	37
Table 2.2-12 Flow coefficient, C_v -calculations ($p_1 = 100$ bar, $p_2 = 45$ bar)	37
Table 2.2-13 Swagelok SS-31RS4	38
Table 2.2-14 Capillary tube data	41
Table 3.1-1 Instrument list.....	45
Table 3.1-2 Thermocouple specifications	46
Table 3.1-3 Druck PTX-510 Specifications.....	49
Table 3.1-4 Druck PTX-1400 Specifications.....	50
Table 3.1-5 Rheonik RHE 08 - Advanced transmitter.....	53
Table 3.1-6 Vaisala HMP 233	55
Table 3.1-7 KIMO AMI 300 Temperature and humidity transmitter	55
Table 3.1-8 L-unit LWT Watt transducer.....	56
Table 3.1-9 Total uncertainty estimation.....	60
Table 5.2-1 Average CO ₂ values : 1000-8000 seconds.....	67
Table 5.2-2 Water and fabric	68
Table 5.3-1 Average CO ₂ values: 1000 – 7000 seconds	71
Table 5.3-2 Water and fabric	72
Table 5.4-1 CO ₂ average values: 1000-6000 seconds	74
Table 5.4-2 Fabric and water	75
Table 5.5-1 Average values CO ₂ : 1000-7000 seconds	77
Table 5.5-2 Fabric and water	78
Table 5.6-1 Average CO ₂ values 1000-6000 seconds	80
Table 5.6-2 Fabric and water	81
Table 5.7-1 CO ₂ average values: 1000-4000 seconds	83
Table 5.7-2 Fabric and water	84
Table 5.8-1 Average values 1000-5000 seconds.....	86
Table 5.8-2 Water and air values	86
Table 5.9-1 Average CO ₂ values 1000-6000 seconds	88
Table 5.9-2 Water and air values	89
Table 5.9-1 Assumptions COP calculations.....	90

Table B-1 Dew point table.....	122
--------------------------------	-----

Table of equations

Equation 1.1-1 Energy consumption heat pump [kW]	4
Equation 1.1-2 Total energy consumption [kW].....	4
Equation 1.1-3 Heat pump coefficient of performance.....	4
Equation 1.1-4 Coefficient of performance	4
Equation 1.1-5 Energy savings heat pump.....	4
Equation 1.3-1 Isentropic efficiency	6
Equation 1.3-2 Isentropic efficiency real	7
Equation 1.3-3 Compressor volumetric efficiency.....	7
Equation 1.3-4 Volumetric refrigeration capacity	8
Equation 1.4-1 Absolute humidity content.....	11
Equation 1.4-2 Relative humidity content.....	11
Equation 1.4-3 Dryer efficiency	11
Equation 1.4-4 Specific moisture extraction rate heat pump [$\text{kg}_{\text{water}}/\text{kW}$].....	12
Equation 1.4-5 Kiln efficiency	13
Equation 1.4-6 Air cooler efficiency.....	13
Equation 1.4-7 Air heater efficiency	13
Equation 2.2-1 Power factor for single phase.....	24
Equation 2.2-2 Low pressure drop flow.....	36
Equation 2.2-3 High pressure drop flow	36
Equation 2.2-4 Ideal gas law	37
Equation 2.2-5 Miller's friction factor correlation	39
Equation 2.2-6 Capillary tube length	39
Equation 2.2-7 Sum of tube intervals	39
Equation 2.2-8 Mass flux.....	40
Equation 2.2-9 Liquid friction factor	40
Equation 2.2-10 Gas friction factor.....	40
Equation 2.2-11 Multiphase flow coefficient.....	40
Equation 2.2-12 Froude number.....	40
Equation 2.2-13 Weber number	40
Equation 2.2-14 Two phase throttling length.....	41
Equation 2.2-15 Sum of two-phase throttling length.....	41
Equation 2.2-16 Inner diameter.....	42
Equation 3.1-1 Measured series average	58
Equation 3.1-2 Standard deviation	58
Equation 3.1-3 Gaussian normal distribution	58
Equation 3.1-4 Total uncertainty	59

Appendices

Appendix A: Experiment performance figures

The figures shown below in the attachments are visualizations of the measured and calculated values from the experiments performed in the project. For all the experiments there are presented figures of: Measured CO₂ temperatures, pressures, mass flow, evaporating and gas cooling performance (main and external gas cooler in the same graph), energy consumption, COP and energy savings and finally the measured relative humidity and temperature of the air through the cycle.

Due to some measurement errors in the thermocouple device at the discharge gas at the compressor, the calculated value from the isentropic efficiency is included in the performance figures.

Experiment 1: Manual throttle valve, no external fan

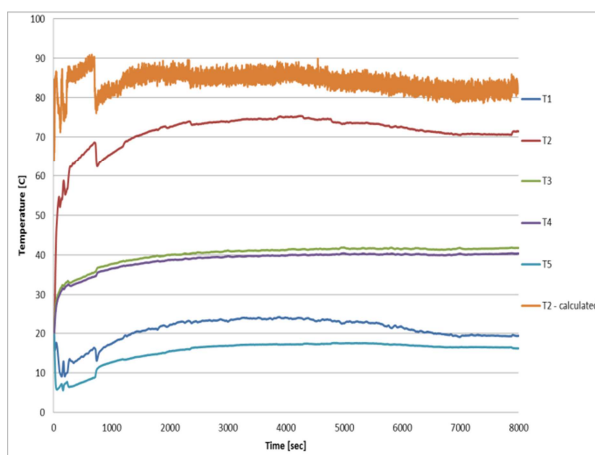


Figure A-1 Measured temperatures CO₂ circuit

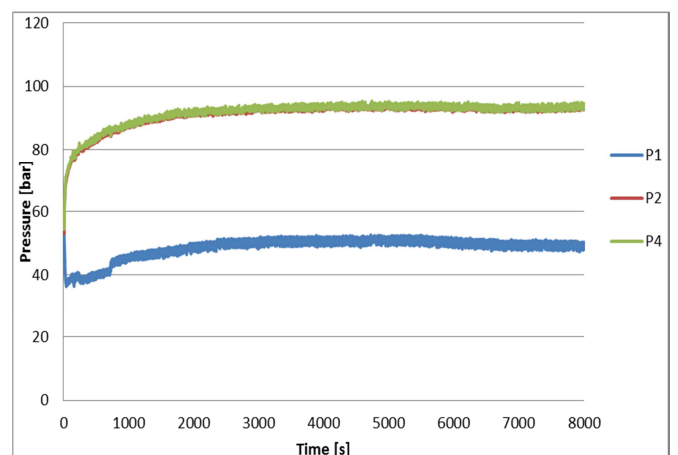


Figure A-2 Measured pressures

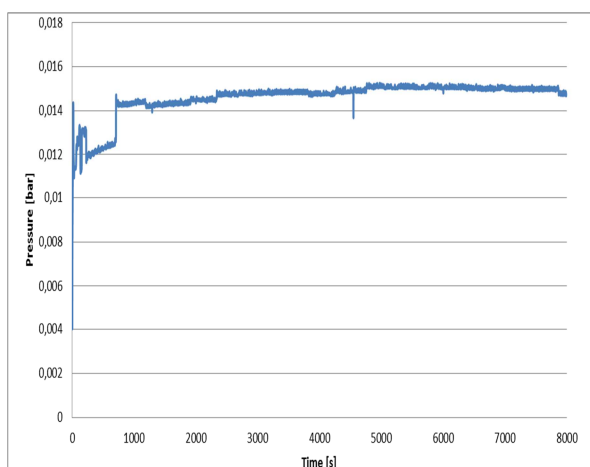


Figure A-3 Measured mass flow

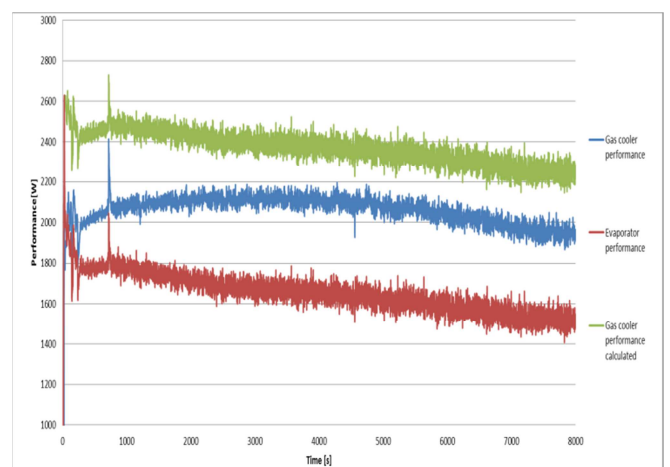


Figure A-4 Gas cooler and evaporator performance

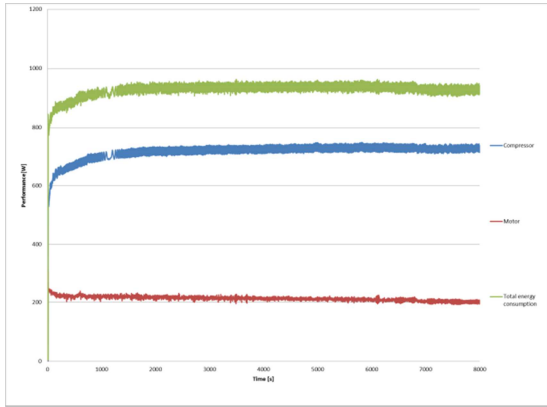


Figure A-5 Energy consumption

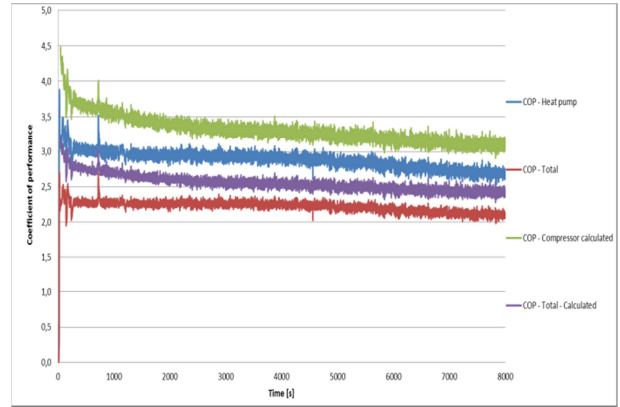


Figure A-6 Coefficient of performance

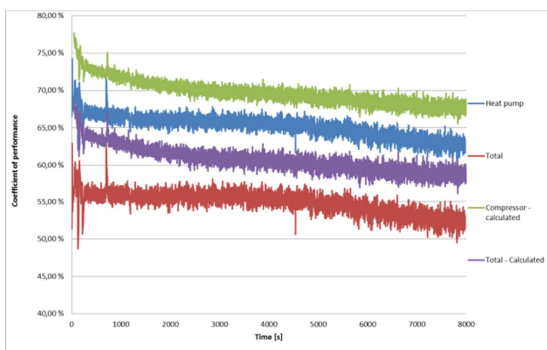


Figure A-7 Energy savings

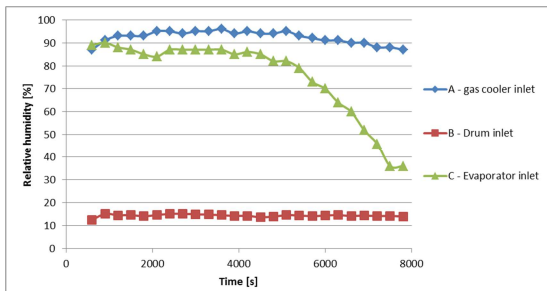


Figure A-8 Air relative humidity

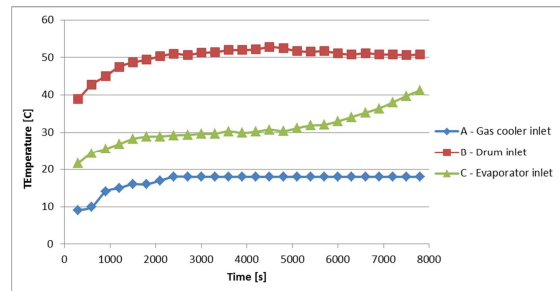


Figure A-9 Air temperatures

Experiment 2: Manual throttling external gas cooler fan connected

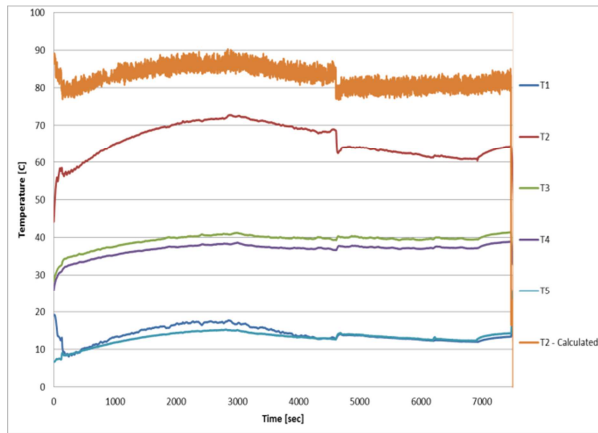


Figure A-10 Measured temperatures CO₂-cycle

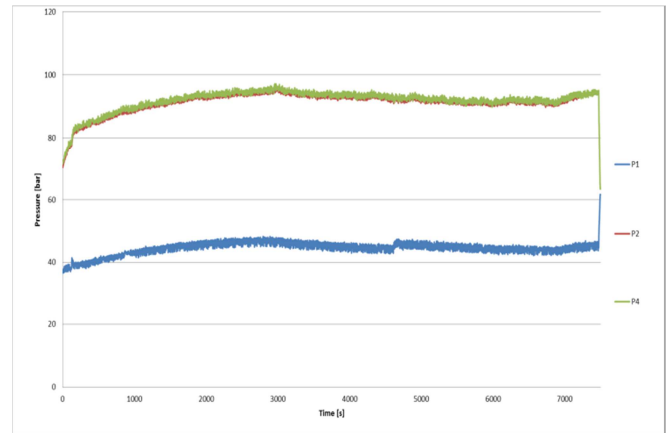


Figure A-11 Measured pressures CO₂-cycle

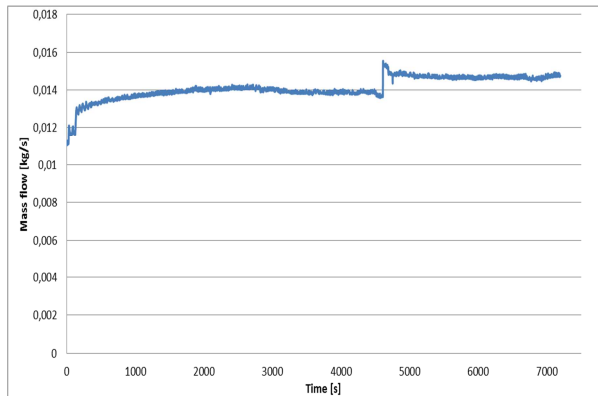


Figure A-12 Measured mass flow CO₂

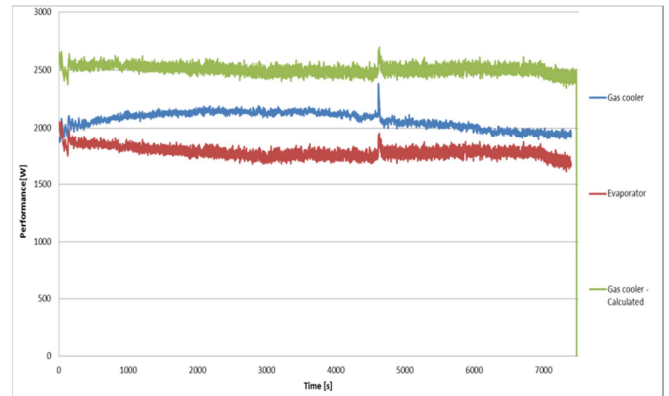


Figure A-13 Gas cooler and evaporator performance

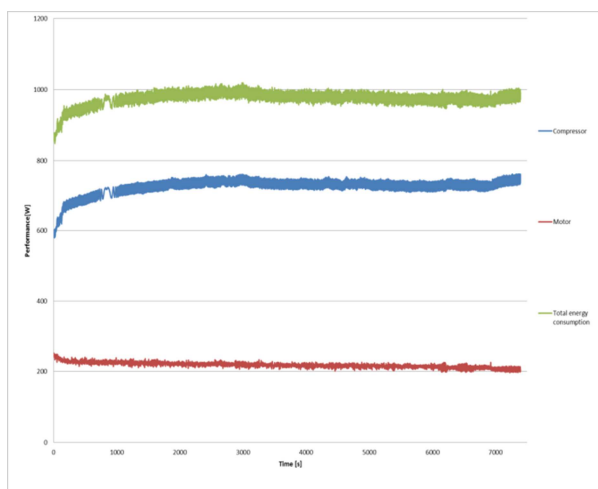


Figure A-14 Energy consumption

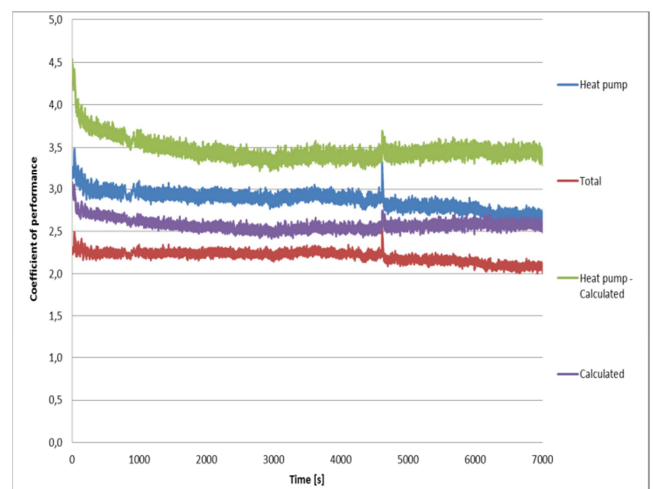


Figure A-15 Coefficient of performance

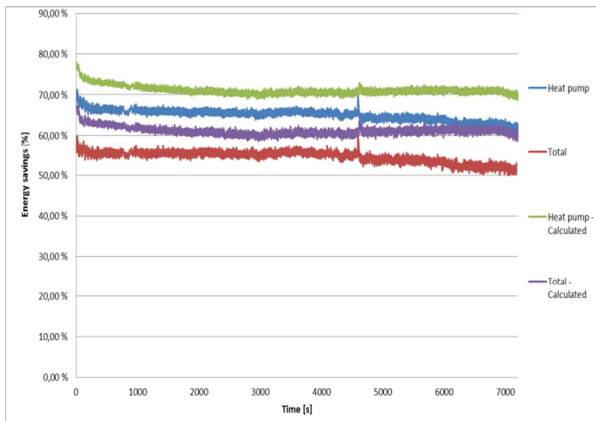


Figure A-16 Energy savings

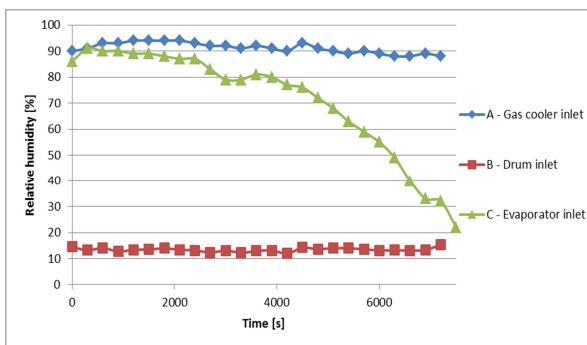


Figure A-17 Air relative humidity

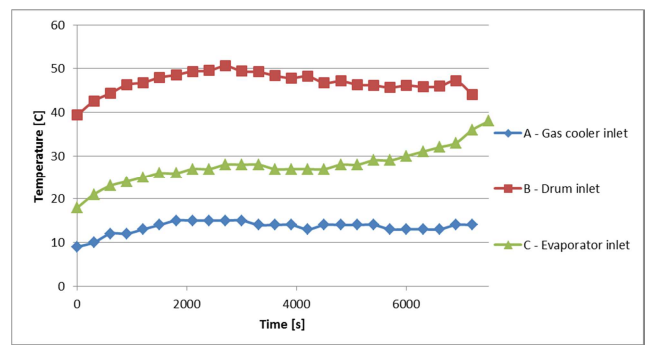


Figure A-18 Air temperatures

Experiment 3: Capillary tube (900 mm), external fan

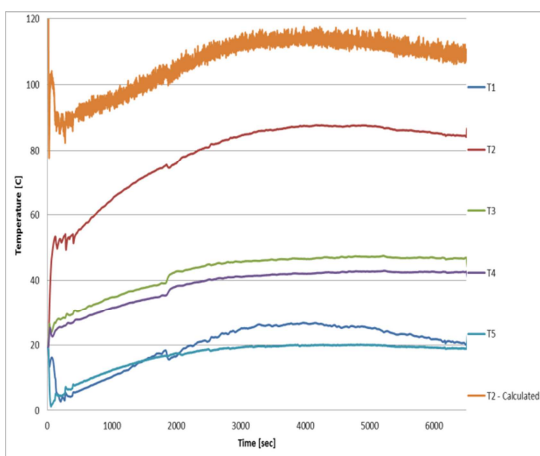


Figure A-19 CO₂ Temperatures

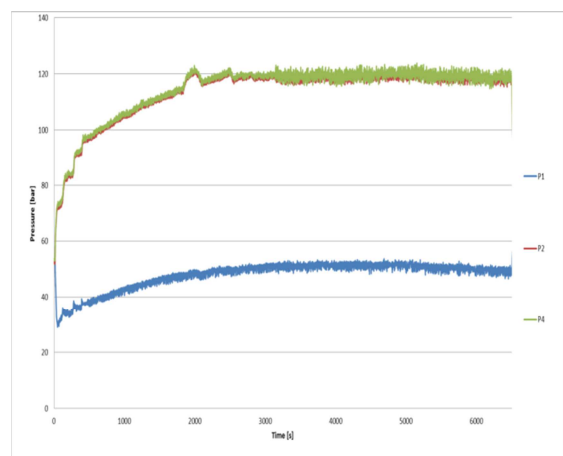


Figure A-20 CO₂ pressure measurements

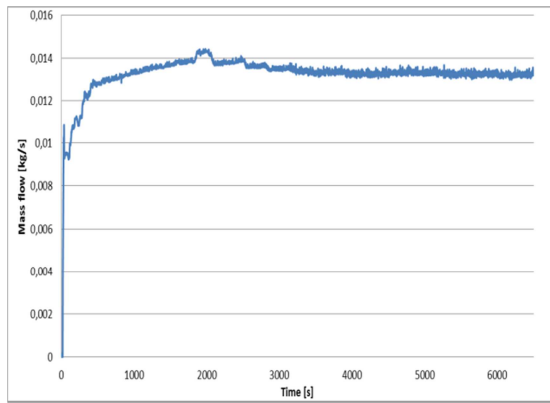


Figure A-21 Mass flow

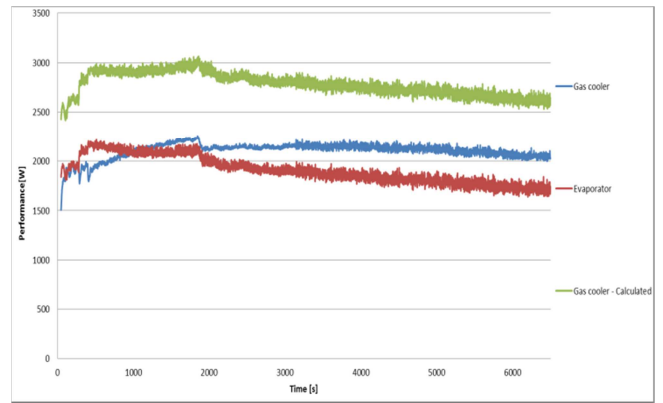


Figure A-22 Evaporator and gas cooler performance

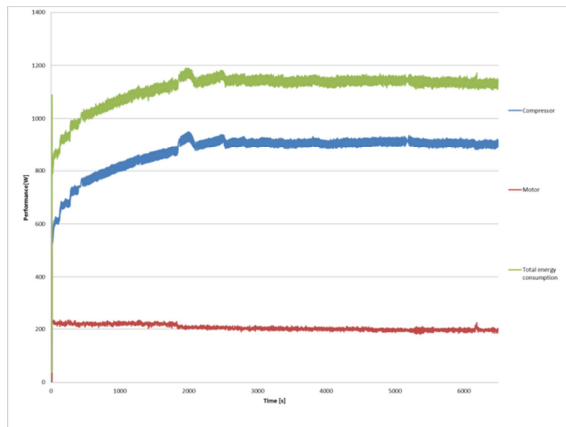


Figure A-23 Energy consumption

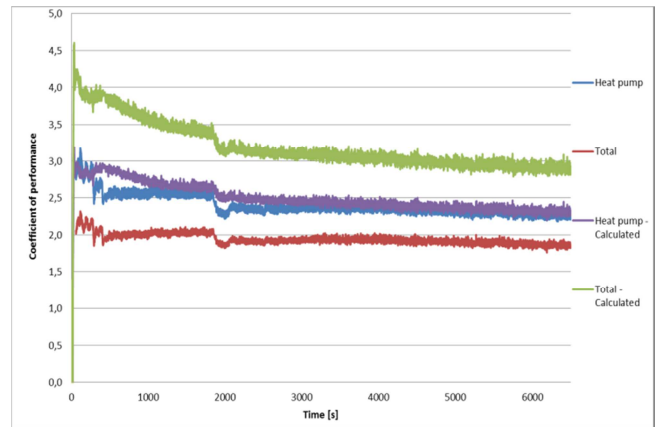


Figure A-24 Coefficient of performance

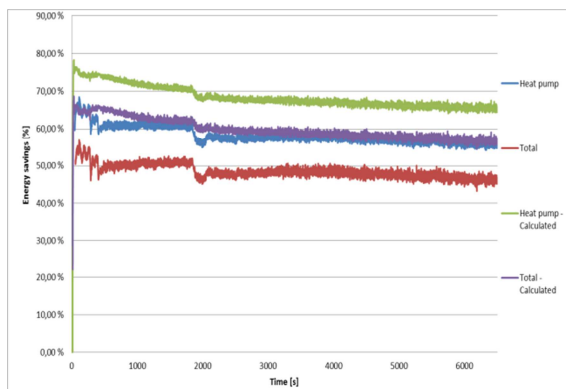


Figure A-25 Energy savings

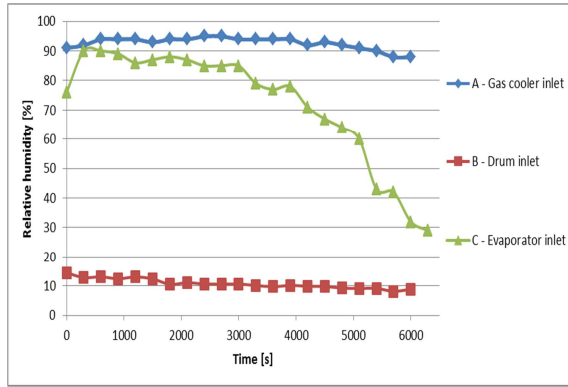


Figure A-26 Relative humidity

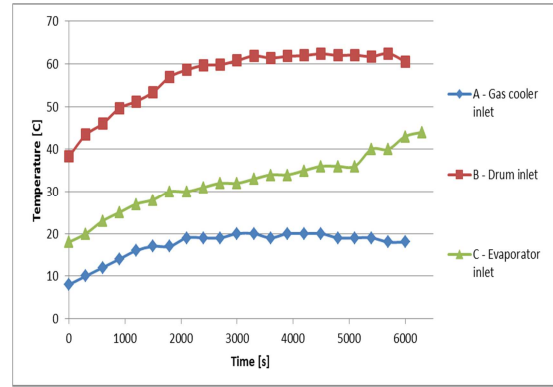


Figure A-27 Air temperatures

Experiment 4: Capillary tube 740 mm

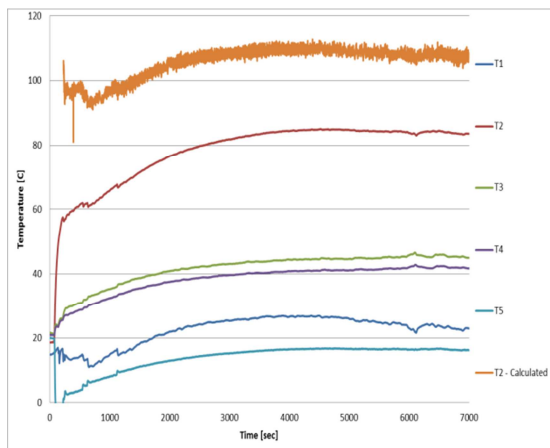


Figure A-28 Measured CO₂ temperatures

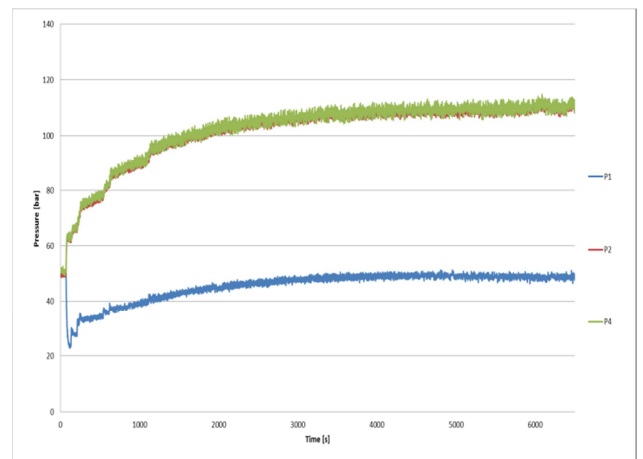


Figure A-29 Measured CO₂ pressures

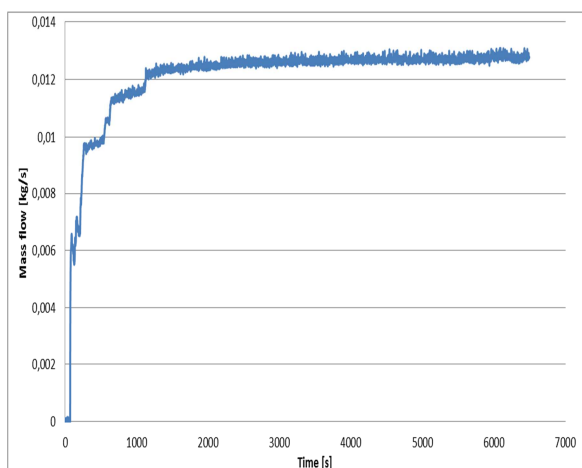


Figure A-30 Measured mass flow

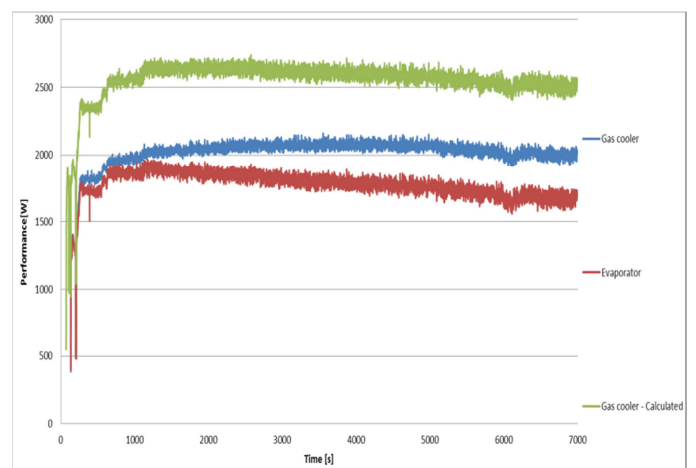


Figure A-31 Evaporator and gas cooler performance

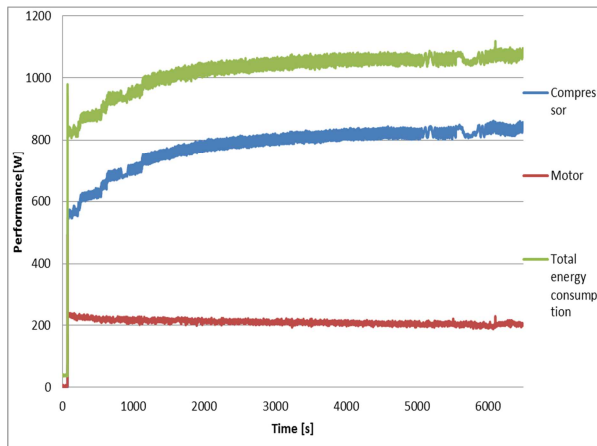


Figure A-32 Energy consumption

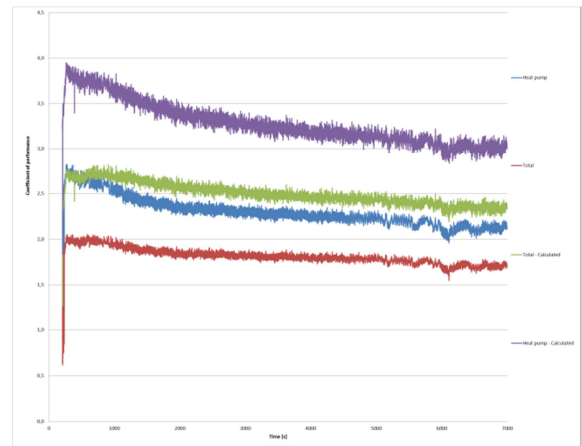


Figure A-34 Coefficient of performance

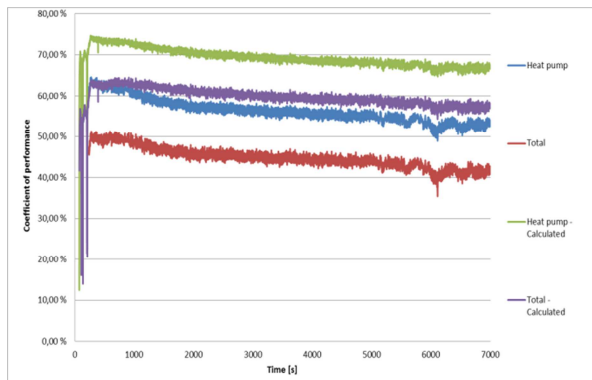


Figure A-33 Energy savings

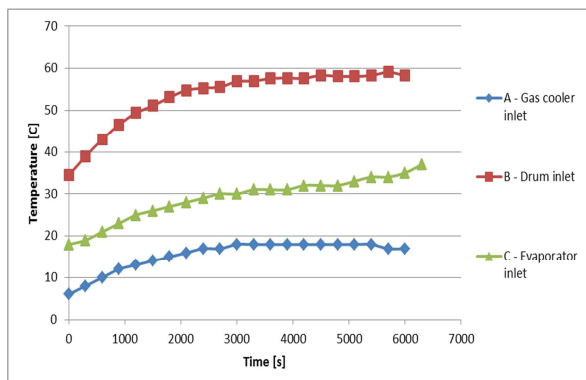


Figure A-35 Measured air temperatures

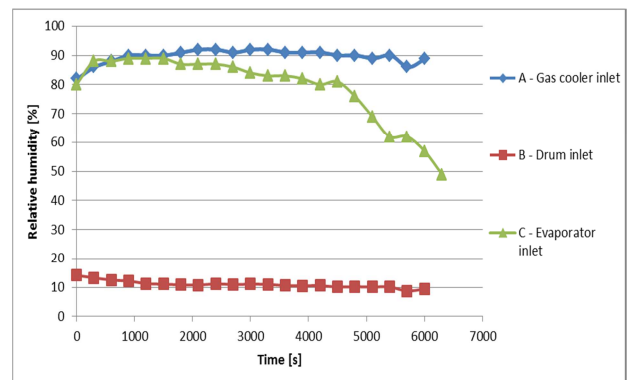


Figure A-36 Measured air relative humidity

Experiment 5: Capillary tube 660 mm – 1

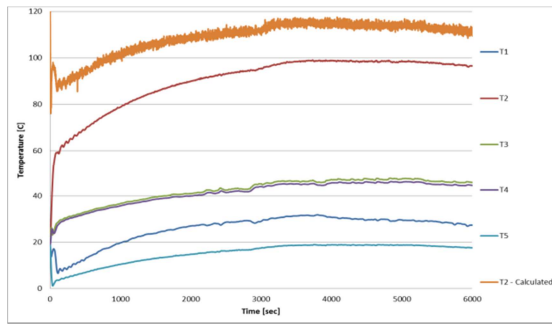


Figure A-37 Measured CO₂ temperatures

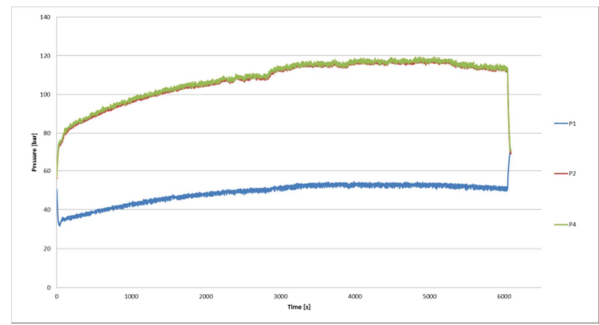


Figure A-38 Measured CO₂ pressures

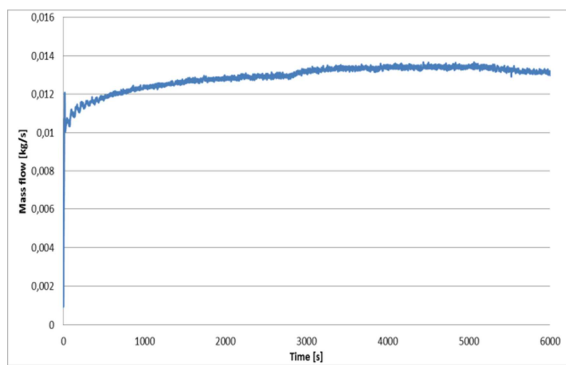


Figure A-39 Measured mass flow

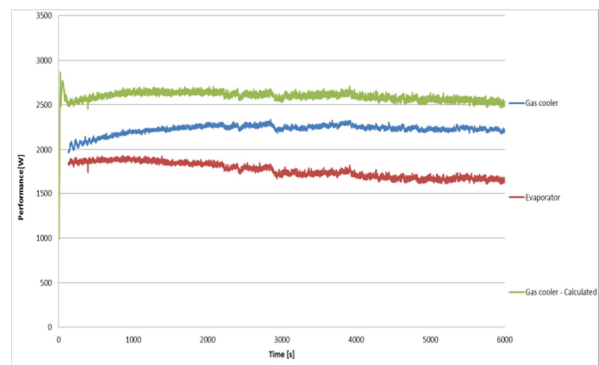


Figure A-40 Evaporator and gas cooler performance

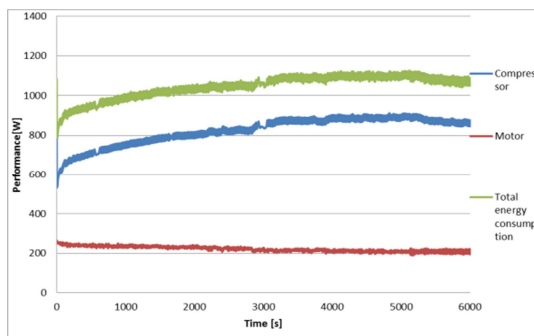


Figure A-41 Energy consumption

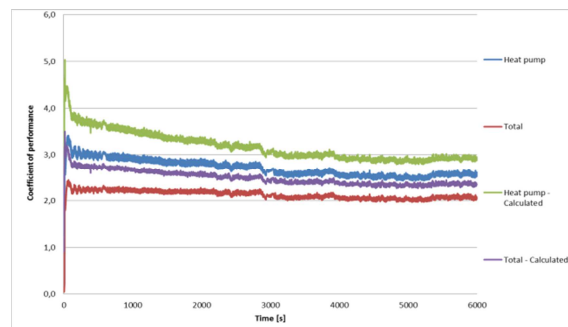


Figure A-42 Coefficient of performance

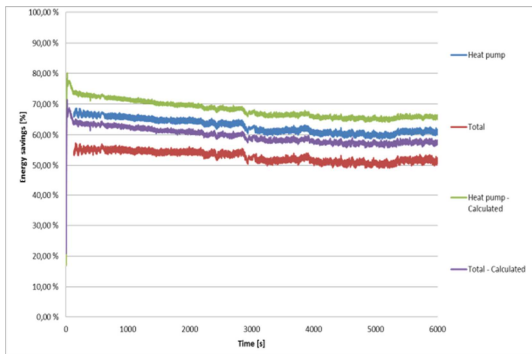


Figure A-43 Energy savings

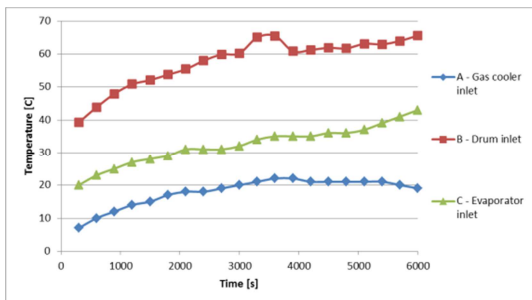


Figure A-44 Measured air temperatures

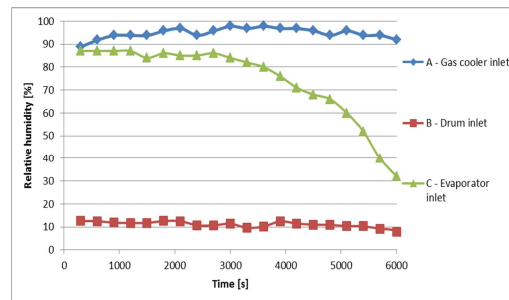


Figure A-45 Measured air relative humidity

Experiment 6: Capillary tube 660 mm – 2: reduced refrigerant charge

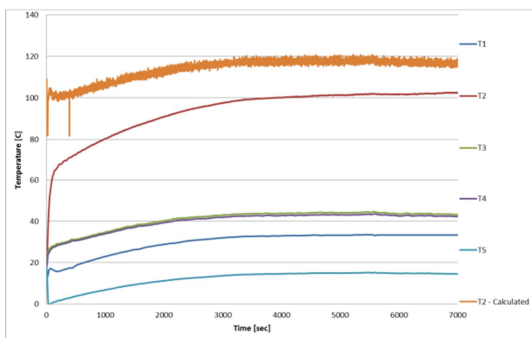


Figure A-46 Measured CO₂ temperatures

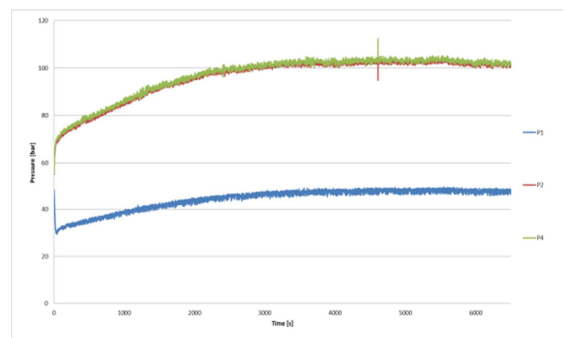


Figure A-47 Measured CO₂ pressures

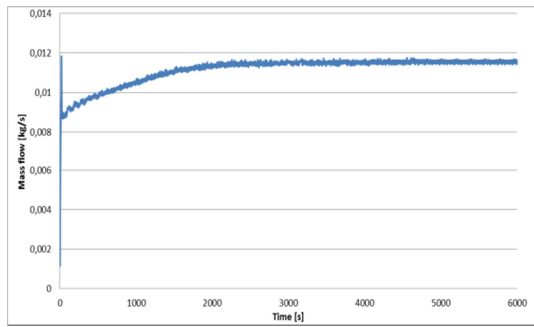


Figure A-48 Measured CO₂ mass flow

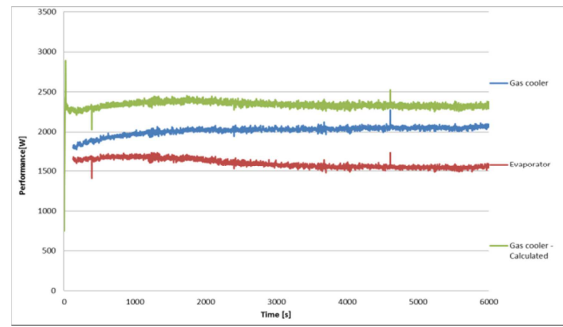


Figure A-49 Calculated CO₂ performance

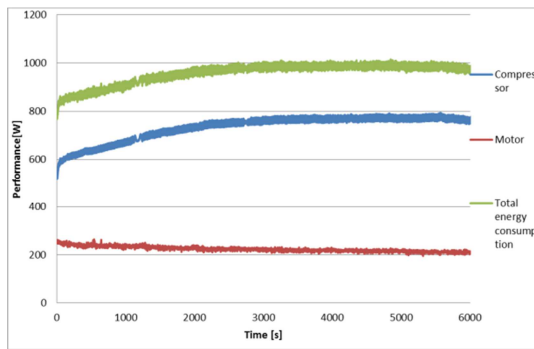


Figure A-50 Energy consumption

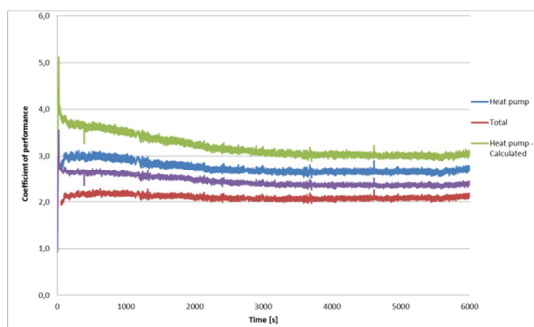


Figure A-51 Coefficient of performance

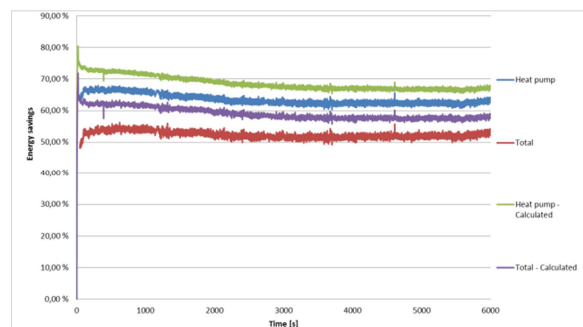


Figure A-52 Energy savings

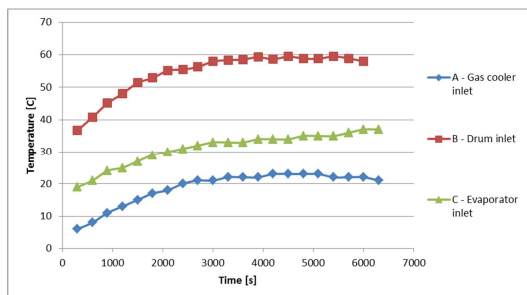


Figure A-53 Air temperatures

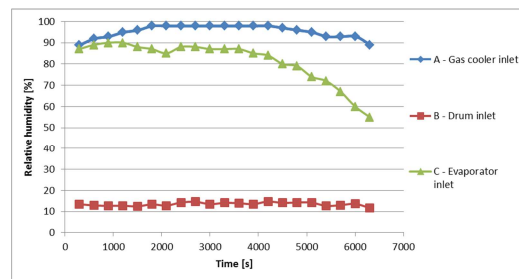


Figure A-54 Air relative humidity

Experiment 7: Capillary tube 660 mm – 3: increased refrigerant charge

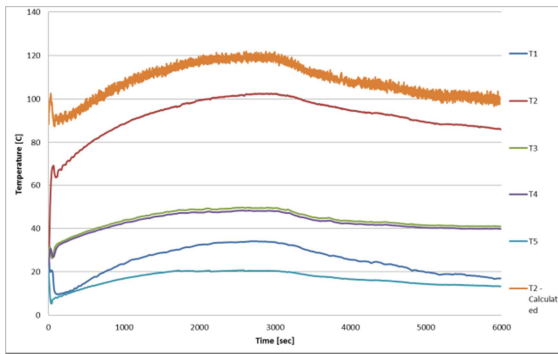


Figure A-55 Measured CO₂ temperatures

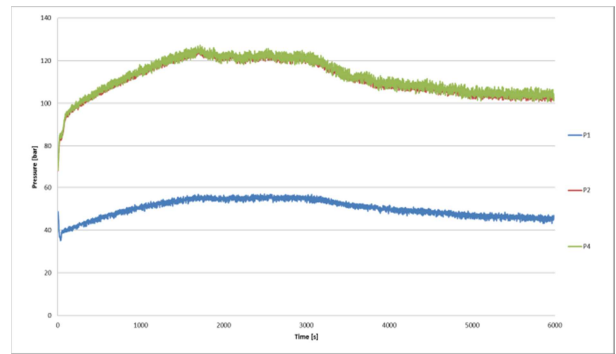


Figure A-56 Measured CO₂ pressures

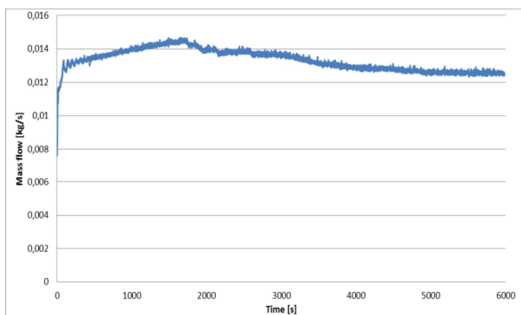


Figure A-57 Measured CO₂ mass flow

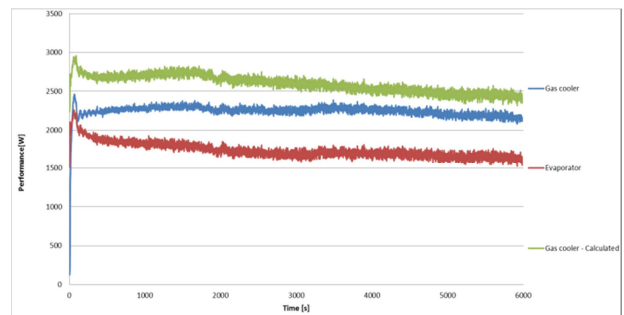


Figure A-58 Calculated CO₂ performance

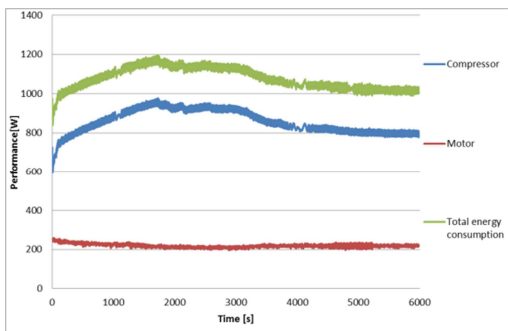


Figure A-59 Energy consumption

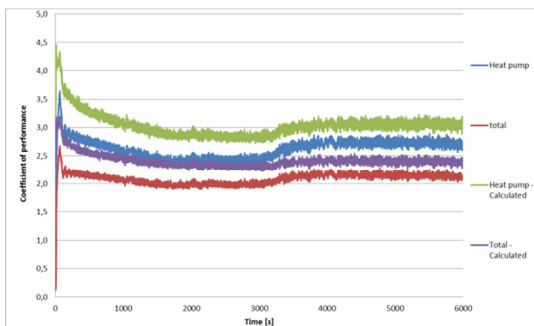


Figure A-60 Coefficient of performance

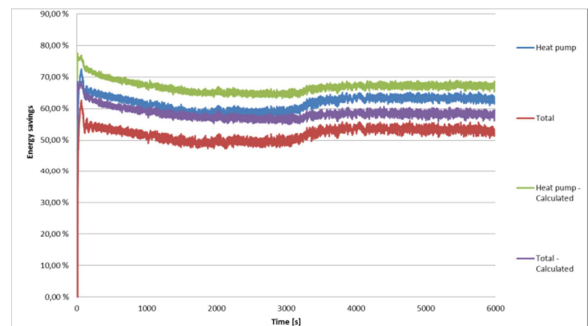


Figure A-61 Energy savings

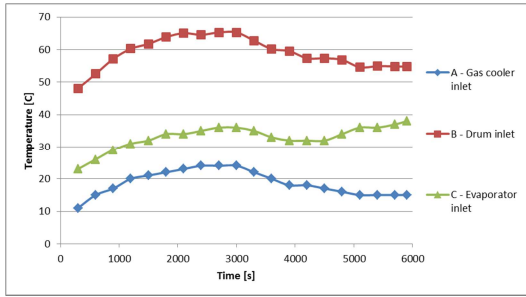


Figure A-62 Air temperatures

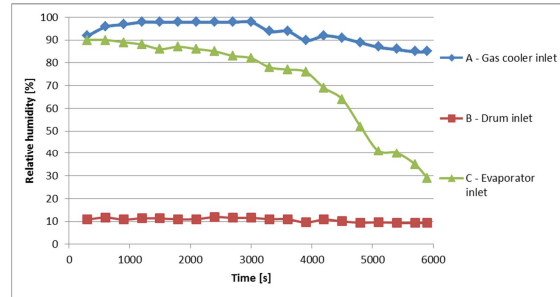


Figure A-63 Air relative humidity

Experiment 8: Capillary tube 660 mm – 3: increased refrigerant charge

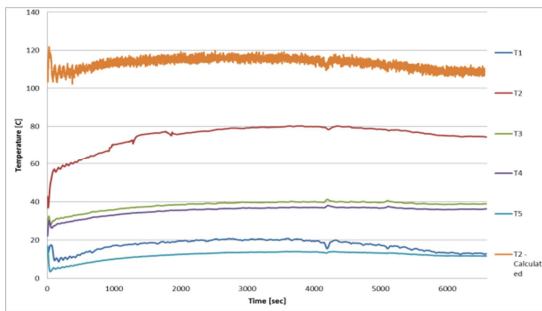


Figure A-64 Measured CO₂ temperatures

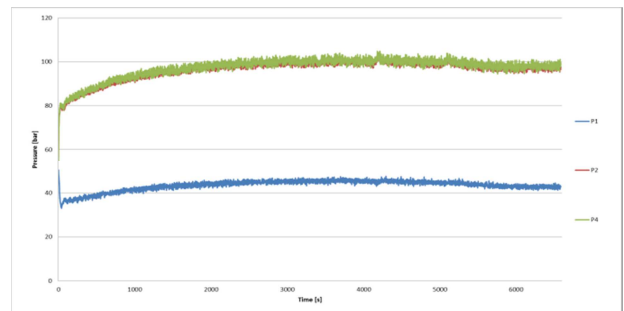


Figure A-65 Measured CO₂ pressures

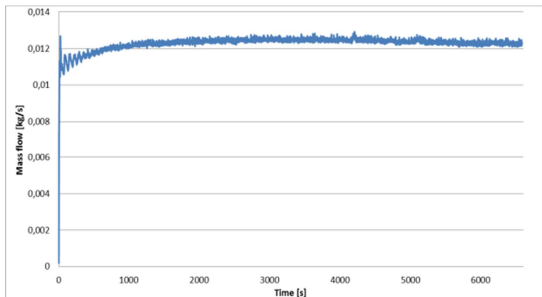


Figure A-66 Measured CO₂ mass flow

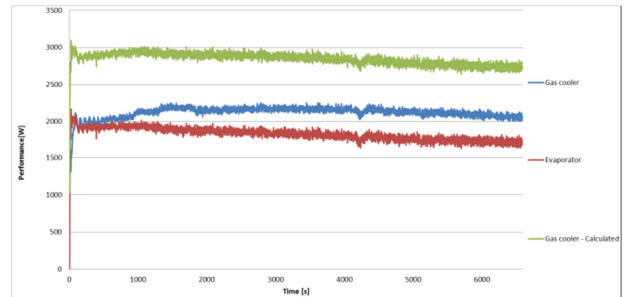


Figure A-67 Calculated CO₂ performance

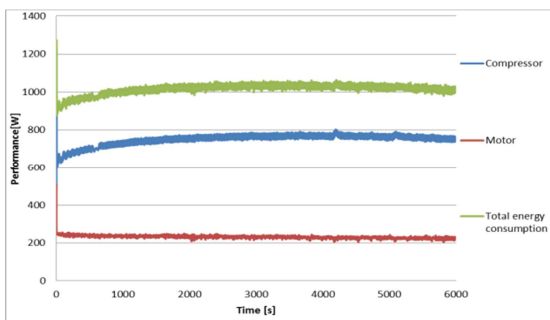


Figure A-68 Energy consumption

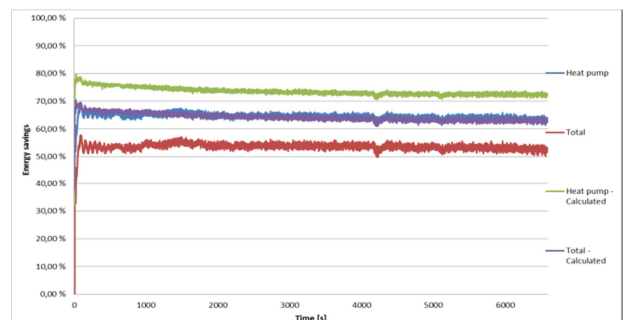


Figure A-69 Energy savings

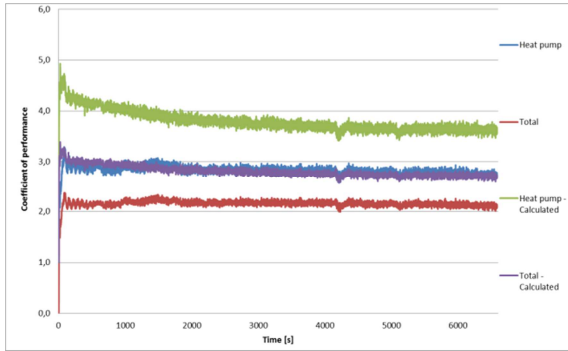


Figure A-70 Coefficient of performance

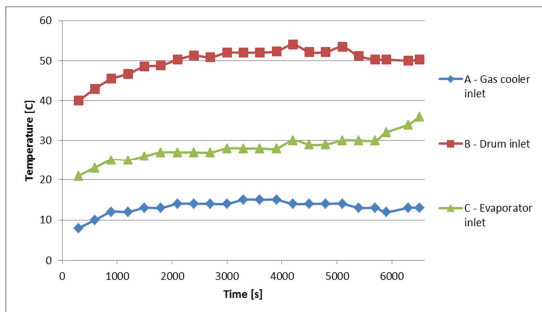


Figure A-71 Air temperatures

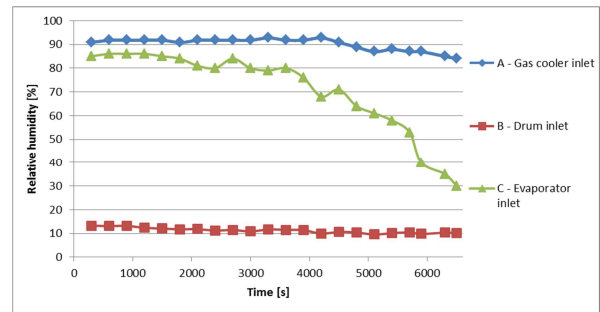


Figure A-72 Air relative humidity

Appendix B: Dew point table

The red values represent all dew point temperatures at the evaporator surface above 20 °C. If the temperature of the inlet air to the evaporator surface is 20 °C and 90% relative humidity, the temperature of the evaporator surface must be 21.3 °C or below for humidity in the air to condense.

Air relative humidity and temperatures are values in blue.

Table B-1 Dew point table

Air temperature evaporator inlet		Calculated dew point temperature for the air entering the evaporator														% RH
		95,0	90,0	85,0	80,0	75,0	70,0	65,0	60,0	55,0	50,0	45,0	40,0	35,0	30,0	
40,0	°C	39,0	38,0	37,0	35,9	34,7	33,5	32,1	30,7	29,2	27,6	25,8	23,8	21,6	19,1	
39,0	°C	38,0	37,1	36,0	34,9	33,7	32,5	31,2	29,8	28,3	26,7	24,9	22,9	20,7	18,3	
38,0	°C	37,1	36,1	35,0	33,9	32,8	31,6	30,3	28,9	27,4	25,8	24,0	22,0	19,9	17,4	
37,0	°C	36,1	35,1	34,0	33,0	31,8	30,6	29,3	27,9	26,5	24,8	23,1	21,2	19,0	16,6	
36,0	°C	35,1	34,1	33,1	32,0	30,9	29,7	28,4	27,0	25,5	23,9	22,2	20,3	18,1	15,7	
35,0	°C	34,1	33,1	32,1	31,0	29,9	28,7	27,4	26,1	24,6	23,0	21,3	19,4	17,3	14,8	
34,0	°C	33,1	32,1	31,1	30,1	28,9	27,7	26,5	25,1	23,7	22,1	20,4	18,5	16,4	14,0	
33,0	°C	32,1	31,1	30,1	29,1	28,0	26,8	25,5	24,2	22,8	21,2	19,5	17,6	15,5	13,1	
32,0	°C	31,1	30,1	29,2	28,1	27,0	25,8	24,6	23,3	21,8	20,3	18,6	16,7	14,6	12,3	
31,0	°C	30,1	29,2	28,2	27,1	26,0	24,9	23,6	22,3	20,9	19,4	17,7	15,8	13,8	11,4	
30,0	°C	29,1	28,2	27,2	26,2	25,1	23,9	22,7	21,4	20,0	18,4	16,8	14,9	12,9	10,5	
29,0	°C	28,1	27,2	26,2	25,2	24,1	23,0	21,8	20,5	19,0	17,5	15,9	14,0	12,0	9,7	
28,0	°C	27,1	26,2	25,2	24,2	23,2	22,0	20,8	19,5	18,1	16,6	15,0	13,2	11,1	8,8	
27,0	°C	26,1	25,2	24,3	23,3	22,2	21,1	19,9	18,6	17,2	15,7	14,1	12,3	10,2	8,0	
26,0	°C	25,1	24,2	23,3	22,3	21,2	20,1	18,9	17,6	16,3	14,8	13,2	11,4	9,4	7,1	
25,0	°C	24,1	23,2	22,3	21,3	20,3	19,1	18,0	16,7	15,3	13,9	12,3	10,5	8,5	6,2	
24,0	°C	23,1	22,3	21,3	20,3	19,3	18,2	17,0	15,8	14,4	12,9	11,3	9,6	7,6	5,4	
23,0	°C	22,2	21,3	20,3	19,4	18,3	17,2	16,1	14,8	13,5	12,0	10,4	8,7	6,7	4,5	
22,0	°C	21,2	20,3	19,4	18,4	17,4	16,3	15,1	13,9	12,6	11,1	9,5	7,8	5,9	3,6	
21,0	°C	20,2	19,3	18,4	17,4	16,4	15,3	14,2	12,9	11,6	10,2	8,6	6,9	5,0	2,8	
20,0	°C	19,2	18,3	17,4	16,4	15,4	14,4	13,2	12,0	10,7	9,3	7,7	6,0	4,1	1,9	
19,0	°C	18,2	17,3	16,4	15,5	14,5	13,4	12,3	11,1	9,8	8,4	6,8	5,1	3,2	1,0	
18,0	°C	17,2	16,3	15,4	14,5	13,5	12,5	11,3	10,1	8,8	7,4	5,9	4,2	2,3	0,2	
17,0	°C	16,2	15,3	14,5	13,5	12,5	11,5	10,4	9,2	7,9	6,5	5,0	3,3	1,4	-0,6	
16,0	°C	15,2	14,4	13,5	12,6	11,6	10,5	9,4	8,2	7,0	5,6	4,1	2,4	0,6	-1,4	
15,0	°C	14,2	13,4	12,5	11,6	10,6	9,6	8,5	7,3	6,0	4,7	3,2	1,5	-0,3	-2,1	
14,0	°C	13,2	12,4	11,5	10,6	9,6	8,6	7,5	6,4	5,1	3,8	2,3	0,6	-1,1	-2,9	
13,0	°C	12,2	11,4	10,5	9,6	8,7	7,7	6,6	5,4	4,2	2,8	1,4	-0,2	-1,9	-3,7	
12,0	°C	11,2	10,4	9,6	8,7	7,7	6,7	5,6	4,5	3,2	1,9	0,4	-1,0	-2,6	-4,5	
11,0	°C	10,2	9,4	8,6	7,7	6,7	5,7	4,7	3,5	2,3	1,0	-0,4	-1,8	-3,4	-5,2	
10,0	°C	9,2	8,4	7,6	6,7	5,8	4,8	3,7	2,6	1,4	0,1	-1,2	-2,6	-4,2	-6,0	

Appendix C: Dryer template ASKO – CO₂

Test results from measured data on the CO₂ system; the table shows the drying and energy use from the given input for the 8 experiments. They are not directly comparable due to that there are changing factors in the 8 different experiments.

TORKTUMLARTEST TD60.3 Kondens

Program	Bomull	Syntet	Akryl
P1 Extra torr		Temp °C	Normal
P2 Skåp torr			Låg
P3 Normal torr			
P4 Stryktorr			

Klimat % RH	55	Temperatur °C	22
Tolerans	± 5	Tolerans	± 2
Serienr.	Prototype 1		
Int.nr.		Lufflöde (m ³ /h)	
Provserie		Elementeffekt (W)	

Nominell vikt, W (g)	6316	Nominell fukt start, μ_{i0}	60 %	Nominell fukt slut, μ_{i0}	0 %
Vikt tom kondensvattentank (g)	0				
Konditionerad vikt, W_0 (g)	6316				

Datum	2011-08-11	2011-09-11	2011-11-11	2011-15-11	2011-17-11	2011-18-11	2011-23-11	2011-24-11	
Starttid	10:30	12:00	09:00	13:00	14:00	10:30	09:00	12:30	
Körning nr.	1	2	3	4	5	6	7	8	Medelvärden
Centrifugerad vikt, W_f (g)	9500	9500	9500	9972	9500	9908	9500	9810	9649
Torkad vikt, W_t (g)	6310	6326	6315	6328	6323	6362	6325	6332	6328
Programtid, t_m (min)	126	115	100	116	116	116	100	110	112
Energiförbrukning, E_m (kWh)	1,96	1,99	1,89	2,00	1,87	1,87	1,69	1,85	1,890
Vikt kondensvattentank slut (g)	1970	1928	2247	2537	1611	2314	1988	2094	2086
	Resultat								
Returvatten i tank, W_w (g)	1970	1928	2247	2537	1611	2314	1988	2094	
Fukttinhåll Start, μ_i (%)	50,4%	50,4%	50,4%	57,9%	50,4%	56,9%	50,4%	55,3%	52,8%
Fukttinhåll Slut, μ_{if} (%)	-0,1%	0,2%	0,0%	0,2%	0,1%	0,7%	0,1%	0,3%	0,2%
Förbrukning kWh / liter borttorkat vatten	0,61	0,63	0,59	0,55	0,59	0,53	0,53	0,53	0,57
Kondenseringsseffekt, C (%)	62 %	61 %	71 %	70 %	51 %	65 %	63 %	60 %	63 %
	Korrigerade resultat till nominell fukt								
Korrigerad energiförbrukning, E (kWh)	2,33	2,38	2,25	2,08	2,23	2,00	2,02	2,02	2,16
Korrigerad programtid, t (min)	150	137	119	121	138	124	119	120	129
	Korrigerade resultat till EN61121:2005								
Korrigerad energiförbrukning, E_{cor} (kWh)	2,65	2,71	2,56	2,37	2,54	2,28	2,30	2,30	2,46
Korrigerad energiförbrukning (kWh/kg gods)	0,42	0,43	0,41	0,38	0,40	0,36	0,36	0,36	0,39
Energiklass	A								

Figure C-1 - Experiment overview – CO₂

Appendix D: Dryer template ASKO – R134a

Test results from measured data of the R134a system from the manufacturer, which shows the measured data from the testing on the previous system. 4 experiments have been performed on this system.

TORKTUMLARTEST TD70 prototyp

Program	Bomull	Syntet	Akryl
P1 Extra torr	Temp °C	Normal	
P2 Skåp torr		Låg	
P3 Normal torr			
P4 Stryktorr	Tidsprogram		

Klimat % RH	55	Temperatur °C	23
Tolerans	± 5	Tolerans	± 2
Serienr.	Prototypserie 1-1		
Int.nr.	13051	Luftflöde (m³/h)	
Provserie	788	Elementeffekt (W)	

Nominell vikt, W (g)	8000	Nominell fukt start, μ_{i0}	60 %	Nominell fukt slut, μ_{i0}	0 %
Vikt tom kondensvattentank (g)	325				
Konditionerad vikt, W_0 (g)	7991				

Datum	2009-08-17	2009-08-17	2009-08-18	2009-08-18				
Starttid	10,15	13,30	8,40	11,55				
Körning nr.	10072	10073	10074	10075				Medelvärden
Centrifugerad vikt, W_i (g) Starting load + water	12786	12786	12786	12786				12786
Torkad vikt, W_f (g) Dry Load after drying	8099	8090	8249	8239				8169
Programtid, t_m (min)	145	145	145	145				145
Energiförbrukning, E_m (kWh) Energiconsumption	2,110	2,118	2,035	2,091				2,089
Vikt kondensvattentank slut (g) Endgewicht Kondensatbehälter	4271	4315	4162	4139				4222
	Resultat							
Returvatten i tank, W_w (g) Return Water	3946	3990	3837	3814				
Fuktnnehåll Start, μ_i (%) Feuchtigkeitsgehalt Start	60,0%	60,0%	60,0%	60,0%				60,0%
Fuktnnehåll Slut, μ_f (%) Feuchtigkeitsgehalt Ende	1,4%	1,2%	3,2%	3,1%				2,2%
Förbrukning kWh / liter borttorkat vatten Verbrauch kWh / Liter Wasser zu entfernen getrocknet	0,45	0,45	0,45	0,46				0,45
Kondenseringsseffekt, C (%)	84 %	85 %	85 %	84 %				84 %
	Korrigerade resultat till nominell fukt							
Korrigerad energiförbrukning, E (kWh)	2,16	2,16						2,16
Korrigerad programtid, t (min)	148	148						148
	Korrigerade resultat till EN61121:2005							
Korrigerad energiförbrukning, E_{cor} (kWh)	2,46	2,47						2,47
Korrigerad energiförbrukning (kWh/kg gods)	0,31	0,31						0,31
Energiklass								A

Figure D-1 - Experiment overview - R134a

Appendix E: Draft article

Development of new heat pump cloth dryer with CO₂ as working fluid

Trygve Magne Eikevik, Håvard Rekstad, Åsmund Elnan

Norwegian University of Science and Technology

Abstract

Focus on energy consumption in the commercial home appliances become more and more imminent day by day. For the consumer to maintain the luxury of appliances like tumble dryers, new technology must be introduced. Applying a heat pump in a tumble dryer will be an option to replace existing energy demanding devices. In the original design there was an R134a heat pump, this has been replaced by a heat pump using R744 as refrigerant. R134a is commonly used in heat pumps due to good heat transfer characteristics, however it has a global warming potential of 1300. The R744 heat pump will operate in a transcritical state; absorbing heat from humid air by evaporating the refrigerant and rejecting heat to dry air by cooling supercritical gas. In this article data from experiments on the two refrigerants will be compared to see if R744 is a feasible option.

Introduction

HFCs in refrigerating processes has been the first choice for many years, R134a was introduced in early in the 1990s as a replacement for R-12. In many heat pump and refrigerating appliances the HFCs has been the preferred choice as working fluid, due to good heat transfer characteristics and temperature levels. The use of HFCs has been controlled by the Montreal Protocol due to their ozone depleting effects. The Kyoto protocol of December 1997 accepted by many countries decided to control the use of HFCs due to their high global warming effects. By phasing out a preferred choice for many commercial and household appliances the alternative must have less global warming effects and be highly energy efficient. The alternative to be discussed in this article is carbon dioxide or R744; it has a global warming potential of 1 and good heat transfer characteristics.

According to (Colak, et al., 2009) the first work on a heat pump dryer started in 1973, and it was stated that energy consumption was less than for a conventional heated dryer. Later heat pumps in drying appliances has been more and more widely used and developed. For a small appliance like

the tumble dryer the energy consumption and the operational costs must be set to a minimum for the household consumer.

In this article the heat pump tumble dryer with R134a and R744 will be compared; specific moisture extraction, COP of the heat pump and the drying time will be factors to consider. The next sections of the article will include the basic design of the tumble dryer, experimental test procedure and the results from the experiments.

Heat pump tumble dryer concept and design

The concept of the heat pump dryer has been developed for many years, and attempts to improve the energy efficiency has been analysed comprehensively. The basic model is made with a simple and cheap solution with a heating element that consumes extensively amount of energy. Energy consumption and environmentally friendly technology become more and more in the centre of attention. To be able to maintain the luxury of domestic clothes tumble dryer the energy consumption and environmental impacts must be set to a minimum, the old fashion dryers must be phased out. According to (Klöcker, et al., 2001) a solution with heat pump in convective hot air dryers is the optimal solution. Depending on the system configuration a heat pump in a traditional system will decrease energy by 60-80% (Strømmen, et al., 2002).

The basic principle of the heat pump dryer is shown in Figure 2. The system will have two main circuits; a general heat pump circuit and an air cycle. The main fan connected to the same motor running the drum, flows hot air from the gas cooler and into the drum. In the drum hot air will reduce in temperature, while the absolute humidity will increase. The air continues through a lint air filter to remove fabric particles before entering the evaporator. In the evaporator humid and relative hot air will be dehumidified by the cold surfaces. The moisture in the air will condense on the colder surfaces in the evaporator where the water will be drained and pumped away to water storage.

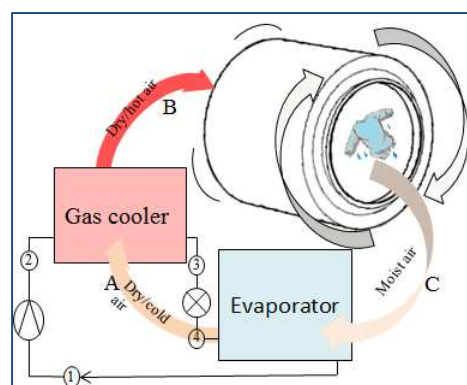


Figure 2 - Heat pump dryer concept

The heat pump system is based on an originally R134a system; the old system has been tested to find the drying time, specific moisture extraction rate and heat pump performance. The new R744 system will be working in a transcritical state; this implies a subcritical evaporating process and a gas cooling process in the supercritical state. The critical temperature of CO₂ is as low as 31.1 °C, and the temperature demand of the air heating process much higher, a supercritical gas cooling is required. The corresponding critical pressure for R744 is 73.4 bars, thus the components are designed to handle working pressures above 100 bars. The new components have been designed from the air side conditions of the R134a cycle.

As for the R134a system there is chosen to have an extra gas cooler as shown in Figure 3, a fan will blow ambient air to reduce the temperature of the CO₂ as much as possible. The extra cooling of the refrigerant is important to reduce throttling losses before the throttling process. During the drying cycle when the humidity content decrease the temperature of the air will increase out of the main gas cooler, which will result in a reduced cooling of the refrigerant and a reduced COP. The external gas cooler will maintain the same cooling capacity through the full cycle, since the ambient air has a constant temperature.

The heat exchangers are tube-in-fin; copper tubes and aluminium – both metals with very good heat transfer characteristics. The evaporator has coated fins to make the water droplets easily drained away from the surface. The compressor is a 2.44 cm³ piston compressor, for this first prototype the compressor has too large outer dimensions to fit in the chassis, and is mounted outside. Further analyses will investigate to find an alternative to the chosen compressor to be able to mount it inside. The expansion process is performed by a capillary tube in parallel to a manual expansion valve, where the experimental data will be compared to the theoretical calculated values. Figure 3 shows the chosen system configuration for the R744 process.

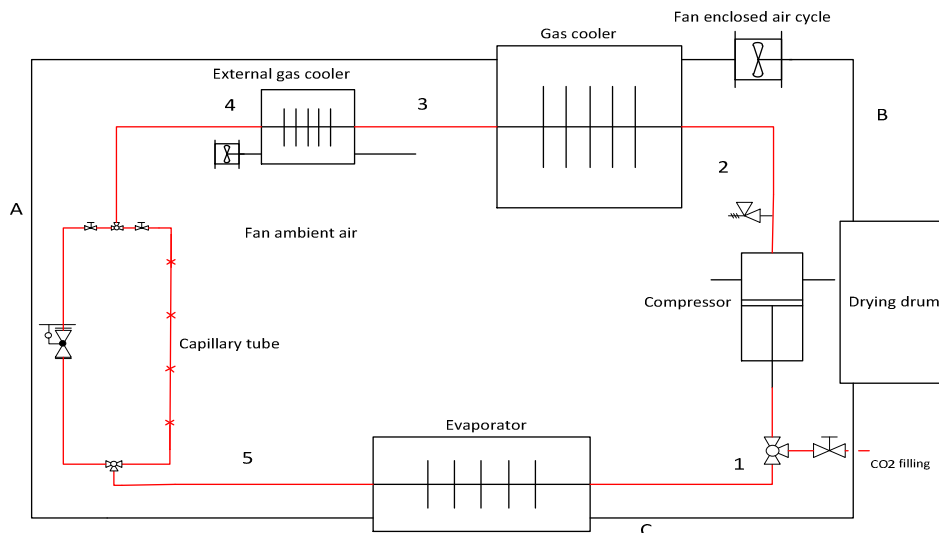


Figure 3 - R744 system configuration

Table 3 shows some important properties of R134a and R744 compared at an evaporation temperature of 0 °C.

Table 3 Refrigerant property data R134a and R744

Property	R134a	CO ₂ (R744)	Units
Molecular weight	102,0	44,01	[g/mol]
Heat of evaporation	198,4	231,6	[kJ/kg]
Thermal conductivity liquid	0,092	0,105	[W/mK]
Thermal conductivity gas	0,012	0,023	[W/mK]
Specific volume liquid	0,768	1,073	[m ³ /kg]
Specific volume gas	71,0	10,2	[m ³ /kg]
Kinematic viscosity liquid	0,212	0,095	[10 ⁻⁶ m ² /s]
Kinematic viscosity gas	0,880	0,156	[10 ⁻⁶ m ² /s]
Critical temperature	101.1	31.1	[°C]
Critical pressure	40.6	73.8	[bars]
Global warming potential	1300	1	[-]
Ozone depletion potential	0	0	[-]

Except from the global warming aspects of the refrigerant selection; there are some thermodynamically differences. R744 has a small gas density which implies that the volumetric

heating capacity of R744 is very good. Nonetheless the low critical temperature at R744 and the supercritical gas cooling process is the largest difference between the refrigerants.

Theoretical background

During the drying cycle the air is heated with constant absolute humidity in the gas cooler, enthalpic humidification process in the drum, and finally a dehumidification process in the evaporator, before the air again enters the gas cooler.

The CO₂ process and the air cycle process are shown in Figure 4 and Figure 5 respectively. The T-x chart shows the changes of temperature and humidity in the enclosed air cycle, while the T-h diagram shows the changes of state in the refrigerant. In the T-x diagram; A represent the inlet of the gas cooler where the air is heated with constant absolute humidity, B is the inlet of the drum where the hot air with constant enthalpy will be humidified from the wet fabric, in point C the air enters the evaporator to be dehumidified.

In the T-x diagram; 1 is saturated refrigerant in the evaporator outlet, 2 represent a 5 K overheat at the outlet of the evaporator. The gas cooling process is represented by point 3 to 5, from point 5 to 6 the gas is expanded into the evaporator.

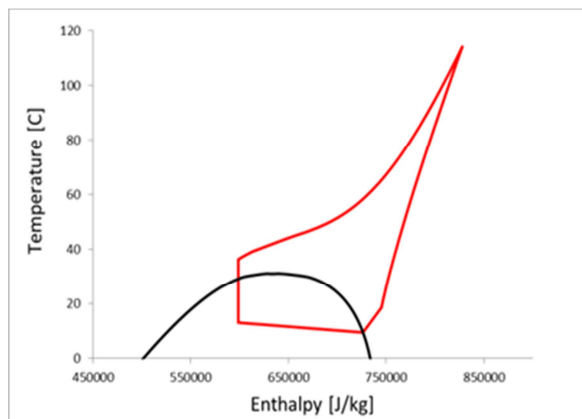


Figure 4 - T-h diagram CO₂

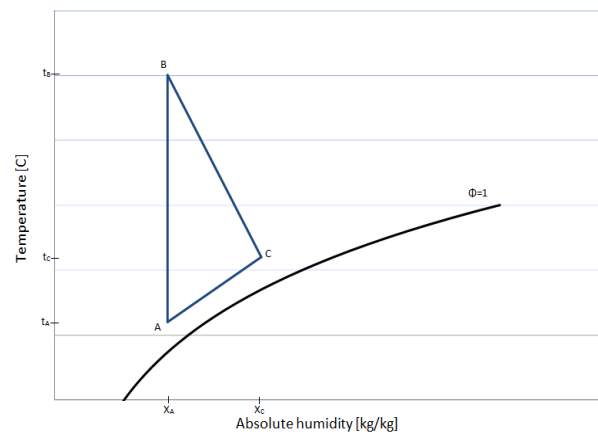


Figure 5 - t-x diagram air cycle

The energy consumption is considered for the heat pump alone and the total system configuration; shown in Equation 5 and Equation 6 respectively.

$$EC_{HP} = \dot{m}_{Ref}(h_3 - h_2)$$

Equation 5 - Energy consumption heat pump [kW]

The compressor and the drum/main fan motor will have varying load through the cycle and will have continuous measurement of energy, while the external fan will have almost constant load through the cycle and will be calculated as a constant value.

$$EC_{Total} = EC_{HP} + EC_{Motor} + EC_{Fan}$$

Equation 6 - Total energy consumption [kW]

Moisture extraction rate (SMER) and coefficient of performance (COP) of the heat pump will indicate the base of comparison of the two refrigerants. The SMER value indicates moisture removed per unit energy input, represented here by [kg_w/kW].

$$SMER_{HP} = \frac{\Delta x_{C-A}}{P_{El}}$$

Equation 7 - Specific moisture extraction rate heat pump [kg_w/kW]

The COP of the system will be represented in the same way; COP_{hp} and COP for the total energy consumption. Except for the compressor the energy consuming components include; drum motor, main fan and external gas cooler fan. The calculations of the heat pump and system performance will be calculated in Equation 8 and Equation 9 respectively.

$$COP_{HP} = \frac{(\Delta h_{gas\ cooler})}{(\Delta h_{Compressor})} = \frac{(h_3 - h_5)}{(h_3 - h_2)}$$

Equation 8 - Heat pump coefficient of performance

$$COP = \frac{\dot{m}_{Ref}(h_3 - h_5)}{EC_{Total}}$$

Equation 9 - Coefficient of performance

Another way to represent the performance of the system is the energy savings, this value represent how much energy is saved at a certain COP value.

$$Energy\ savings = 1 - \frac{1}{COP}$$

Equation 10 – Energy savings [%]

To determine the compressor isentropic efficiency the actual power input to the compressor will be considered together with the measured mass flow and suction specific volume. The compressor isentropic efficiency will be determined from Equation 11.

$$\eta_{is} = \frac{\dot{m}_{ref}(h_{2s} - h_2)}{W_{Compressor}}$$

Equation 11 - Isentropic efficiency actual

Prototype design

This first prototype was made to see if it actually it has a feasible potential to compete with the R134a model. This included that a model that was built in the same chassis as the R134a process delivered from a large manufacturer for these products. The new prototype included that new heat exchangers, compressor and throttling devices had to be dimensioned, ordered and installed.

Selection of the compressor was solely done on the performance data required for the given capacity of the system. A compressor with a displacement volume of 2.44 cm³ specially made for CO₂ applications were chosen for the first prototype. This compressor had a design that had too large outer dimensions to fit within the existing chassis and had to be placed on the outside.

The heat exchangers include an evaporator, a main gas cooler and an external gas cooler; all that have been dimensioned from software from SINTEF. These components are also specially designed for use with CO₂ as refrigerant due to the high pressure they have to withstand.

The system is designed with a manual expansion device in parallel to a capillary tube. The manual valve is installed to be used in the start-up operation for the first experiments, while the results presented are with operation with capillary tube. The dimension of the capillary tube is 660 mm long and an inner diameter of 0.9 mm.

All components have been pressure proven both from manufacturer and locally before experimental operation. A safety report including start and stop procedures, chemical data sheets and hazard operation evaluation has also been performed.

The system has been tested with several refrigerant charges to alter the pressure level to find a best possible operation. For the experiment presented in this article the refrigerant charge was 450 g.

The ambient temperature in the testing facility is not controlled but it will not deviate in a large manner, measurements indicate a temperature of 21 °C +/- 2 K during operation.

Experimental results

The base for the background of this report is on results from the former R134a system; temperature and humidity values have been direct input for simulations to find the sizes of the heat exchangers and compressor.

While the R134a operation is a subcritical process with evaporation at 5 Bara and condensation at 15 Bara, will the CO₂ system operate with evaporation pressure at 45 Bara and gas cooler pressures up to 120 Bara.

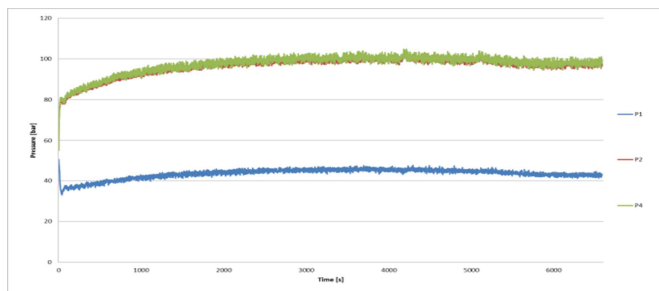


Figure 6 - Pressure levels CO₂

During the experiments it was focused on testing of different factors rather than verifying results through a large repeatability of the chosen configuration. This is considered to be performed for the continued work on the prototype. In the experiments various refrigerant charges, with and without fan to the external gas cooler and with different throttling devices were tried out.

The new designed system was tested with different configurations to find a set-point that would combine a low energy use, short drying time and a smooth operation. The dry load of clothes used in the experiments had a mass of 6.316 kg and was wetted and centrifuged to be close to 10 kg. The clothing load in the R134a experiment compared to the R744 are larger a bit larger and thus the two systems will be compared on the specific value. The tests data from the R134a system has an average dry fabric mass of 8 kg and wetted and centrifuged to become 12.7 kg.

After several experiments the length of the capillary tube for the throttling process was chosen and the required temperature at the inlet of the drum. This temperature is directly dependent on the gas cooler pressure and the discharge temperature from the compressor.

It was observed during experiments that the with an air temperature into the drum around 55 °C the drying time was reduced close to 100 minutes, and thus the energy efficiency would increase.

By using the fan to the external gas cooler the temperature before throttling was drastically reduced and this lead to an increased drying rate in the evaporator. Applying the fan for further prototypes is recommended to reduce drying time.

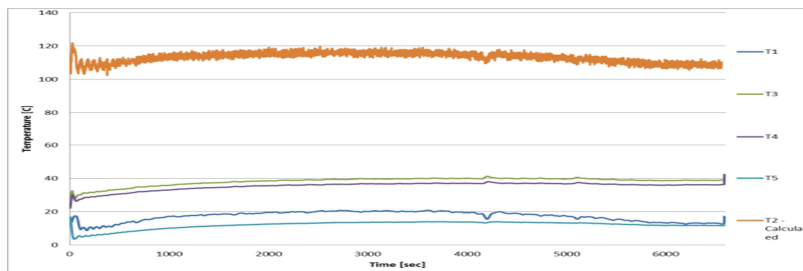


Figure 7 - Operation temperatures

The operational temperatures of the CO₂ cycle were measured with thermocouple measurement devices on the outside of the copper tubes in the system. However it was discovered a rather large error in the measurement of the discharge temperature thus the value shown in Figure 7 have been deduced from measurement of electrical consumption of the compressor.

The gas cooler capacity has an average value around 2900 W, while the evaporator is around 1900 W, both are decreasing towards the end of the drying operation when the fabric is dried.

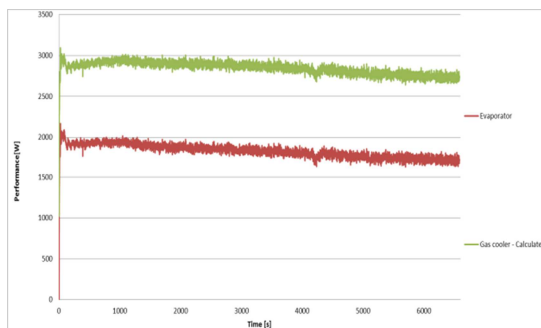


Figure 8 - Gas cooler and evaporator capacity

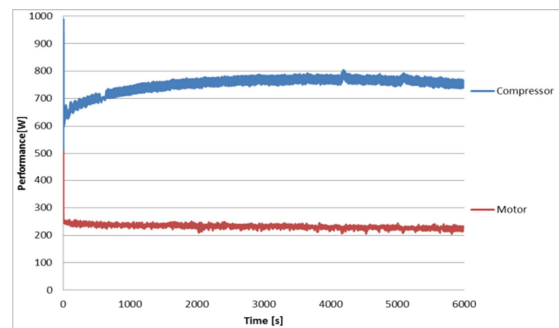


Figure 9 - Power consumption

The power consumed by the motor is running at a stable level during the while drying time just above 200 W, while the compressor reaches a stable value around 760 W after 2000 seconds. For the total energy consumption the external fan with an effect of 33.4 W is added as well.

The total drying time for the CO₂ process is 110 minutes which results in a total energy use of 1.85 kWh to return the fabric to dry state. Similarly are the drying times for the R134a system 145 minutes for the given clothing load, and consumes a total of 2.1 kWh. The specific energy used for this system is calculated to be 0.31 kWh/kg_{Dry fabric}, this value is corrected in relation to EN 61121:2005. The comparable value for the R744 system returns a specific corrected value of 0.36

kWh/kg_{Dry fabric}, thus 13.8 % more energy spent per mass fabric. However data given on specific energy use from the manufacturer for the R134a system has given 0.27 kWh/kg_{Dry fabric} as a reference value to compare the R744 system with.

The registered air leakages from the R744 system are above an acceptable level, this is caused by that the chassis is originally designed and fitted for the R134a system. The air leaks during the drying process are registered with the collected water in the water storage and are around 30 %.

Conclusion

This article is made on the basis of an R134a system, with new R744 components designed for the existing chassis. This results in a non-optimal air cycle due to components with slightly larger core dimensions. Largest are the deviation from the compressor which are placed outside the chassis, but the gas coolers' and the evaporators' core sizes are also not perfect fit for the existing chassis.

The reason to develop this new system using R744 as refrigerant is based on the global warming potential of R134a, which is 1300, while the natural refrigerant R744 has a similar value of 1.

Experiments have been compared from the two similar systems and the first prototype using R744 compared to the R134a system is slightly less energy efficient. Experiments on the two systems have not been performed parallel to each other so there have been some deviations in experiment factors for the two systems. The air leakage ratio from the R744 system is also too large to have a perfect comparable system.

Due to factors mentioned more work should be performed to develop the next prototype based on the design from this first prototype. However at the current point the R744 as refrigerant is less energy efficient than the R134a as refrigerant for the same system. However more experiments should be performed with a new chassis and compressor mounted inside it.

References

Colak Neslian and Hepbasli Arif A review of heat pump drying: Part 1 – Systems, models and studies [Article] // Energy Conversion and management. - [s.l.] : Elsevier, 2009. - 50. - pp. 2180-2186.

Klöcker K, Schmidt E L and Steimle F Carbon dioxide as a working fluid in drying heat pumps [Article] // International journal of refrigeration. - 2001. - 24. - pp. 100-107.

Strømmen Ingvald [et al.] Low temperature drying with heat pump new generations of high quality dried products [Journal]. - Trondheim : [s.n.], 2002. - 13th International drying symposium.

Appendix F: Safety report

Attached on the next page are the safety report for the system, this includes procedures to operate the system, safety brochures for the refrigerant and chemicals applied and a risk assessment.

Risikovurderingsrapport

CO₂ tørketrommel

Prosjekttittel	Development of new heat pump cloth dryer with CO ₂ as working fluid
Prosjektleder	Åsmund Elnan
Enhet	NTNU
HMS-koordinator	Erik Langørgen
Linjeleder	Olav Bolland
Plassering	VVS-lab
Romnummer	
Riggansvarlig	Åsmund Elnan
Risikovurdering utført av	Erik Langørgen

INNHALDSFORTEGNELSE

1	INNLEDNING	1
2	ORGANISERING.....	1
3	RISIKOSTYRING AV PROSJEKTET	1
4	TEGNINGER, FOTO, BESKRIVELSER AV FORSØKSOPPSETT	2
5	EVAKUERING FRA FORSØKSOPPSETNINGEN.....	4
6	VARSLING.....	5
6.1	Før forsøkskjøring.....	5
6.2	Ved uønskede hendelser	5
7	VURDERING AV TEKNISK SIKKERHET	6
7.1	Fareidentifikasjon, HAZOP.....	6
7.2	Brannfarlig, reaksjonsfarlig og trykksatt stoff og gass	6
7.3	Trykkpåkjent utstyr	6
7.4	Påvirkning av ytre miljø (utslipp til luft/vann, støy, temperatur, rystelser, lukt)	8
7.5	Stråling.....	8
7.6	Bruk og behandling av kjemikalier	8
7.7	El sikkerhet (behov for å avvike fra gjeldende forskrifter og normer).....	9
8	VURDERING AV OPERASJONELL SIKKERHET.....	9
8.1	Prosedyre HAZOP	9
8.2	Drifts og nødstopps prosedyre.....	9
8.3	Opplæring av operatører.....	9
8.4	Tekniske modifikasjoner.....	9
8.5	Personlig verneutstyr	10
8.6	Generelt.....	10
8.7	Sikkerhetsutrustning	10
8.8	Spesielle tiltak.....	10
9	TALLFESTING AV RESTRISIKO – RISIKOMATRISSE	10
10	KONKLUSJON	10
11	LOVER FORSKRIFTER OG PÅLEGG SOM GJELDER.....	10
12	VEDLEGG.....	12
•	VEDLEGG A – NODE 1	13
•	VEDLEGG B – NODE 2	14
•	VEDLEGG C: DATABLAD CO2	16
•	VEDLEGG D - PRØVESERTIFIKAT FOR LOKAL TRYKKTESTING	23
•	VEDLEGG E HAZOP MAL PROSEDYRE	25
•	VEDLEGG F FORSØKSPROSEDYRE.....	26
•	VEDLEGG G OPPLÆRINGSPLAN FOR OPERATØRER	27

VEDLEGG H SKJEMA FOR SIKKER JOBB ANALYSE	28
13 VEDLEGG H APPARATURKORT UNITCARD	30
VEDLEGG I FORSØK PÅGÅR KORT	31
VEDLEGG J OLJEDATABLAD	31

1 INNLEDNING

Riggen er en tørketrommel for klær med varmepumpeteknologi, i utgangspunktet var systemet basert på R134a som kuldemedium. Den opprinnelige riggen har blitt demontert og rigget med nye komponenter som er godkjent for overkritisk CO₂. Eksperimentets formål er å undersøke effektiviteten til CO₂ i forhold til R134a i en tørketrommel. Det har vært gjennomført testing av R134a anlegget tidligere som vil være referanse for testresultatene.

Nye deler som er introdusert til systemet er kompressor, gasskjøler, ekstern gasskjøler og fordampner, i tillegg til rørføring/ventiler og instrumentering.

Riggen er montert på et bord i VVS-laben, hoveddelene er plassert inne i en opprinnelig tørketrommel, med kompressoren utenfor på grunn av plassmangel inni selve kabinettet. I tillegg til selve riggen vil det være et stativ med skap for instrumenteringen plassert ved siden av selve riggen.

Rørføringen er med kobberør og er loddet med sølvlodding og sammenkoblet med Swagelok tilkoblinger som er godkjente for høye trykk.

2 ORGANISERING

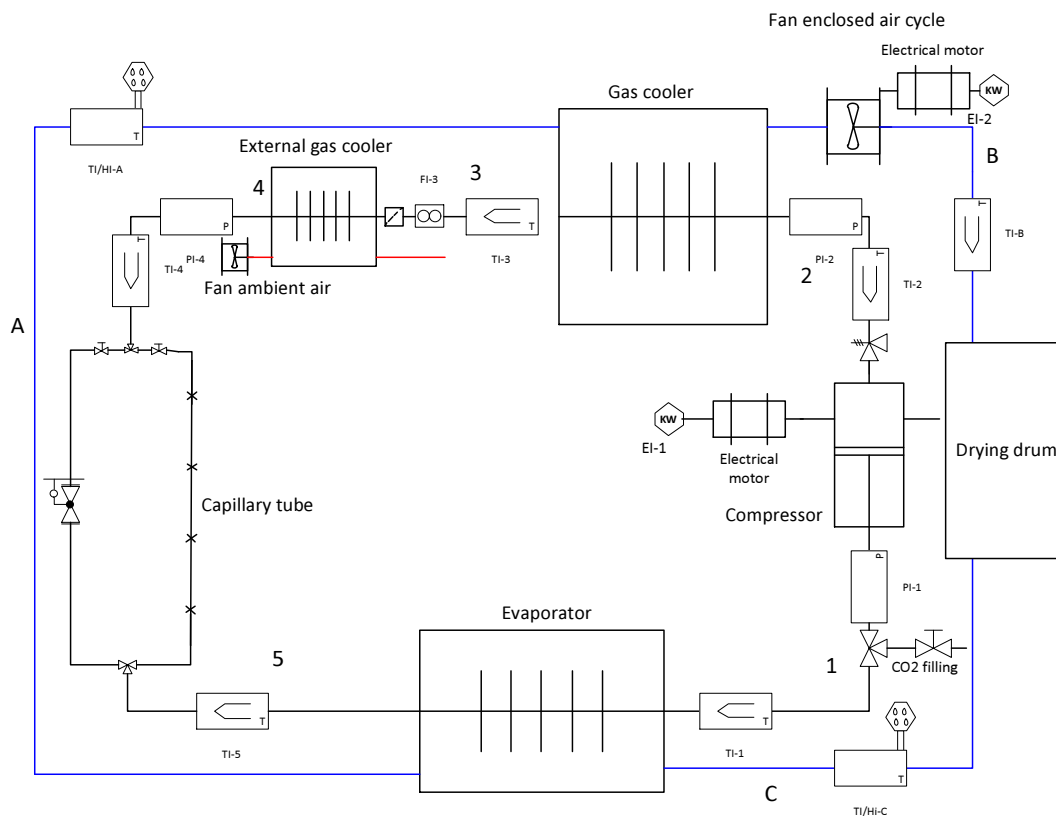
Rolle	NTNU	Sintef
Lab Ansvarlig:	Morten Grønli	Harald Mæhlum
Linjeleder:	Olav Bolland	Mona J. Mølsvik
HMS ansvarlig:	Olav Bolland	Mona J. Mølsvik
HMS koordinator	Erik Langørgen	Harald Mæhlum
HMS koordinator	Bård Brandåstrø	
Romansvarlig:	Håvard Rekstad	
Prosjektleder:	Åsmund Elnan, NTNU	
Ansvarlig riggoperatører:	Åsmund Elnan, NTNU	

3 RISIKOSTYRING AV PROSJEKTET

Hovedaktiviteter risikostyring	Nødvendige tiltak, dokumentasjon	DTG
Prosjekt initiering	Prosjekt initiering mal	
Veiledningsmøte	Skjema for Veiledningsmøte med pre-risikovurdering	
Innledende risikovurdering	Fareidentifikasjon – HAZID Skjema grovanalyse	
Vurdering av teknisk sikkerhet	Prosess-HAZOP Tekniske dokumentasjoner	
Vurdering av operasjonell sikkerhet	Prosedyre-HAZOP Opplæringsplan for operatører	
Sluttvurdering, kvalitetssikring	Uavhengig kontroll Utstedelse av apparaturkort Utstedelse av forsøk pågår kort	

4 TEGNINGER, FOTO, BESKRIVELSER AV FORSØKSOPPSETT

Vedlegg:



Svart krets: CO₂-krets

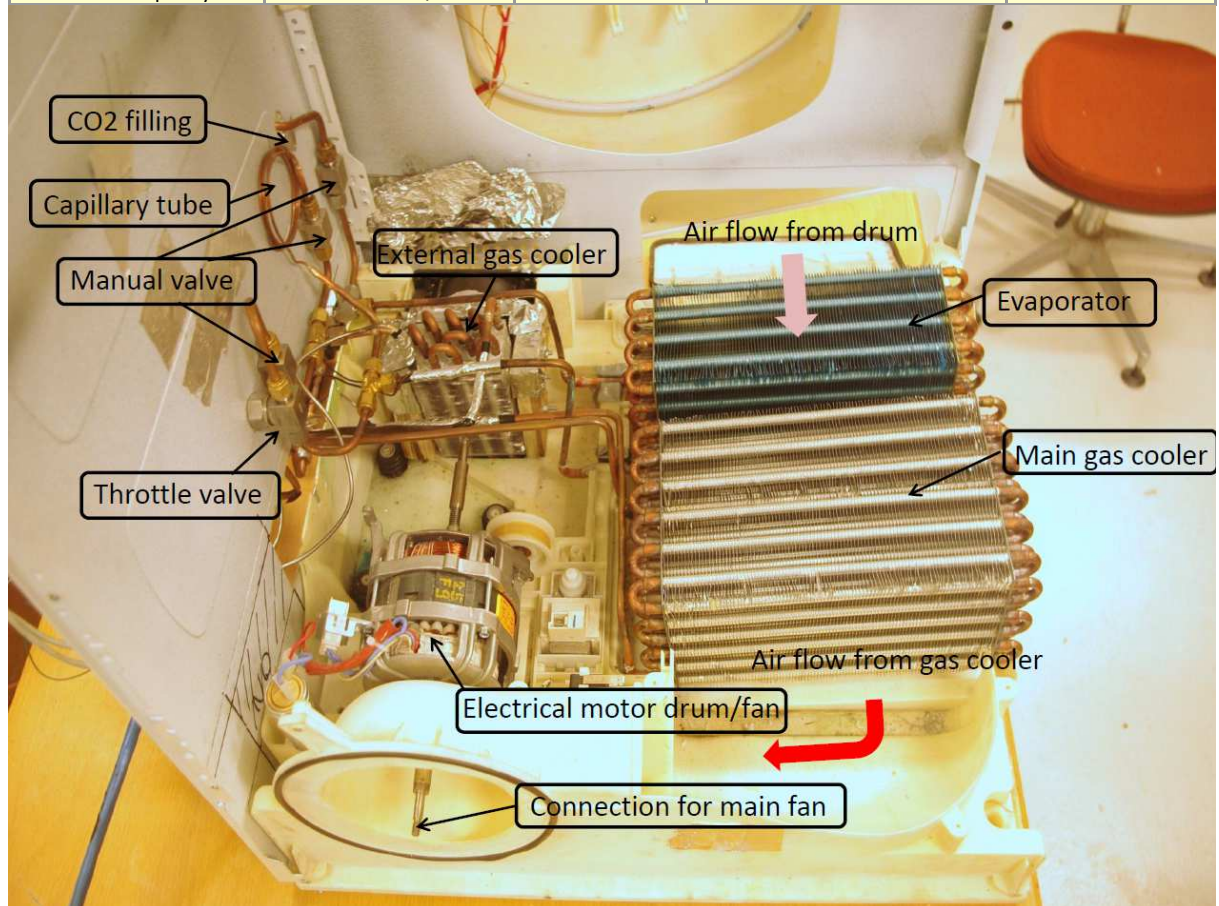
Blå krets: intern luftkrets

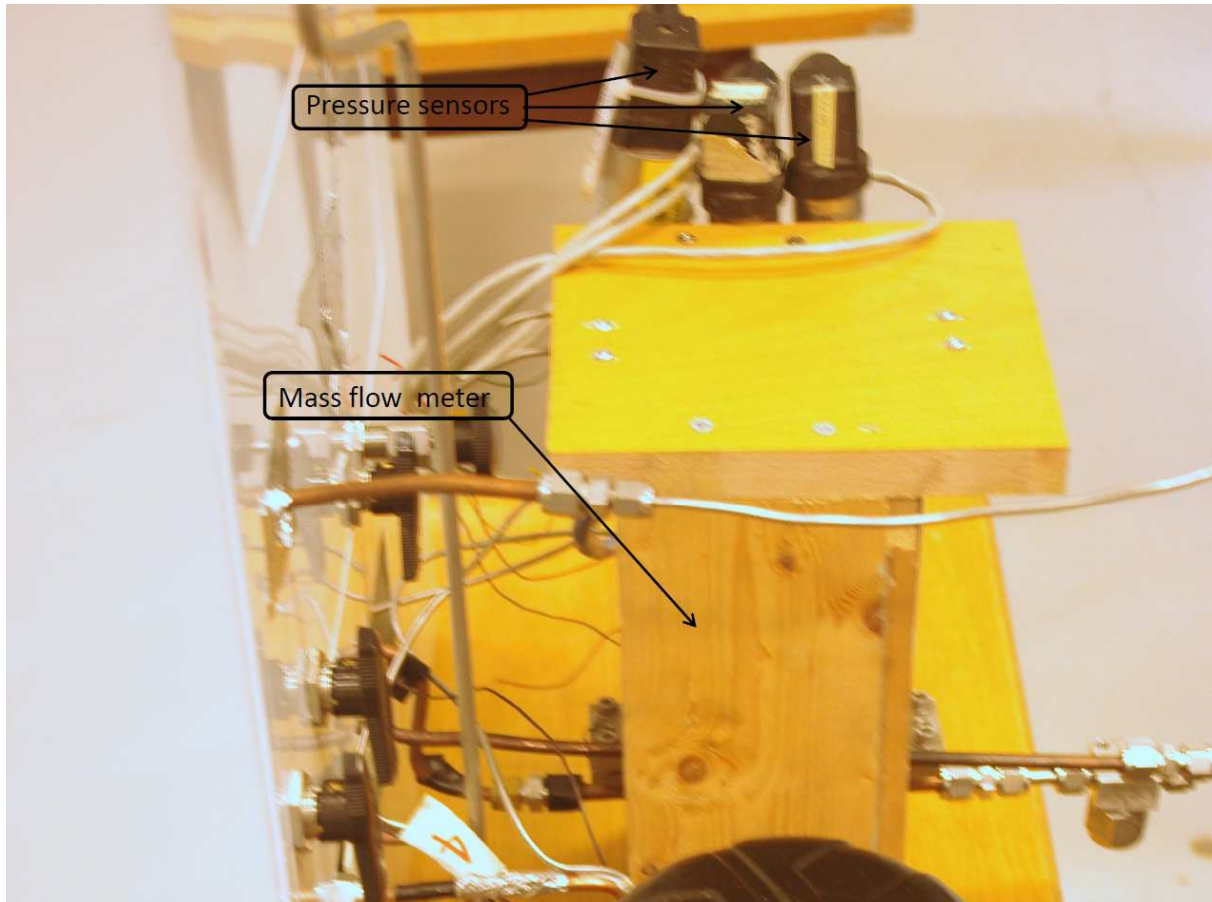
Rød krets: omgivelses luft

Instrument List					
Displayed Text	Description	Connection Type	Output signal	Manufacturer	Model
FI-3	Coriolis Mass flowmeter with fast response	8 mm	4-20 mA	RHEOINK	RHM04
PI-1	Pressure sensor	(1/8)"	0.4-2.0 V	Druck	PTX 1400
PI-2	Pressure sensor	(1/8)"	0.8-4.0 V	Druck	PTX 1400
PI-4	Pressure sensor	(1/8)"	4-20 mA	Druck	PTX 510-00
TI-1	Thermocouple	Outer tube surface		National instruments	9211
TI-2	Thermocouple	Outer tube surface		National instruments	9211
TI-2a	Thermocouple	In air cycle		National instruments	9211
TI-3	Thermocouple	Outer tube surface		National instruments	9211
TI-4	Thermocouple	Outer tube surface		National Instruments	9211
TI-5	Thermocouple	Outer tube surface		National Instruments	9211
TI/Hi-A	Temp and humidity transmitter	In air cycle	4-20 mA	Vaisala	HMP233
TI/Hi-C	Temp and humidity transmitter	In air cycle	4-20 mA	Vaisala	HMP233
EI-1	Wattmeter	Compressor	4-20 ma	M-system CO Ltd	LWT-24A1-H
EI-2	Wattmeter	Drum power supply	4-20 mA	M-system CO Ltd	LWT-24A1-H

Equipment List				
Displayed Text	Description	Manufacturer	Material	Model
Compressor	CO2 compressor	Embraco	Iron	EK 6214 CD
Gas cooler	CO2 HX	Sierra	Cu/Al	Custom made
External gas cooler	CO2 HX	Sierra	Cu/Al	Custom made
Evaporator	CO2 HX	Sierra	Cu/Al	Custom made
Dryer components		ASKO		

Valve and pipeline list				
Description	Valve Class	Manufacturer	Model	Number/length
Swagelok Tee		Swagelok	316L-400-3 Stainless Steel	#3
Manual metering valve	Cv 0.04	Swagelok	SS-31RS4	#1
Standard 2-way		Swagelok	SS-43GS4	#3
Pressure safety valve	Max t/p 121 C/ 338 Bar	Swagelok	SS-4R3A, High pressure	#1
CO2 tubes	(1/4)"		CO2 copper tubes	ca 3.7 meter
Capillary tube	Ø0.9 mm			ca 1 meter





Operatør vil oppholde seg rett i nærheten av systemet da det er en manuell strupeventil som skal opereres montert på selve tørketrommelveggen. CO₂ flaske for påfylling vil være i direkte nærhet av riggen for å kunne regulere mengde CO₂ under selve eksperimentet. Datalogger med direkte overvåking av trykk, temperatur og massestrøm vil overvåkes gjennom hele eksperimentet.

Avstengningsventiler for CO₂ vil være på rigg.

Er ingen vannkjøling på anlegget så det er ingen ventiler for vann direkte relatert til riggen.

Avstengningsprosedyr forekommer ved å kutte elektristet til kompressoren da dette vil avslutte trykkøkning på høytrykkside av varmepumpesyklusen og trykket vil etter hvert stabilisere seg gjennom strupeventilen.

Systemet er testet for trykk opp til 160 bar uten kompressor og trykkceller innkoblet, og lekkasjetestet for 100 bar med kompressor og trykkceller innkoblet.

5 EVAKUERING FRA FORSØKSOPPSETNINGEN

Evakuering skjer på signal fra alarmklokker eller lokale gassalarmstasjon med egen lokal varsling med lyd og lys utenfor aktuelle rom, se 6.2

Evakuering fra rigg området foregår igjennom merkede nødutganger til møteplass, (hjørnet gamle kjemi/kjelhuset eller parkeringsplass 1a-b.)

Aksjon på rigg ved evakuering: Ved evakuering under forsøk vil elektrisitet tilkoblet systemet slås AV. Det vil ikke være noen avtapping av CO₂ i forbindelse med evakuering, eventuell lekkasje av medium til omgivelsene sees på som ufarlig da fyllingen i anlegget er veldig liten og forsøk vil gjennomføres i rom med store luftvolum. Dette vil ikke føre til noen kvelningsfare.

CO₂ er brannhemmende og vil ikke være noen eksplosjons/brann-fare ved eventuell brann i rigg eller i nærområdet.

6 VARSLING

6.1 Før forsøkskjøring

Varsling per e-post, med opplysning om forsøkskjøringens varighet og involverte til:

- HMS koordinator NTNU/SINTEF
Erik.langorgen@ntnu.no
Baard.brandaastro@ntnu.no

All forsøkskjøringen skal planlegges og legges inn i aktivitetskalender for lab. Forsøksleder må få bekreftelse på at forsøkene er klarert med øvrig labdrift før forsøk kan iverksettes.

6.2 Ved uønskede hendelser

BRANN

Ved brann en ikke selv er i stand til å slukke med rimelige lokalt tilgjengelige slukkemidler, skal nærmeste brannalarm utløses og arealet evakueres raskest mulig. En skal så være tilgjengelig for brannvesen/bygningsvaktmester for å påvise brannsted.

Om mulig varsles så:

NTNU	SINTEF
Labsjef Morten Grønli, tlf: 918 97 515	Labsjef Harald Mæhlum tlf: 930 149 86
HMS: Erik Langørgen, tlf: 91897160	Forskningsjef Lars Sørnum tlf:928 049 25
Instituttleder: Olav Bolland: tlf:91897209	

GASSALARM

Ved gassalarm skal gassflasker stenges umiddelbart og området ventileres. Klarer man ikke innen rimelig tid å få ned nivået på gasskonsentrasjonen så utløses brannalarm og laben evakueres. Dedikert personell og eller brannvesen sjekker så lekkasjested for å fastslå om det er mulig å tette lekkasje og lufte ut området på en forsvarlig måte.

Varslingsrekkefølge som i overstående punkt.

PERSONSKADE

- Førstehjelpsutstyr i Brann/førstehjelpsstasjoner,
- Rop på hjelp,

- Start livreddende førstehjelp
- **Ring 113** hvis det er eller det er tvil om det er alvorlig skade.

ANDRE UØNSKEDE HENDELSER (AVVIK)

NTNU:

Rapporteringskjema for uønskede hendelser på

http://www.ntnu.no/hms/2007_Nettsider/HMSRV0401_avvik.doc

SINTEF:

Synergi

7 VURDERING AV TEKNISK SIKKERHET

7.1 Fareidentifikasjon, HAZOP

Forsøksoppsetningen deles inn i følgende noder:

Node 1	Varmepumpeenhet
Node 2	Tørketrommelenhet (roterende trommel)

Vedlegg: Hazop mal

Vurdering:

7.2 Brannfarlig, reaksjonsfarlig og trykksatt stoff og gass

Inneholder forsøkene brannfarlig, reaksjonsfarlig og trykksatt stoff

<input type="checkbox"/>	JA. Eksplosjonsverndokument utarbeides og eller dokumentert trykktest, (kap 7.3)
--------------------------	--

Vedlegg : Se 7.3

Vurdering: Maks arbeidstrykk er 120 bar, ingen eksplosjonsfare.

7.3 Trykkpåkjent utstyr

Inneholder forsøksoppsetningen trykkpåkjent utstyr:

<input type="checkbox"/>	JA. Utstyret trykktestes i henhold til norm og dokumenteres
--------------------------	---

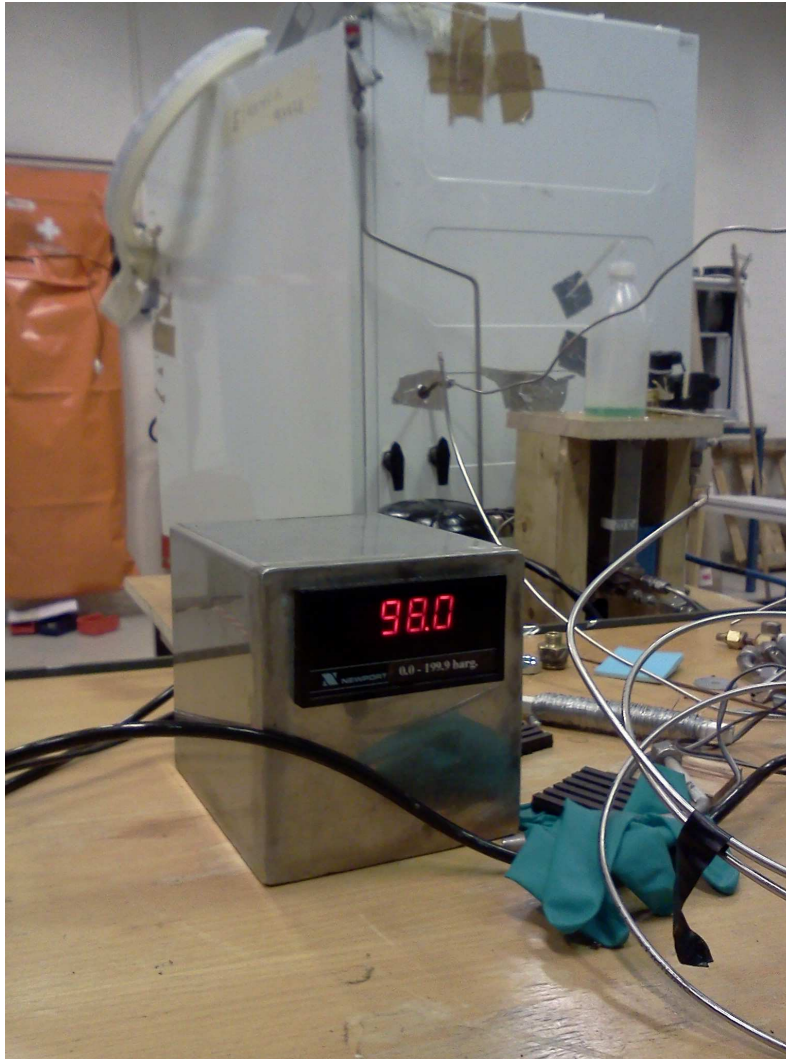
Trykkutsatt utstyr skal trykktestes med driftstrykk gange faktor 1.4, for utstyr som har usertifiserte sveiser er faktoren 1.8. Trykktesten skal dokumenteres skriftlig hvor fremgangsmåte framgår.

Anleggets maksimale driftstrykk vil være 120 bar.

Anlegget ble trykksatt med nitrogen opp til 160 bar, der med mindre lekkasjer det gikk ned til ca. 154 bar i løpet av en time. Her var kompressor ikke inkludert i testingen da den har et makstrykk på 120 bar. Det ble påført såpevann for å avdekke lokasjon av eventuelle lekkasjer. Der det ble funnet lekkasjer ble enten Swagelok kobling skrudd fastere, eller utskiftet på grunn av slitasje, da noen deler er gjenbruksdeler. Anlegget ble igjen trykksatt opp til samme trykk for å teste utskiftede koblinger.



Anlegget ble satt opp med alle komponenter inkludert kompressoren og trykceller innkoblet, maks trykk ble ført opp til 100 bar og i løpet av første timen var trykket redusert til ca. 99 bar. I løpet av de neste 14 timene under trykk var trykket redusert ned til 98 bar.



Vedlegg: Sertifikat for trykkpåkjent utstyr.

Vurdering:

7.4 Påvirkning av ytre miljø (utslipp til luft/vann, støy, temperatur, rystelser, lukt)

NEI	
-----	--

Vurdering: Vil eksperimentene generere utslipp av røyk, gass, lukt eller unormalt avfall.? Mengder/konsistens. Er det behov for utslippstillatelse, ekstraordinære tiltak? Eventuelle utslipp til omgivelser vil være mindre mengder CO₂, dette vil ikke ha noen påvirkning på hverken lokale eller globale skalaer.

7.5 Stråling

NEI	
-----	--

Vedlegg:

Vurdering:

7.6 Bruk og behandling av kjemikalier

JA	CO ₂ (gass)
----	------------------------

Vedlegg: Sikkerhetsdatablad for CO₂

Vurdering: Riggene inneholder små mengder, utslipp vil ikke føre til kvelningsfare.

7.7 El sikkerhet (behov for å avvike fra gjeldende forskrifter og normer)

NEI	JA, El sikkerhet gjennomgås å risikovurderes
-----	--

Her forstås montasje og bruk i forhold til normer og forskrifter med tanke på berøringsfare

Vurdering: NA

8 VURDERING AV OPERASJONELL SIKKERHET

Sikrer at etablerte prosedyrer dekker alle identifiserte risikoforhold som må håndteres gjennom operasjonelle barrierer og at operatører og teknisk utførende har tilstrekkelig kompetanse.

8.1 Prosedyre HAZOP

Metoden er en undersøkelse av operasjonsprosedyrer, og identifiserer årsaker og farekilder for operasjonelle problemer.

Vedlegg: Ingen

Vurdering:

8.2 Drifts og nødstopps prosedyre

Driftsprosedyren er en sjekklister som skal fylles ut for hvert forsøk.

Nødstopps prosedyren skal sette forsøksoppsetningen i en harmløs tilstand ved uforutsette hendelser.

Vedlegg "Procedure for running experiments

Nødstopps prosedyre: Elektristet til kompressor, trommel og vifte kuttes ved å trykke på nødstoppbryter vil systemet vil umiddelbart stoppes. Ingen elektrisitet tilføres til systemet. CO₂ under trykk i varmpumpesyklusen vil falle til balansetrykket i systemet gjennom strupeventilen over tid.

8.3 Opplæring av operatører

Dokument som viser Opplæringsplan for operatører utarbeides for alle forsøksoppsetninger.

Vedlegg H

- Hvilke krav er det til opplæring av operatører.
- Hva skal til for å bli selvstendig operatør
- Arbeidsbeskrivelse for operatører

Vedlegg: Opplæringsplan for operatører

8.4 Tekniske modifikasjoner

- Tekniske modifikasjoner som kan gjøres av Operatør
 - Utføres av sertifisert personell
- Tekniske modifikasjoner som må gjøres av Teknisk personale:
 - Modifikasjon på trykkpåkjent utstyr
- Hvilke tekniske modifikasjoner utløser krav om ny risikovurdering

- Endringer av CO₂ krets

8.5 Personlig verneutstyr

- Det er påbudt med vernebriller i sonen anlegget er plassert i.

8.6 Generelt

- Området rundt forsøksoppsetningen avskjermes.
- Traverskran og truck kjøring skal ikke foregå i nærheten under eksperimentet.
- Gassflasker skal plasseres i godkjent stativ med avstengningsventil lett tilgjengelig.
- Vann og trykklufttilførsel i slanger skal stenges/kobles fra ved nærmeste fastpunkt når riggen ikke er i bruk.

8.7 Sikkerhetsutrustning

- Ingen utover det som er montert på riggen

8.8 Spesielle tiltak

- Det vil være full overvåkning under eksperiment.
- Sikker jobb analyse ved modifikasjoner,(SJA)
 - Brannfarlig/giftig gass eller kjemikalier

9 TALLFESTING AV RESTRISIKO – RISIKOMATRISSE

Risikomatrissen vil gi en visualisering og en samlet oversikt over aktivitetens risikoforhold slik at ledelse og brukere får et mest mulig komplett bilde av risikoforhold.

IDnr	Aktivitet-hendelse	Frekv-Sans	Kons	RV
1	Utblåsning CO ₂ krets - CO ₂ i kontakt med hud - frostskafer	1	B	B1
2	Roterende deler	1	A	A1
3	Utblåsning varm side	3	C	C3

Vurdering restrisiko: Akseptabel

10 KONKLUSJON

Riggen er bygget til god laboratorium praksis (GLP).

Hvilke tekniske endringer eller endringer av driftsparametere vil kreve ny risikovurdering.

Annet medium, trykk, mekaniske inngrep

Apparaturkortet får en gyldighet på **2 måneder**

Forsøk pågår kort får en gyldighet på **2 måneder**

11 LOVER FORSKRIFTER OG PÅLEGG SOM GJELDER

Se <http://www.arbeidstilsynet.no/regelverk/index.html>

- Lov om tilsyn med elektriske anlegg og elektrisk utstyr (1929)
- Arbeidsmiljøloven

- Forskrift om systematisk helse-, miljø- og sikkerhetsarbeid (HMS Internkontrollforskrift)
- Forskrift om sikkerhet ved arbeid og drift av elektriske anlegg (FSE 2006)
- Forskrift om elektriske forsyningsanlegg (FEF 2006)
- Forskrift om utstyr og sikkerhetssystem til bruk i eksplosjonsfarlig område NEK 420
- Forskrift om håndtering av brannfarlig, reaksjonsfarlig og trykksatt stoff samt utstyr og anlegg som benyttes ved håndteringen
- Forskrift om Håndtering av eksplosjonsfarlig stoff
- Forskrift om bruk av arbeidsutstyr.
- Forskrift om Arbeidsplasser og arbeidslokaler
- Forskrift om Bruk av personlig verneutstyr på arbeidsplassen
- Forskrift om Helse og sikkerhet i eksplosjonsfarlige atmosfærer
- Forskrift om Høytrykksspyling
- Forskrift om Maskiner
- Forskrift om Sikkerhetsskiltning og signalgivning på arbeidsplassen
- Forskrift om Stillaser, stiger og arbeid på tak m.m.
- Forskrift om Sveising, termisk skjæring, termisk sprøyting, kullbuemeisling, lodding og sliping (varmt arbeid)
- Forskrift om Tekniske innretninger
- Forskrift om Tungt og ensformig arbeid
- Forskrift om Vern mot eksponering for kjemikalier på arbeidsplassen (Kjemikalieforskriften)
- Forskrift om Vern mot kunstig optisk stråling på arbeidsplassen
- Forskrift om Vern mot mekaniske vibrasjoner
- Forskrift om Vern mot støy på arbeidsplassen

Veiledninger fra arbeidstilsynet

se: <http://www.arbeidstilsynet.no/regelverk/veiledninger.html>

Vedlegg til Risikovurderingsrapport

CO₂ tørketrommel

Prosjekttittel	Development of new heat pump cloth drum dryer with CO ₂ as working fluid
Prosjektleder	Åsmund Elnan
Enhet	NTNU
HMS-koordinator	Erik Langørgen
Linjeleder	Olav Bolland
Plassering	VVS-lab
Romnummer	VVS-Lab
Riggansvarlig	Åsmund Elnan

• VEDLEGG A – NODE 1

Project: Node: 1 – CO ₂ krets							Page
Ref #	Guideword	Causes	Consequences	Safeguards	Recommendations	Action	Date Sign
1	No flow	Defekt rørføring	Ingen strømning	Følge trykk og massestrøm gjennom eksperiment			
2	More flow	For stor åpning i strupningen	Overfylt fordampner, kan føre til for liten overhetning og risiko for væske i kompressor	Følge trykk og massestrøm gjennom eksperiment			
3	Less flow	Strupning er tett	Økt trykk, redusert kjølekapasitet, varmt innsug til kompressor - tap	Følge trykk og massestrøm gjennom eksperiment			
4	More pressure	Strupning er tett	Økt trykk, redusert kjølekapasitet	Åpne strupning, for å redusere trykk			
5	Less pressure	Lekkasje	Kompressor suger luft, trykk faller	Overvåke målinger på trykk og massestrøm			
6	More temperature	Fuktighet i klær er borte	Høytrykk øker i mindre grad – tørkeprosess avsluttes når utløp fra trommel er på gitt nivå	Pressostat i LabView dersom det overgår kritisk nivå			

Project: Node: 1 – CO ₂ krets							Page
Ref #	Guideword	Causes	Consequences	Safeguards	Recommendations	Action	Date Sign
7	Contamination	Se ref #3	Se ref #3	Se ref #3			
8	Relief	Ukontrollert trykkoppbygning	CO ₂ utslipp til atmosfære – ingen lokal konsekvens	Overtrykksventil	Holde seg unna varm oljedamp.		

- **VEDLEGG B – NODE 2**

Project: Node: 2 – Tørketrommelenhet (motor, trommel, vannpumpe)							Page
Ref #	Guideword	Causes	Consequences	Safeguards	Recommendations	Action	Date Sign
1	Obstructed rotation	Trommel i kontakt med kabinett	Ytre skader på ulike deler	Passe på, lytte etter ulyder			
2	Water over flow	Defekt pumpe	Vann renner ut av trommel	Teste at pumpe går som den skal, se etter evt. lekkasjer			
3	Smoke	Brent motor, trommel i kontakt med kabinett	Ødeleggelser av kritiske deler til tørketrommelen	Være observant på unormale lukter, lyder, røyk			

Project: Node: 2 – Tørketrommelenhet (motor, trommel, vannpumpe)							Page
Ref #	Guideword	Causes	Consequences	Safeguards	Recommendations	Action	Date Sign

- **VEDLEGG C: DATABLAD**
CO2

HMS-DATABLAD

 Linde Gas | **AGA**

Sist endret: 26.05.2006

Internt nr: 0011

Erstatter dato:30.01.2003

KARBONDIOKSID (FLYTENDE)

1. IDENTIFIKASJON AV KJEMIKALIET OG ANSVARLIG FÖRETAK

HANDELSNAVN	KARBONDIOKSID (FLYTENDE)
KJEMISK NAVN	Karbondioksid
SYNONYMER	Dypkjølt karbondioksid, kondensert karbondioksid, ; Flytende karbondioksid, liquid karbondioksid,
FORMEL	CO ₂
Cas-nr.	124-38-9
EC-nr.	204-696-9
Indeksnr.	

NASJONAL PRODUSENT/IMPORTØR

Foretak	AGA AS
Adresse	Pb 13 Grefsen
Postnr./sted	0409 Oslo
Land	Norge
Internett	www.aga.no
Telefon	+ 47 23 17 72 00
Faks	+ 47 22 02 78 04

2. OPPLYSNINGER OM KJEMISK SAMMENSETNING

Nr.	Ingrediensnavn	EC-nr.	Cas-nr.	Vekt-%	Merking
1	Karbondioksid, flytende	204-696-9	124-38-9	ca 100%	

Tegnforklaring: T+=meget giftig, T=giftig, C=etsende, Xn=helseskadelig, Xi=irriterendeE=eksplosiv, O=oksiderende, F+=ekstremt brannfarlig, F=meget brannfarlig, N=miljøskadelig, Kreft=kreftfremkallende, Mut=arvestoffskadelig, Rep=reproduksjonsskadelig, Kons.=konsentrasjon

3. VIKTIGSTE FAREMOMENTER

GENERELT

Vurdert ikke merkepliktig.

HELSE

Fare for kvelning ved utslipp i trange rom. Frostskafer ved kontakt med flytende karbondioksid.

4. FØRSTEHJELPSTILTAK

HMS-DATABLAD

Linde Gas | AGA

Sist endret: 26.05.2006

Internr nr: 0011

Erstatter dato:30.01.2003

GENERELT

Gass eller damp fortrenger oksygen og kan medføre kvelningsfare. Bring pasienten ut i frisk luft og sikkerhet. Ved bevisstløshet: Løs stramtsittende klær, stabilt sideleie. Gi kunstig åndedrett ved åndedrettsstans. Ved hjertestans gis hjertemassasje. Sørg for ro, varme og frisk luft. Skaff øyeblikkelig legehjelp.

INNÅNDING

Vanlig førstehjelp; ro, varme og frisk luft. Ved åndedrettsstans: Gi kunstig åndedrett, evt. oksygen. Ved alvorlige pustevansker kan oksygentilførsel være nødvendig. Ved bevisstløshet løses tetsittende klær, plasser i stabilt sideleie. Kunstig åndedrett ved munn til munn-metoden og hjertemassasje om nødvendig. Kontakt lege.

HUDKONTAKT

Gassen er meget kald når den kommer ut av beholderen, og det kan forårsake frostskafer på hud. Skyll huden med store mengder vann, samtidig som tilsølte klær, armbåndsur o.l. fjernes. Fortsett å skylle i minst 15 minutter. Tildekkes med steril kompress. Konsulter lege.

ØYEKONTAKT

Skyll øyeblikkelig med lunkent, rennende vann i minst 15 minutter. Hold øyelokkene godt fra hverandre. Unngå store vanntrykk mot øyet. Kontakt lege hvis ubehag vedvarer etter skylling.

SVELGING

Ikke aktuelt (produktet er en gass).

MEDISINSK INFORMASJON

Symptomatisk behandling. Kontakt evt. Giftinformasjonssentralen (tlf. 22 59 13 00, fax. 22 60 85 75).

5. TILTAK VED BRANNSLUKKING

EGNET BRANNSLUKKINGSMIDDEL

Vann, CO₂, skum, pulver. Slukningsmiddel velges mht. omgivende brann.

UEGNET BRANNSLUKKINGSMIDDEL

Bruk ikke full vannstråle.

BRANN- OG EKSPLOSJONSFARE

Produktet er ikke brannfarlig. Eksplosjonsrisiko ved brann i lukkede beholdere eller rom.

PERSONLIG VERNEUTSTYR VED SLUKKING AV BRANN

Egnet åndedrettsvern vil være nødvendig. Brannen bekjempes fra mest mulig beskyttet plass pga. eksplosjonsfare hvis trykkbeholdere utsettes for sterk varme.

HMS-DATABLAD

Linde Gas | AGA

Sist endret: 26.05.2006

Internt nr: 0011

Erstatter dato:30.01.2003

ANNEN INFORMASJON

Brann-/varmeutsatte beholdere kjøles med vann eller dekkes med f.eks karbondioksid-pulver, evt. fjernes dersom det er uten risiko for personellet. Brannen bekjempes fra mest mulig beskyttet plass pga. eksplosjonsfare hvis trykkbeholdere utsettes for sterk varme. Kontakt brannvesenet for hjelp.

6. TILTAK VED UTILSIKTET UTSLIPP

SIKKERHETSTILTAK FOR Å BESKYTTE PERSONELL

Advar personer i nærheten, og hold uvedkommende borte. Sørg for nødvendig ventilasjon for å forhindre oksygenmangel (kvelningsfare). Stopp gasslekkasje hvis det er mulig uten risiko. Hvis lekkasje ikke kan stoppes; evakuer området. Gassen er meget kald når den kommer ut av beholderen, og det kan forårsake frostskafer på hud. Vær oppmerksom på at temperaturen i/på beholder vil synke ved lekkasje og at dette kan ha en sterkt nedkjølende effekt. Gassen er tyngre enn luft og vil legge seg langs bakken eller i fordypninger. Kontakt brannvesenet for hjelp.

SIKKERHETSTILTAK FOR Å BESKYTTE YTRE MILJØ

Miljøopplysninger er ikke oppgitt for produktet.

METODER FOR OPPRYDDING OG RENGJØRING

Behandles i henhold til lover og regler for avfallshåndtering (se pkt. 13). Bring evt. flasken(e) ut i friluft hvor lekkasjen kan skje uten fare for omgivelsene. Kontakt brannvesenet for hjelp.

ANNEN INFORMASJON

Gass eller damp fortrenger oksygen og kan medføre kvelningsfare.

7. HÅNTERING OG OPPBEVARING

HÅNTERING

Gass eller damp fortrenger oksygen og kan medføre kvelningsfare. Anvend bare utstyr og materialer godkjent for denne gassen. Sørg for god ventilasjon. Ventiler skal åpnes og stenges langsomt. Unngå å åpne flaskeventilen mot ansiktet. Gassen er tyngre enn luft og vil legge seg langs bakken eller i fordypninger.

OPPBEVARING

Lagres godt ventileret på et godkjent, brannsikret sted beskyttet mot direkte sollys og varme. Påse at ventilen er stengt og at ventilbeskyttelsen er montert. Gassen er tyngre enn luft og vil legge seg langs bakken eller i fordypninger. Varselskilt "GASS UNDER TRYKK" og "FLYTENDE KARBONDIOKSID" må benyttes.

8. EKSPONERINGSKONTROLL OG PERSONLIG VERNEUTSTYR

BEGRENSNING OG KONTROLL AV EKSPONERING

Sørg for god ventilasjon. I kontakt med flater som holder romtemperatur vil den flytende gassen koke voldsomt og sprute.

HMS-DATABLAD

Linde Gas | AGA

Sist endret: 26.05.2006

Intern nr: 0011

Erstatter dato:30.01.2003

ÅNDEDRETTSVERN

Må ikke brukes i trange rom uten god ventilasjon og/eller bruk av åndedrettsvern.

ØYEVERN

Bruk godkjente vernebriller eller ansiktsskjerm.

HÅNDVERN

Benytt arbeidshansker tilpasset det øvrige arbeidet.

ANNET HUDVERN ENN HÅNDVERN

Bruk vernesko. Bruk egnede verneklær.

ANNEN INFORMASJON

Arbeidstilsynet har fastsatt forskrift om personlig verneutstyr på arbeidsplassen, se Best.nr. 524.

ADMINISTRATIVE NORMER

Ingrediensnavn	Cas-nr.	Intervall	ppm	mg/m ³	År	Anm.
Karbondioksid, flytende	124-38-9	8 timer	5000,0	9000,0		

9. FYSISKE OG KJEMISKE EGENSKAPER

TILSTANDSFORM

Dypkjølt flytende gass, inert.

FARGE

Fargeløs.

LUKT

Svak, stikkende syrlig lukt.

LØSELIGHET

Løselig i vann.

FYSISKE OG KJEMISKE PARAMETERE

Tetthet:	1,85	Løselighet i vann:	0,878 l/kg
Damptrykk:	50 bar	Rel. tetth. i m. luft (l=1):	1,53
Kokepunkt:	-78,4°C	Molvekt:	44,01
Viskositet:		Trippelpunkt:	-56,57°C

10. STABILITET OG REAKTIVITET

HMS-DATABLAD

Linde Gas | AGA

Sist endret: 26.05.2006

Internt nr: 0011

Erstatter dato:30.01.2003

STABILITET

Lite reaktivt. Korroderer basismetaller.

MATERIALER SOM SKAL UNNGÅS

Ved høye temperaturer: Wolfram. Molybden. Jern. Nikkel. Fuktig karbondioksid reagerer med mange stoffer ved lave temperaturer og det må bare benyttes syrefast utstyr.

FARLIGE SPALTINGSPRODUKTER

-

ANNEN INFORMASJON

Søk råd hos leverandør.

11. OPPLYSNINGER OM HELSEFARE

GENERELT

Gass eller damp fortrenger oksygen og kan medføre kvelningsfare.

INNÅNDING

Gass eller damp fortrenger oksygen og kan medføre kvelningsfare. Kan ha dødelig utgang.

HUDKONTAKT

Gassen er meget kald når den kommer ut av beholderen, og det kan forårsake frostskafer på hud.

ØYEKONTAKT

Kan gi frotskade.

SVELGING

Ikke aktuelt (produktet er en gass).

ALLERGI

-

MUTAGENE EFFEKTER

-

FOSTERSKADELIGE EFFEKTER

-

AKUTTE OG KRONISKE SKADEVIRKNINGER

-

HMS-DATABLAD

Linde Gas | AGA

Sist endret: 26.05.2006

Internt nr: 0011

Erstatter dato:30.01.2003

12. MILJØOPPLYSNINGER

ØKOTOKSISITET

-

MOBILITET

Spres hurtig i luft.

PERSISTENS OG NEDBRYTBARHET

Produktet løses og fortynnes raskt ved utslipp til vann.

BIOAKKUMULERINGSPOTENSIAL

Bioakkumulerer ikke.

ANDRE SKADEVIRKNINGER

Vær oppmerksom på faren for frostskafer. Må ikke slippes ut i kloakk eller avløp.

ANNEN INFORMASJON

Ikke miljøskadelig.

13. FJERNING AV KJEMIKALIEAVFALL

GENERELT

Ikke klassifisert som spesialavfall. Ved tilstrekkelig ventilasjon og forøvrig under betryggende kontroll kan gassen slippes til friluft.

14. OPPLYSNINGER OM TRANSPORT

Kjemikaliet er klassifisert som farlig gods: Ja

HMS-DATABLAD

 Linde Gas | 

Sist endret: 26.05.2006 Internett nr: 0011 Erstatte dato:30.01.2003

UN-nr: 2187

VARENAVN OG BESKRIVELSE:

KARBONDIOKSID, NEDKJØLT FLYTENDE

ADR/RID (VEITRANSPORT/JERNBANETRANSPORT)

Klasse:	2	Forpakkingsgr:	
----------------	---	-----------------------	--

Fareseddel:	2.2		
--------------------	-----	--	--

Farenummer:	22		
--------------------	----	--	--

Dypkjølt flytende gass, inert.

IMDG (SJØTRANSPORT)

Klasse:	2.2	Forpakkingsgr:	-
----------------	-----	-----------------------	---

Sub. risiko:	-	EMS:	2-12
---------------------	---	-------------	------

Marin forurensning:	-		
----------------------------	---	--	--

IATA (LUFTTRANSPORT)

Klasse:		Forpakkingsgr:	
----------------	--	-----------------------	--

ANNEN INFORMASJON

Transport i samsvar med nasjonale regler og ADR (vei), RID (jernbane) og IMDG (sjø). Sikkerhetsventilen på større tanker vil avlaste overtrykk.

15. OPPLYSNINGER OM LOVER OG FORSKRIFTER

EF-etikett	Ikke vurdert
-------------------	--------------

SAMMENSETNING
YL-gruppe
YL-tall :
REFERANSER

Arbeidstilsynet: Forskrift om stoffliste. Produktet er klassifisert og merket i henhold til EEC-forskrifter eller respektive nasjonale lover. Transport av farlig gods: ADR, RID, IMDG, IATA.

ANNEN INFORMASJON

Orientering: "Arbeidstilsynets publikasjonskatalog". Orientering: "Hva du må vite, når du bruker åndedrettsvern". Veiledning: "Arbeide i trange rom". Forskrift: "Bruk av personlig verneutstyr på arbeidsplassen".

16. ANDRE OPPLYSNINGER AV BETYDNING FOR HMS

INFORMASJONSKILDER

AGAs publikasjon: "ABC for gassikkerhet". AGA's publikasjon. "AGA sikkerhetskurs - om gassenes egenskaper, bruk og håndtering". AGAs publikasjon: "Gassikkerhet i alle ledd (industri)". AGAs publikasjon: "Sikker gassflasketransport".

LEVERANDØRENS ANMERKNINGER

Flasken skal returneres til leverandør med minst 2 bar resttrykk. Informasjonen i dette dokument skal gjøres tilgjengelig til alle som håndterer produktet.

• VEDLEGG D - PRØVESERTIFIKAT FOR LOKAL TRYKKTESTING



• VEDLEGG D - PRØVESERTIFIKAT FOR LOKAL TRYKKTESTING

Trykktesten skal utføres i følge NS-EN 13445 del 5 (Inspeksjon og prøving).
Se også prosedyre for trykktesting gjeldende for VATL lab

Trykkpåkjent utstyr: Tarbotrammel, CO₂ vannpumpe

Benyttes i rigg:

Design trykk for utstyr:bara

Maksimum tillatt trykk: 150bara
(i.e. burst pressure om kjent)

Maksimum driftstrykk i denne rigg: 120bara

Prøvetrykket skal fastlegges i følge standarden og med hensyn til maksimum tillatt trykk.

Prøvetrykk: 99,8bara (..... x maksimum driftstrykk)
I følge standard

Test medium: Nitrogen

Temperatur: 21 °C

Start: Tid: 13. sept 2011 - 17.20

Trykk: 99.8 bara

Slutt: Tid: 14. sept 2011 - 10.00

Trykk: 98 bara

Eventuelle repetisjoner fra atm. trykk til maksimum prøvetrykk: 1

Test trykket, dato for testing og maksimum tillatt driftstrykk skal markers på (skilt eller innslått)

Troulbe 21.10.2011
Sted og dato

[Signature]
Signatur

SWAGELOK RELIEF VALVE R3A		
NR 61		
Test medie N2 dato: 2011.09.09 utført av: MR		
Ref nr. KN09-007		
Åpningstrykk 150 Bar	Helt åpen	stengt
148,2	155	134,5
151	155	135,1
149,1	156	133,3
151,8	157	134,9
151,9	155	135,8

Test medie N2 dato: utført av:		

Test medie N2 dato: utført av:		

Test medie N2 dato: utført av:		

- **VEDLEGG E HAZOP MAL PROSEDYRE**

Project: Node: 1							Page
Ref #	Guideword	Causes	Consequences	Safeguards	Recommendations	Action	Date Sign
	Uklar	Prosedyre er laget for ambisiøs eller preget av forvirring					
	Trinn på feil plass	Prosedyren vil lede til at handlinger blir gjennomført i feil mønster/rekkefølge					
	Feil handling	Prosedyrens handling er feil spesifisert					
	Uriktig informasjon	Informasjon som er gitt i forkant av handling er feil spesifisert					
	Trinn utelatt	Manglende trinn, eller trinn krever for mye av operatør					
	Trinn mislykket	Trinn har stor sannsynlighet for å mislykkes					
	Påvirkning og effekter fra andre	Prosedyrens prestasjoner vil trolig bli påvirket av andre kilder					

• **VEDLEGG F FORSØKSPROSEDYRE**

Experiment, name, number: CO ₂ Tørketrommel		Date/ Sign
Project Leader: Trygve Magne Eikevik		
Experiment Leader: Åsmund Elnan		
Operator, Duties: Åsmund Elnan		
	Conditions for the experiment:	Completed
	Experiments should be run in normal working hours, 08:00-16:00 during winter time and 08.00-15.00 during summer time. Experiments outside normal working hours shall be approved.	
	One person must always be present while running experiments, and should be approved as an experimental leader.	
	An early warning is given according to the lab rules, and accepted by authorized personnel.	
	Be sure that everyone taking part of the experiment is wearing the necessary protecting equipment and is aware of the shut down procedure and escape routes.	
	Preparations	Carried out
	Post the "Experiment in progress" sign.	
	<i>Start up procedure</i> <ul style="list-style-type: none"> - Labview operative – computer ready to log experiment - CO2 refrigerant charge - Weighing of dry fabric - Weighing of wet fabric - Check standstill conditions for temperature and pressure - Check correct throttling for start-up(valves and throttling valve) 	
	During the experiment	
	<i>LabView control of temperature and pressure</i>	
	Regulate manual throttling valve if necessary	
	End of experiment	
	<i>Turn off compressor, motor, external fan, water pump</i>	
	<i>Stop LabView logging</i>	
	Remove all obstructions/barriers/signs around the experiment.	
	Tidy up and return all tools and equipment.	
	Tidy and cleanup work areas.	
	Return equipment and systems back to their normal operation settings (fire alarm)	
	To reflect on before the next experiment and experience useful for others	
	Was the experiment completed as planned and on scheduled in professional terms?	
	Was the competence which was needed for security and completion of the experiment available to you?	
	Do you have any information/ knowledge from the experiment that you should document and share with fellow colleagues?	

• **VEDLEGG G OPPLÆRINGSPLAN FOR OPERATØRER**

Experiment, name, number: CO2 tørketrommel	Date/ Sign
Project Leader: Trygve Magne Eikevik	
Experiment Leader: Åsmund Elnan	
Operator Åsmund Elnan	

	Kjennskap til EPT LAB generelt	
	Lab - adgang -rutiner/regler -arbeidstid	
	Kjenner til evakueringsprosedyrer	
	Aktivitetskalender	
	Kjennskap til forsøkene	
	Prosedyrer for forsøkene	
	Nødstop	
	Nærmeste brann/førstehjelpsstasjon	
	Kjenne til faremomenter ved kontakt med CO2, se sikkerhetsdatablad	
	- Har gjennomgått E-kurs med Yara	
	Drift av tørketrommel	
	- Oppbygning av riggen	
	- LabView virkemåte	
	- Oppstartsprosedyrer	
	- Trykkbegrensninger	
	- Avstengningsprosedyrer	

Operatør

HMS ansvarlig

Dato

Dato

Signert

Signert

VEDLEGG H SKJEMA FOR SIKKER JOBB ANALYSE

SJA tittel:		
Dato:		Sted:
Kryss av for utfylt sjekkliste:	<input type="checkbox"/>	

Deltakere:		
SJA-ansvarlig:		

<p>Arbeidsbeskrivelse: (Hva og hvordan?) Tørking av tøy ved hjelp av tørketrommel med varmepumpeteknologi. Varmepumpen er med CO₂ som medium i en transkritisk prosess. Dvs. oppvarming av luft i overkritisk fase og avfuktning i underkritisk fase.</p>
<p>Risiko forbundet med arbeidet: Rørsammenbrudd med påfølgende lekkasje</p>
<p>Beskyttelse/sikring: (tiltaksplan, se neste side) Vernebriller</p>
<p>Konklusjon/kommentar: Er liten eller ingen fare for personskade ved kjøring av disse forsøkene.</p>

Anbefaling/godkjenning:	Dato/Signatur:	Anbefaling/godkjenning:	Dato/Signatur:
SJA-ansvarlig:		Områdeansvarlig:	
Ansvarlig for utføring:		Annen (stilling):	
HMS aspekt	Ja	Nei	Ikke aktuelt
Kommentar / tiltak			Ansv.

Dokumentasjon, erfaring, kompetanse				
Kjent arbeidsoperasjon?				
Kjennskap til erfaringer/uønskede hendelser fra tilsvarende operasjoner?				
Nødvendig personell?				
Kommunikasjon og koordinering				
Mulig konflikt med andre operasjoner?				
Håndtering av en evt. hendelse (alarm, evakuering)?				
Behov for ekstra vakt?				
Arbeidsstedet				
Uvante arbeidsstillinger?				
Arbeid i tanker, kummer el.lignende?				
Arbeid i grøfter eller sjakter?				
Rent og ryddig?				
Verneutstyr ut over det personlige?				
Vær, vind, sikt, belysning, ventilasjon?				
Bruk av stillaser/lift/seler/stropper?				
Arbeid i høyden?				
Ioniserende stråling?				
Rømningsveier OK?				
Kjemiske farer				
Bruk av helseskadelige/giftige/etsende kjemikalier?				
Bruk av brannfarlige eller eksplosjonsfarlige kjemikalier?				
Må kjemikaliene godkjennes?				
Biologisk materiale?				
Støv/asbest?				
Mekaniske farer				
Stabilitet/styrke/spenning?				
Klem/kutt/slag?				
Støy/trykk/temperatur?				
Behandling av avfall?				
Behov for spesialverktøy?				
Elektriske farer				
Strøm/spenning/over 1000V?				
Støt/krypstrøm?				
Tap av strømtilførsel?				
Området				
Behov for befarings?				
Merking/skilting/avsperring?				
Miljømessige konsekvenser?				
Sentrale fysiske sikkerhetssystemer				
Arbeid på sikkerhetssystemer?				
Frakobling av sikkerhetssystemer?				
Annet				

13 VEDLEGG H APPARATURKORT UNITCARD

Apparatur/unit

Dette kortet SKAL henges godt synlig på apparaturen! *This card MUST be posted on a visible place on the unit!*

Faglig Ansvarlig (Scientific Responsible) Trygve Magne Eikevik	Telefon mobil/privat (Phone no. mobile/private) 97508853
Apparaturansvarlig (Unit Responsible) Åsmund Elnan	Telefon mobil/privat (Phone no. mobile/private) 97508853
Sikkerhetsrisikoer (Safety hazards) <ul style="list-style-type: none">- Lekkasje av CO2 til omgivelser- små mengder i stort rom vil ikke føre til fare for personskade.- Ved akutt lekkasje vil det føre til at karbondioksiden ekspanderer og det vil være kalde overflater, fordampningstemperatur på 10 C vil ikke føre til akutt fare- Varme overflater på høytykkside ut til kompressor plassert på utsida av tørketrommelen – disse kan ha temperatur rundt 100 C, en bør derfor vere observant ved arbeid rundt disse rørene.	
Sikkerhetsregler <ul style="list-style-type: none">- Bruk av vernebriller påbudt under forsøk	
Nødstop prosedyre Nødstoppbryter er montert på styringsskap, denne vil kutte strøm til alle kontaktorer og medføre at systemet umiddelbart vil stoppe.	

Her finner du (Here you will find):

Prosedyrer (Procedures)
Bruksanvisning (Users manual)

Nærmeste (nearest)

Brannslukningsapparat (fire extinguisher)	
Førstehjelpsskap (first aid cabinet)	

NTNU
Institutt for energi og prosessteknikk

Dato

Signert

VEDLEGG I FORSØK PÅGÅR KORT

Forsøk pågår! Experiment in progress!

Dette kort skal settes opp før forsøk kan påbegynnes This card has to be posted before an experiment can start

Ansvarlig / Responsible	Telefon jobb/mobil/hjemme 97508853
Operatører/Operators Åsmund Elnan	Forsøksperiode/Experiment time(start – slutt) 20.10.2011-31.11.2011
Prosjektleder Åsmund Elnan	Prosjekt CO2 Tørketrommel

Eksperimentet innebærer tørking av klær i en tørketrommel. Til dette benyttes en CO₂ – varmepumpe som skal operere transkritisk; varmeopptak i underkritisk fase og med varmeavgivelse i overkritisk fase. Driftspunkt er 100 bar i gasskjøler og 45 bar i fordampere.

Hele eksperiment vil være overvåket fra start til slutt.

Eventuelle farer inkluderer brist i rørføringer med påfølgende lekkasjer av kuldemedium til omgivelsene. Fyllingen er liten og forsøk gjøres i et større rom som ikke vil medføre noen kvelningsfare ved lekkasje.

NTNU
Institutt for energi og prosessteknikk

Dato

Signert

VEDLEGG J OLJEDATABLAD

Safety Data Sheet

according to 1907/2006/EC, Article 31

Printing date 01.11.2008

Revision: 01.11.2008

1 Identification of the substance/preparation and of the company/undertaking

- Product details
- Trade name: RENISO TRITON SEZ 68
- Article number: 600418212
- Application of the substance / the preparation Lubricant
- Manufacturer/Supplier:
FUCHS LUBRICANTS (UK) PLC.
New Century Street
Hanley
Stoke-on-Trent, Staffordshire, ST1 5HU
UK
Emergency telephone: (UK) 08701 200400
e-mail: product.safety@fuchs-oil.com
- Further information obtainable from: Product safety department.
- Information in case of emergency: Emergency telephone: (UK) 08701 200400

2 Hazards identification

- Hazard description: Not applicable.
- Information concerning particular hazards for human and environment: Not applicable.

3 Composition/information on ingredients

- Chemical characterization:
- CAS No. Description
SYNTHETIC ESTER
- Identification number(s)
- Additional information: A blend of synthetic esters

4 First aid measures

- General information: No special measures required.
- After inhalation: Supply fresh air; consult doctor in case of complaints.
- After skin contact:
Immediately wash with water and soap and rinse thoroughly.
If skin irritation continues, consult a doctor.
- After eye contact:
Check for and remove any contact lenses.
Rinse opened eye for several minutes under running water. Then consult a doctor.
- After swallowing:
Wash mouth out with water
Do not induce vomiting; call for medical help immediately.
- Information for doctor:
High pressure injection injuries through the skin require prompt surgical intervention and possibly steroid therapy, to minimise tissue damage and loss of function. Because entry wounds are small and do not reflect the seriousness of the underlying damage, surgical exploration to determine the extent of involvement may be necessary. Local anaesthetics or hot soaks should be avoided because they can contribute to swelling, vasospasm and ischaemia. Prompt surgical decompression, debridement and evacuation of foreign material should be performed under general anaesthetics, and wide exploration is essential.

5 Fire-fighting measures

- Suitable extinguishing agents:
CO₂, powder or water spray. Fight larger fires with water spray or alcohol resistant foam.
- For safety reasons unsuitable extinguishing agents: Water with full jet

(Contd. on page 2)

GB

Safety Data Sheet

according to 1907/2006/EC, Article 31

Printing date 01.11.2008

Revision: 01.11.2008

Trade name: RENISO TRITON SEZ 68

(Contd. of page 1)

- **Protective equipment:**
- Wear self-contained respiratory protective device.
- Wear fully protective suit.

6 Accidental release measures

- **Person-related safety precautions:** Particular danger of slipping on leaked/spilled product.
- **Measures for environmental protection:**
- Do not allow to enter sewers/ surface or ground water.
- Do not allow to penetrate the ground/soil.
- **Measures for cleaning/collecting:**
- Absorb with liquid-binding material (sand, diatomite, acid binders, universal binders, sawdust).
- Send for recovery or disposal in suitable receptacles.
- **Additional information:** No dangerous substances are released.

7 Handling and storage

- **Handling:**
- **Information for safe handling:** Prevent formation of aerosols.
- **Information about fire - and explosion protection:** No special measures required.
- **Storage:**
- **Requirements to be met by storerooms and receptacles:** Prevent any seepage into the ground.
- **Information about storage in one common storage facility:** Store away from oxidizing agents.
- **Further information about storage conditions:** Store in cool, dry conditions in well sealed receptacles.

8 Exposure controls/personal protection

- **Additional information about design of technical facilities:** No further data; see item 7.
- **Ingredients with limit values that require monitoring at the workplace:** Not required.
- **Additional information:** The lists valid during the making were used as basis.
- **Personal protective equipment:**
- Select PPE appropriate for the operations taking place taking into account the product properties.
- **General protective and hygienic measures:**
- Wash hands before breaks and at the end of work.
- Avoid close or long term contact with the skin.
- Do not eat, drink, smoke or sniff while working.
- Do not carry product impregnated cleaning cloths in trouser pockets.
- Avoid contact with the eyes.
- **Respiratory protection:** Not required.
- **Protection of hands:**
- The glove material has to be impermeable and resistant to the product/ the substance/ the preparation.
- **Material of gloves**
- The selection of the suitable gloves does not only depend on the material, but also on further marks of quality and varies from manufacturer to manufacturer.
- **Penetration time of glove material**
- The exact break through time has to be found out by the manufacturer of the protective gloves and has to be observed.
- **Eye protection:**
- Safety glasses
- Goggles recommended during refilling
- **Body protection:** Protective work clothing

(Contd. on page 3)

Safety Data Sheet

according to 1907/2006/EC, Article 31

Printing date 01.11.2008

Revision: 01.11.2008

Trade name: RENISO TRITON SEZ 68

(Contd. of page 1)

- **Protective equipment:**
- Wear self-contained respiratory protective device.
- Wear fully protective suit.

6 Accidental release measures

- **Person-related safety precautions:** Particular danger of slipping on leaked/spilled product.
- **Measures for environmental protection:**
- Do not allow to enter sewers/ surface or ground water.
- Do not allow to penetrate the ground/soil.
- **Measures for cleaning/collecting:**
- Absorb with liquid-binding material (sand, diatomite, acid binders, universal binders, sawdust).
- Send for recovery or disposal in suitable receptacles.
- **Additional information:** No dangerous substances are released.

7 Handling and storage

- **Handling:**
- **Information for safe handling:** Prevent formation of aerosols.
- **Information about fire - and explosion protection:** No special measures required.
- **Storage:**
- **Requirements to be met by storerooms and receptacles:** Prevent any seepage into the ground.
- **Information about storage in one common storage facility:** Store away from oxidizing agents.
- **Further information about storage conditions:** Store in cool, dry conditions in well sealed receptacles.

8 Exposure controls/personal protection

- **Additional information about design of technical facilities:** No further data; see item 7.
- **Ingredients with limit values that require monitoring at the workplace:** Not required.
- **Additional information:** The lists valid during the making were used as basis.
- **Personal protective equipment:**
- Select PPE appropriate for the operations taking place taking into account the product properties.
- **General protective and hygienic measures:**
- Wash hands before breaks and at the end of work.
- Avoid close or long term contact with the skin.
- Do not eat, drink, smoke or sniff while working.
- Do not carry product impregnated cleaning cloths in trouser pockets.
- Avoid contact with the eyes.
- **Respiratory protection:** Not required.
- **Protection of hands:**
- The glove material has to be impermeable and resistant to the product/ the substance/ the preparation.
- **Material of gloves**
- The selection of the suitable gloves does not only depend on the material, but also on further marks of quality and varies from manufacturer to manufacturer.
- **Penetration time of glove material**
- The exact break trough time has to be found out by the manufacturer of the protective gloves and has to be observed.
- **Eye protection:**
- Safety glasses
- Goggles recommended during refilling
- **Body protection:** Protective work clothing

GB

(Contd. on page 3)

Safety Data Sheet

according to 1907/2006/EC, Article 31

Printing date 01.11.2008

Revision: 01.11.2008

Trade name: RENISO TRITON SEZ 68

(Contd. of page 3)

13 Disposal considerations

- **Product:**
- **Recommendation**
Must not be disposed together with household garbage. Do not allow product to reach sewage system.
Contact waste processors for recycling information.
- **European waste catalogue**
Waste key numbers in accordance with the European Waste catalogue (EWC) are origin-referred defined. Since this product is used in several industries, no waste key can be provided by the supplier. The waste key number should be determined in arrangement with your waste disposal partner or the responsible authority.
- **Uncleaned packaging:**
- **Recommendation:** Disposal must be made according to official regulations.

14 Transport information

- | |
|---|
| <ul style="list-style-type: none"> · Land transport ADR/RID (cross-border) · ADR/RID class: - |
| <ul style="list-style-type: none"> · Maritime transport IMDG: · IMDG Class: - · Marine pollutant: No |
| <ul style="list-style-type: none"> · Air transport ICAO-TI and IATA-DGR: · ICAO/IATA Class: - |
- **Transport/Additional information:** Not dangerous according to the above specifications.

15 Regulatory information

- **Labelling according to EU guidelines:**
Observe the general safety regulations when handling chemicals.
The substance is not subject to classification according to EU lists and other sources of literature known to us.

16 Other information

- This information is based on our present knowledge. However, this shall not constitute a guarantee for any specific product features and shall not establish a legally valid contractual relationship.
- **Department issuing MSDS:** Product safety department.
 - **Contact:** GORDON SHARP

GB